Vascular function in abdominal adipose tissue: vascular tone, angiogenic and secretory capacity

Lei Shen

Adipokines and Metabolism Research Group

Division of Medicine

UCL

A thesis submitted for the degree of Doctor of Philosophy in the Division of Medicine at University College London

Declaration

No part of this thesis has been submitted in support of an application for any other degree or qualification at the University College London or any other university or institute. All the work presented is my own and all collaborations have been acknowledged.

Signature:

Date:

Abstract

Background

Healthy adipose tissue (AT) growth is critically dependent on vascular support and this relationship appears to be reciprocal. Optimal angiogenesis and functional vascular tone ensure normal supply of oxygen, insulin, and nutrients, thus preventing AT hypoxia and insulin resistance. Normal vascular function may also be regulated by factors derived from the healthy AT (adipokines). In obesity AT expansion, especially of the abdominal subcutaneous and omental depots (SAT and OAT respectively), contributes to the increased risk of metabolic and cardiovascular diseases. In addition, perivascular AT (PVAT) may also mediate vascular function by producing vasoactive adipokines, either directly or through indirect effects on components of the adjacent vessel wall. Changes in vascular characteristics during AT expansion in SAT, OAT and PVAT have all been the focus of much recent research.

During the tenure of this project three studies, with separate but related aims, explored the vaso-responsiveness, angiogenic and adipokine secretory capacity of resistance vessels embedded within abdominal adipose tissue depots and the adipokine secretory capacity of PVAT.

Aims

The aims were to investigate in:

Study 1: the depot- and diabetes-specific differences of noradrenaline (NA) synthesis, NA-mediated vasoconstriction and tissue fibrosis in abdominal SAT and OAT of morbidly obese patients.

Study 2: the depot- and diabetes-specific differences of capillary density, angiogenic capacity and angiogenesis-related mRNA and protein expression.

Study 3: the adipokine production of PVAT of the saphenous vein (SV) and internal thoracic artery (ITA).

Methods

Studies 1&2: Abdominal SAT and OAT, from morbidly obese patients undergoing weight-reducing surgery, were used for investigating 1) vascular function (myography); 2) adipokine secretion (explant and ELISAs); 3) adipocyte morphology and capillary density (histochemistry and immunohistochemistry); 4) angiogenic capacity (tissue culture), and 5) vasculature-related gene and protein expression (real-time PCR and western blot).

Study 3: Segments of SV and the ITA with the surrounding PVAT intact, obtained from patients undergoing coronary artery bypass graft surgery (CABG), was used to investigate: 1) PVAT morphology (histochemistry), 2) adiponectin and leptin secretion (immunohistochemistry). PVAT and vessels were isolated respectively for investigating adipokine production by ELISAs. Cultured human umbilical vein endothelial cells (HUVECs) and human coronary artery endothelial cells (HCAECs) used to investigate secretory capacity of adiponectin by the endothelium.

National Ethical Committees approved all studies and patients gave written informed consent.

Results

Study 1: In non-diabetic subjects, the SAT vessels showed significantly greater sensitivity to NA-mediated vasoconstriction, compared to vessels of OAT or to vessels of either depot of diabetic patients. The non-diabetic SAT also exhibited lower NA synthesis and collagen deposition.

Study 2: Lower capillary density, angiogenic capacity and down-regulation of angiogenesis-related genes was also only apparent in the SAT of non-diabetic subjects, compared with OAT or either depot of diabetics.

Study 3: In the PVAT adiponectin mRNA and protein expression was detected in the endothelium and in cultured human endothelial cells (ECs).

Discussion & Conclusion

The SAT of non-diabetics secreted less noradrenaline and exhibited lower tissue collagen deposition. Furthermore, the arterioles from this depot preserved their sensitivity to NA-mediated vasoconstriction. Conversely, elevated local NA production, greater collagen deposition and relative insensitivity of microvessels to NA-medaited vasoconstriction characterised the OAT, as well as both SAT and OAT of diabetics. NA also directly stimulated collagen mRNA expression.

Greater angiogenic capacity of the OAT of non-diabetics and both SAT and OAT of diabetics may reflect local hypoxia, perhaps because of compromised vascular function.

Human ECs displayed the capacity to produce adiponectin. The effect of EC-derived adiponectin on vasculature needs further investigation.

Table of contents

List of figures

List of tables

Abbreviations

ABC	Avidin biotin complex
AC	Adenylate cyclase
ADRF	Adipocyte-derived relaxing factor
Akt	Protein kinase B
Ang	Angiotensin
ANGPIL3	Angiopoietin-like 3
ANPEP	Alanyl (membrane) aminopeptidase
AT	Adipose tissue
ATBF	Adipose tissue blood flow
AU	Arbitrary unit
BCA	Bicinchoninic acid
BMI	Body mass index
Ca^{2+} channel	Calcium channel
CABG	Coronary artery bypass grafting
cAMP	Cyclic adenosine monophosphate
CCL	Chemokine (C-C motif) ligand
cGMP	Cyclic guanosine monophosphate
CNS	Central nervous system
COL4A3	Collagen, type IV, alpha 3
COX	Cyclooxygenase
CS-GAG	Chondroitin sulfate-glycosaminoglycan
CT	Computed tomography
Ct	Cycle threshold
CXCL	Chemokine (C-X-C motif) ligand

DAPI	4',6-diamidino-2-phenylindole, dihydrochloride
DBH	dopamine-ß-hydroxylase
DBP	Diastolic blood pressure
DM	Diabetic obese patients
EBM	Endothelial basal medium
EC	Endothelial cell
EC_{50}	50% maximal effective concentration
ECM	Extracellular matrix
EDCF	Endothelium-derived contracting factors
EDHF	Endothelium-derived hyperpolarizing factor
EDRF	Endothelium-derived relaxing factors
EFNA3	Ephrin-A3
EGF	Epidermal growth factor
EGM	Endothelial growth medium
eNOS	Endothelial isoform of NO synthase
ET-1	Endothelin-1
EVG	Elastic Van Gieson
FBS	Foetal bovine serum
FGF1	Fibroblast growth factor 1 (acidic)
FGFR3	Fibroblast growth factor receptor 3
FIGF	C-fos induced growth factor (vascular endothelial growth factor D)
FITC	Fluorescein isothiocyanate
FPG	Fasting plasma glucose
GLUT-1	Glucose transporter-1
GPCR	G-protein-coupled receptor
GRB2	Growth factor receptor-bound protein 2

GRK-2	G-protein-coupled receptor kinase-2
GS	Griffonia simplicifolia
HAND2	Heart and neural crest derivatives expressed 2
HCAECs	Human coronary artery endothelial cells
HIF-α	Hypoxia inducible factor-α
HMW	High molecular weight
HOMA	Homeostasis model assessment
HUVECs	Human umbilical vein endothelial cells
IFNA1	Interferon, alpha1
IFNB1	Interferon, beta 1, fibroblast
IFNG	Interferon, gamma
IL-6	Interleukin-6
IP3	1, 4, 5-trisphosphate
IRS-1	Insulin receptor substrate-1
ITA	Internal thoracic artery
K^+ channel	Potassium channel
LECT1	Leukocyte cell derived chemotaxin 1
MABP	Mean arterial blood pressure
MAPK	Mitogen-activated protein kinase
MCP-1	Monocyte chemoattractant protein -1
MEK	MAPK/extracellular signal-regulated kinases
MHO	Metabolically healthy but obese
MMP	Matrix metallopeptidase
MRI	Magnetic resonance imaging
NA	Noradrenalin
NEFA	Non-esterified fatty acid

NO	Nitric oxide
Non-DM	Non-diabetic obese patients
NOTCH4	Notch 4
NPSS	Normal physiological salt solution
NPY	Neuropeptide Y
NRP-1	Neuropilin-1
OAT	Omental adipose tissue
OGTT	Oral glucose tolerance test
OSA	Obstructive sleep apnoea
PBS	Phosphate buffered saline
PCR	Polymerase Chain Reaction
PECAM1	Platelet/endothelial cell adhesion molecule
PF4	Platelet factor 4
PGE_2	Prostaglandin E_2
PGI_2	Prostaglandin I_2
PI3-kinase	Phosphatidylinositol 3-kniase
PKA	Protein kinase A
PLC	Phospholipase C
PLG	Plasminogen
PO	Pathological obese
PO_2	AT oxygen tension
PTGS	Prostaglandin-endoperoxide synthase
PVAT	Perivascular adipose tissue
ROS	Reactive oxygen species
SAT	Subcutaneous adipose tissue
SBP	Systolic blood pressure

SOS	Guanine nucleotide exchange factor
SV	Saphenous vein
SVF	Stromal vascular fraction
TG	Triglycerides
TGFB1	Transforming growth factor, beta 1
TH	Tyrosine hydroxylase
TIMP	TIMP metallopeptidase inhibitor
TNFAIP2	Tumor necrosis factor, alpha-induced protein 2
TNF-α	Tumour necrosis factor –α
TXA_2	Thromboxane A_2
TYMP	Thymidine phosphorylase
UEA	Ulex europaeus
VEGF	Vascular endothelial growth factor
VSMC	Vascular smooth muscle cell

Publications arising from this project

Conference Proceedings

Lei Shen, Nelson Orie, Carlo Casale, Nephtali Marina, Mick Dashwood, Pratik Sufi, Dugal Heath, Rosaire Gray and Vidya Mohamed-Ali, *Depot- and disease-specific differences in adipose noradrenaline mediated vascular tone and arteriolar structure*. ENDO 2013, OR51-Obesity: From Genes to Populations Translational (oral presentation)

Lei Shen, Nelson Orie, Carlo Casale, Nephtali Marina, Mick Dashwood, Pratik Sufi, Dugal Heath, Rosaire Gray and Vidya Mohamed-Ali, *Depot- and disease-specific differences in adipose noradrenaline mediated vascular tone and arteriolar structure.* Endocr Rev, 2013, Vol. 34 (03_MeetingAbstracts): OR51-2 (oral presentation)

Carlo Casale, **Lei Shen**, Sana Malik, Rosaire Gray, Pratik Sufi, Dugal Heath, Nephtali Marina and Vidya Mohamed-Ali, *Systemic Neuropeptide Y Levels Are Suppressed in the Metabolically Healthy Obese*. Endocr Rev, 2013, Vol. 33 (03_MeetingAbstracts): SUN-134

Sana Malik, **Lei Shen**, Carlo Casale, Rosaire Gray, Pratik Sufi, Dugal Heath and Vidya Mohamed-Ali, *Effect of Surgical Weight Loss on Insulin Sensitivity and Lipid Profile of Metabolically Healthy Morbidly Obese Subjects*. Obes Surg. pp. 981 - 981

Vidya Mohamed-Ali; Carlo Casale; Sana Malik; **Lei Shen**; Pratik Sufi, Dugal Heath, Nephtali Marina, Rosaire Gray, *Prevalence and Treatment of Depression Are*

Differentially Associated With Pathological Obesity and Metabolically Healthy Obesity. Obesity, 2011. pp. S92 - S92

Manuscripts under review

Lei Shen, Nelson Orie, Carlo Casale, Nephtali Marina, Mohammed Alsayrafi, Pratik Sufi, Rosaire Gray and Vidya Mohamed-Ali, *Norepinephrine-induced contractile insensitivity and collagen deposition in subcutaneous adipose tissue arterioles of diabetic patients,* Submitted to Circulation, 2014.

Lei Shen, Carlo Casale, Rosaire Gray, Pratik Sufi, Dugal Heath and Vidya Mohamed-Ali, *Depot- and diabetes-specific differences of angiogenesis and angiogenesis-related gene on human abdominal adipose tissue,* Submitted to Diabetes, 2014.

Lei Shen, Ian Evans, Souza Dreifaldt, Mick Dashwood, Vidya Mohamed-Ali, *Endothelial adiponectin: putative role in graft patency in patients undergoing coronary artery bypass surgery?* Submitted to Cardiovascular Diabetology, 2014.

Acknowledgement

Here, I acknowledge all the support from my group and my family.

Great thanks to Dr Kalypso Karastergiou, who patiently taught me the basic lab techniques at the beginning of my PhD; Dr Nelson Orie, who taught me how to do the myography and helped me to set up the myograph system; Dr Ian Evans, for teaching me western blot and giving me very strong support in the endothelium study; my colleague and best friend, Mr Carlo Casale, who supported me in all aspects of the lab work; the clinical team in Whittington Hospital, Dr Rosaire Gray, Mr Pratik Sufi and Mr Dugal Heath, who showed great and consistent patience by consenting the patients and collecting the samples for our study, as well as Dr Domingos Souza and Dr Mats Dreifladt in Sweeden, who collected samples for the PVAT study; Dr Mick Dashwood for giving very useful comments and corrections on this thesis;

Special thanks go to my parents in China, Shen Guoren and Chen Hui, who funded me for the past 4 years and gave me great encouragement for doing this PhD.

Finally yet importantly, I am grateful to my supervisor, Dr Vidya Mohamed-Ali, for her patience in explaining everything to me, especially at the very beginning when my spoken English was not great; for her encouragement, even during the most difficult times when I had difficulties generating data; for her immense knowledge when discussing science with me, and for her extremely high standards in scientific work, which made me achieve great improvement during the past 4 years. Her enthusiasm and motivation deeply inspired me and these memories with her will be priceless treasures and cherished forever.

Chapter 1

Introduction and literature review

1.1 Prevalence and definition of obesity

The prevalence of obesity has increased over the past three decades and currently reached epidemic proportions globally [1]. Today, more than 500 million people suffer from obesity and its related complications worldwide, and this number continues increasing each year [2]. Obesity is defined as excessive adipose tissue (AT) deposition that may impair health [2]. A common method used to identify obese patients is by measuring the body mass index (BMI, body weight in kilograms divided by the square of body height in metres, $kg.m^{-2}$). Individuals with BMI over 30 $kg.m^{-2}$ are considered as obese, while those with BMI over 40 $kg.m^{-2}$ are defined as morbidly obese [2]. The morbidly obese patients are associated with high risks of developing metabolic disorders and cardiovascular diseases [3, 4]. In particular, obesity in abdominal area (central obesity) is an important risk factor of insulin resistance, Type II diabetes, hypertension and increased cardiovascular morbidity and mortality [5, 6].

1.2 Metabolically healthy but obese patients (MHO)

A unique phenotype of a sub-set of obese patients has been reviewed recently [7]. This sub-set of patients appears to be protected from obesity-related metabolic and cardiovascular complications and display favourable metabolic profiles despite their excessive adipose mass [7]. They are known as "metabolically healthy but obese" (MHO) patients. MHO individuals are characterized by their preserved insulin sensitivity, absence of hypertension, dyslipidemia and inflammation, and favourable adipokine profiles (**Figure 1**) [7]. Although 30 years has passed since MHO was first described in 1980s [8], it remains difficult to adequately standardize the identification of MHO patients. Several criteria have been used to characterize MHO patients, mainly based upon the assessment of insulin sensitivity by various methods, such as the hyperinsulinemic-euglycemic clamp, homeostasis model assessment (HOMA) and oral

glucose tolerance test (OGTT), or the levels of the metabolic risk factors such as lipid profiles, blood pressure, and C-reactive protein. Due to the lack of consensus in the definition, the reported prevalence of MHO phenotype ranges from 20 - 44% [7]. It is still unclear why the MHO individuals are resistant to the obesity-related complications. In this cohort weight reduction and AT loss after bariatric surgery achieved almost no metabolic benefits, even surprisingly, at least in some studies, leading to deterioration of insulin sensitivity in these individuals [9, 10], which suggests that the excessive AT may play a protective role. The molecular mechanisms that underlie this phenotype, especially in terms of protection from future development of diabetes or cardiovascular diseases, are still being investigated.

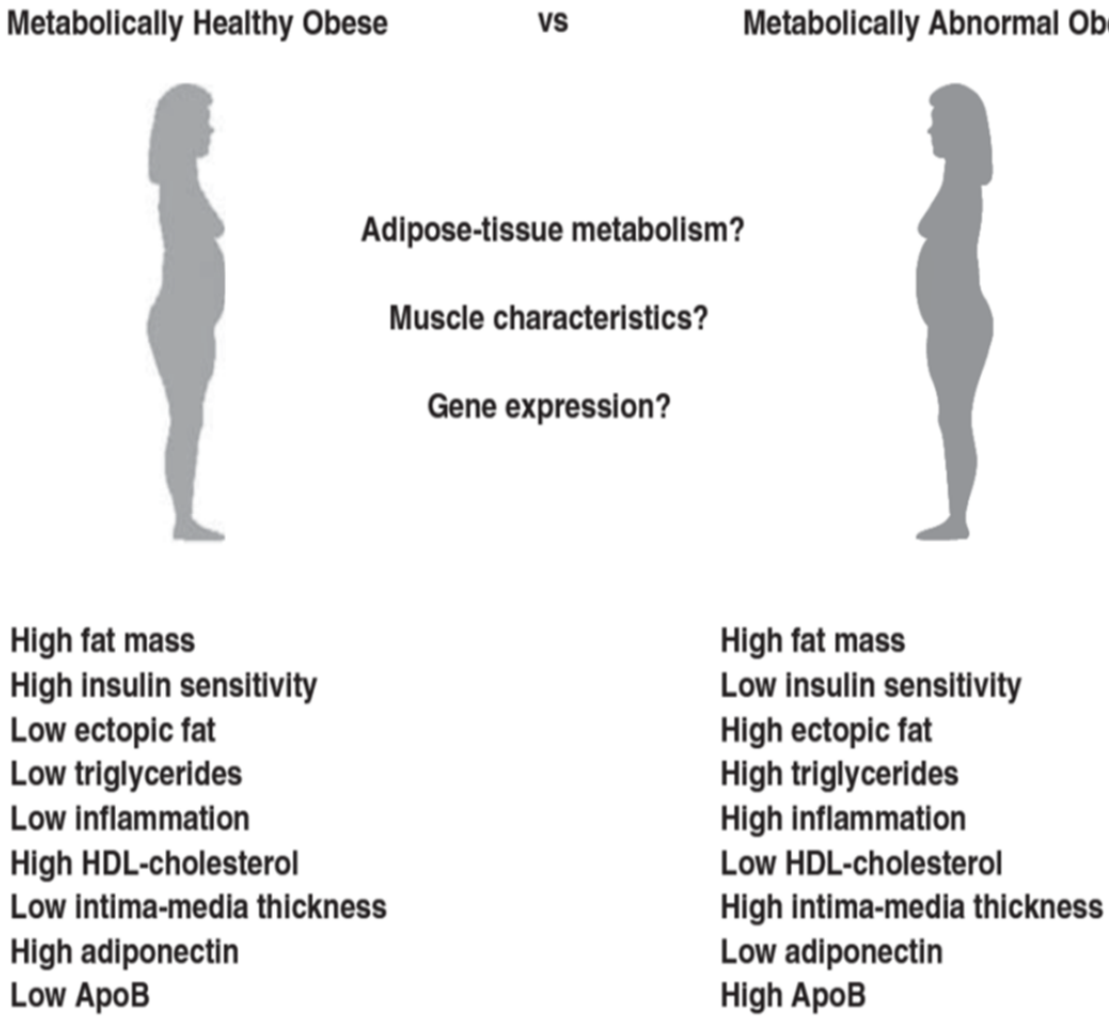

Figure 1 The major factors identifying MHO from metabolically abnormal obese [7]

1.3 AT structure, distribution and abdominal depot-specific differences

1.3.1 AT structure and function

AT is the loose connective organ mainly composed of adipocytes, as well as cells of the stromal vascular fraction (SVF) which includes pre-adipocytes, vascular endothelial cells (ECs) and macrophages. The major function of AT is to store excess energy in the form of triglycerides (TGs) [11], thus it was believed to be involved in body lipid and energy homeostasis. More recently, it has become clear that, in addition to lipid storage, AT is an important secretory organ associated with the production of multiple mediators known as adipokines [12]. These adipokines include pro-inflammatory adipokines such as tumour necrosis factor-α (TNF-α), monocyte chemoattractant protein-1 (MCP-1), and interleukin-6 (IL-6), and anti-inflammatory adipokines such as adiponectin and leptin. The dysregulation of adipokine secretion in obesity may contribute to the development of obesity-associated abnormalities by mechanisms including inhibition of adipogenesis, adipocyte hypertrophy and necrosis, immune cell infiltration and dysregulation of tissue metabolism [12, 13].

1.3.2 AT distribution and depot-specific differences in the abdominal area

Physiological expansion of AT is normal in many sites throughout the body, but only the abnormal AT accumulation in specific depots is associated with the adverse metabolic outcomes [14]. The regional AT expansion mainly includes two patterns of deposition, identified as android (upper body AT expansion) and gynoid pattern (lower body AT expansion). Obese individuals with the gynoid shape are less prone to metabolic disorders and cardiovascular diseases [15, 16], while those with android AT expansion, especially in the abdominal area, are more often associated with elevated risks of metabolic and cardiovascular complications such as insulin resistance, Type II diabetes, hypertension and atherosclerosis [17].

Abdominal AT mainly comprises two depots: the abdominal subcutaneous depot (AT under the skin, SAT) and intra-abdominal omental depot (AT of greater omentum, OAT). In the initial studies, the distribution of AT was assessed by anthropometric measurements such as skinfolds and waist-to-hip circumference ratios [18, 19] which were unable to distinguish SAT from OAT. Later, because of the development of imaging techniques, several studies clearly distinguished SAT from OAT using computed tomography (CT) and magnetic resonance imaging (MRI). It demonstrated that OAT, rather than SAT, was an important risk factor that mediates glucose intolerance in central obesity [20-22]. Recently, the depot-specific differences between SAT and OAT have been widely investigated in rodents and humans. In rodents, the intrinsic difference between the two depots has been shown by fat transplantation technique. Host mice receiving SAT into an omental depot gained less body weight and displayed favourable metabolic profile, but no metabolic benefit was achieved in the reverse situation when OAT transplanted into the subcutaneous region [23]. In addition, transgenic mice with elevated SAT expansion displayed improved insulin sensitivity and higher circulating adiponectin levels compared to their *ob/ob* littermates [24]. In human studies, individuals with higher proportions of OAT and relatively lower SAT were associated with insulin resistance and increased expression of inflammatory markers [5, 6]. Thiazolidinedione-induced AT redistribution (displayed as the SAT/OAT ratio elevation) showed favourable glucose, insulin and lipid profiles [25]. Furthermore, liposuction in SAT depots achieved no impact on circulating cardiovascular risk factors, other than a reduction in leptin [26]. These data implicate SAT as being a weaker risk factor during the development of morbidly obesity or even having a protective effect.

1.3.3 "Spillover" hypothesis

SAT is commonly considered the "good" depot in the context of obesity-related complications. This AT accounts for approximately 80% of the total body AT in human [27], which includes abdominal, gluteal, and femoral SAT (**Figure 2**) [28]. In healthy lean individuals, SAT provides the buffering action to maintain the energy homeostasis after excess calorie intake. This function is thought to be mediated by the "fatty acid trapping" pathway (systemic TG is the source of AT fatty acid) [29], thus SAT becomes the primary depot for lipid accumulation. However, when the buffering action is insufficient to maintain the "fatty acid trapping", elevated fatty acid starts to be deposited ectopically, leading to the AT expansion in OAT and AT infiltration into insulin sensitive organs such as liver, skeletal muscle and heart. When adipocytes enlarged (hypertrophied) by fatty acid intake, their efficiency to buffer excess fatty acid decreases [29] and both lipid synthesis and lipolysis within the bigger adipocytes became more active [30]. Consequently, the elevated transmembrane fatty acids may flow into the circulation and cause the ectopic AT accumulation.

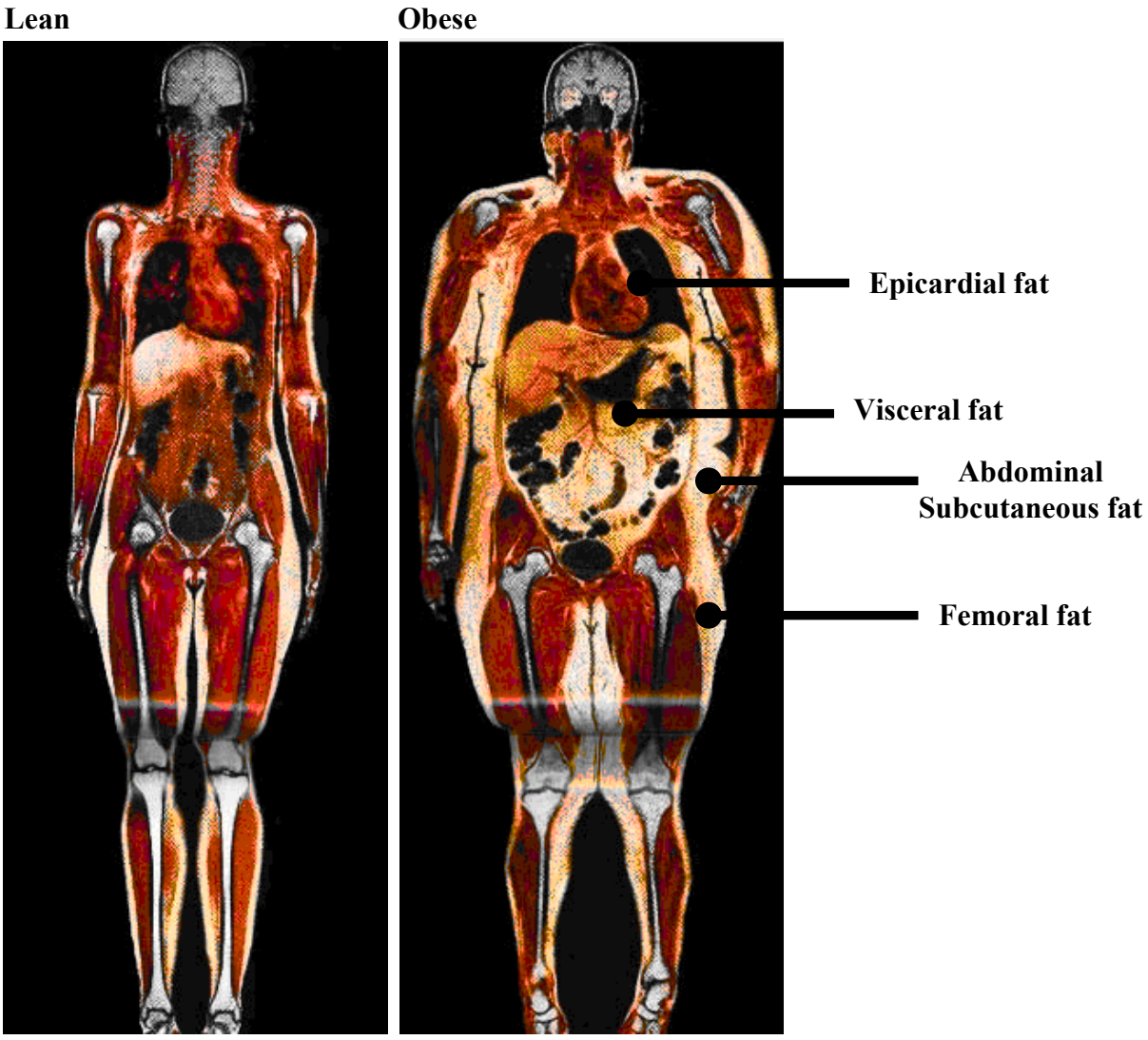

Figure 2 Body fat distribution: normal (left) vs obese (right).
(Extract from http://dietdatabase.com/obesity-facts-and-statistics)

1.4 AT morphology and oxygenation

1.4.1 AT expansion and adipocyte size

AT stores excess energy in the form of TGs. This function makes AT perhaps the only tissue with the capacity to increase and decrease its size dramatically under normal physiological conditions [31]. AT expandability and plasticity are determinants of obesity-related risk of metabolic diseases [14]. In situations of positive energy balance (energy intake exceeds energy expenditure), AT expands by generating new small adipocytes (AT hyperplasia) or increasing the volume of pre-existing adipocytes (AT hypotrophy) or both [32]. There is a negative correlation between subcutaneous adipocyte size and insulin sensitivity in non-diabetic subjects *in vitro*. Hypertrophic adipocytes are associated with insulin resistance, while small adipocytes may contribute to the preserved insulin sensitivity of AT [33]. Small adipocytes are also associated with increased secretion of adiponectin, which is widely accepted as an anti-inflammatory adipokine that protects against insulin resistance and cardiovascular risk [34]. In contrast, large adipocytes secrete more pro-inflammatory adipokines including MCP-1, IL-6, and TNF-α, which are associated with chronic inflammation and metabolic disorders [34]. Paradoxically, adipocyte size, examined in different depots measured by X-ray and CT, were significantly smaller in OAT than SAT [35]. Interestingly, adipocyte hypertrophy and hyperplasia in OAT are associated with hypertriglyceridemia, independent of body composition [36]. Compared with SAT, OAT adipocytes appear to exhibit greater hypoxia- and inflammation-related gene expression, which suggests a more toxic microenvironment in this depot [37]. However, this may be due to inflammatory cells trapped in the adipocyte fraction.

1.4.2 AT oxygenation in obesity

Sufficient oxygen supply is an important determinant of normal AT function [38]. Local tissue hypoxia may occur at the early stages of AT growth and limit healthy AT expansion [39]. In obesity vascular oxygen supply may be compromised by rapid AT expansion.

Much evidence from animal studies suggest AT hypoxia in obesity [40]. Hypoxia-related genes, including hypoxia inducible factor-α (HIF-α) and glucose transporter-1 (GLUT-1), were more highly expressed in AT of obese mice compared with lean mice, hypoxic AT was also associated with increased inflammatory gene expression. Moreover, pimonidazole staining showed a larger hypoxic area in obese mice compared with the lean littermates. Last but not least, AT oxygen tension (PO_2), which is a direct reflection of the local oxygen supply, was lower in AT of obese mice [40].

However, data from human studies are not consistent with the rodent results. To date, there are mainly two studies investigating the local oxygenation in SAT of obese versus lean individuals. One showed that PO_2 was significantly lower in overweight/obese patients, accompanied with local inflammation, compared with lean individuals [41], but the other study pointed to local PO_2 being elevated in obese patients due to the low oxygen consumption [38]. Interestingly, although the human data of AT oxygenation is debatable, both studies found that obesity is associated with decreased AT angiogenesis and capillary rarefaction (low capillary density), which suggests the importance of AT vasculature in maintaining AT normal function.

1.5 AT vasculature: angiogenesis and vasoreactivity

Sufficient vascular support is a key factor maintaining AT growth and functions. Effective vascular network includes optimum angiogenesis, adequate capillary density, and normal vascular function. Vasculature modulates AT in many ways. Firstly, it is an

important source of nutrients, oxygen, and insulin. Adequate blood supply prevents tissue hypoxia and insulin resistance. Secondly, systemic blood is enriched with growth factors and progenitor cells derived from bone marrow and other tissues. This facilitates the cell differentiation into pre-adipocytes or ECs and ensures the capacity of AT expansion. Finally, the vascular network may also enhance the transportation and infiltration of immune cells such as macrophage cells, which may amplify AT inflammation [42].

1.5.1 Interplay between angiogenesis and adipogenesis

In mice, there is a close interplay between angiogenesis and adipogenesis [43]. The initial AT development is characterized by the appearance of fat cell clusters, which is known as "primitive fat organ" [44]. In humans pre-adipocytes and ECs expressed $\alpha_v\beta_3$ integrin and plasminogen activator inhibitor-1(PAI-1), which are involved in the regulation of pre-adipocyte and EC migration [45]. This finding suggests that the formation of the primitive fat organ may be due to the pre-adipocyte migration towards developing capillary ECs. Furthermore, AT-derived SVF *in vitro* differentiated into not only the ECs but also adipocytes [45]. In addition, both SVF and mature adipocytes can induce neovascularization and vessel structure formation [46]. Very recent data also demonstrated that Zfp423, a gene controlling pre-adipocyte determination, was expressed in capillary ECs, which suggests that they may share the same progenitor [47].

1.5.2 Regulation of AT angiogenesis

Normal angiogenesis in AT is through the recruitment and interplay of both adipogenic and angiogenic precursor cells, which leads to an optimum AT expansion. However, angiogenesis in pathological AT expansion may be triggered by hypoxia. In response to AT overexpansion, angiogenesis plays a rate-limiting role constraining AT growth, this may cause tissue hypoxia, immune cell infiltration and chronic inflammation (**Figure 3**)

[39]. Angiogenesis in AT is regulated by multiple factors including classic angiogenic pathway, such as vascular endothelial growth factor (VEGF) and neuropilin-1 (NRP-1), as well as the adipokines released from AT.

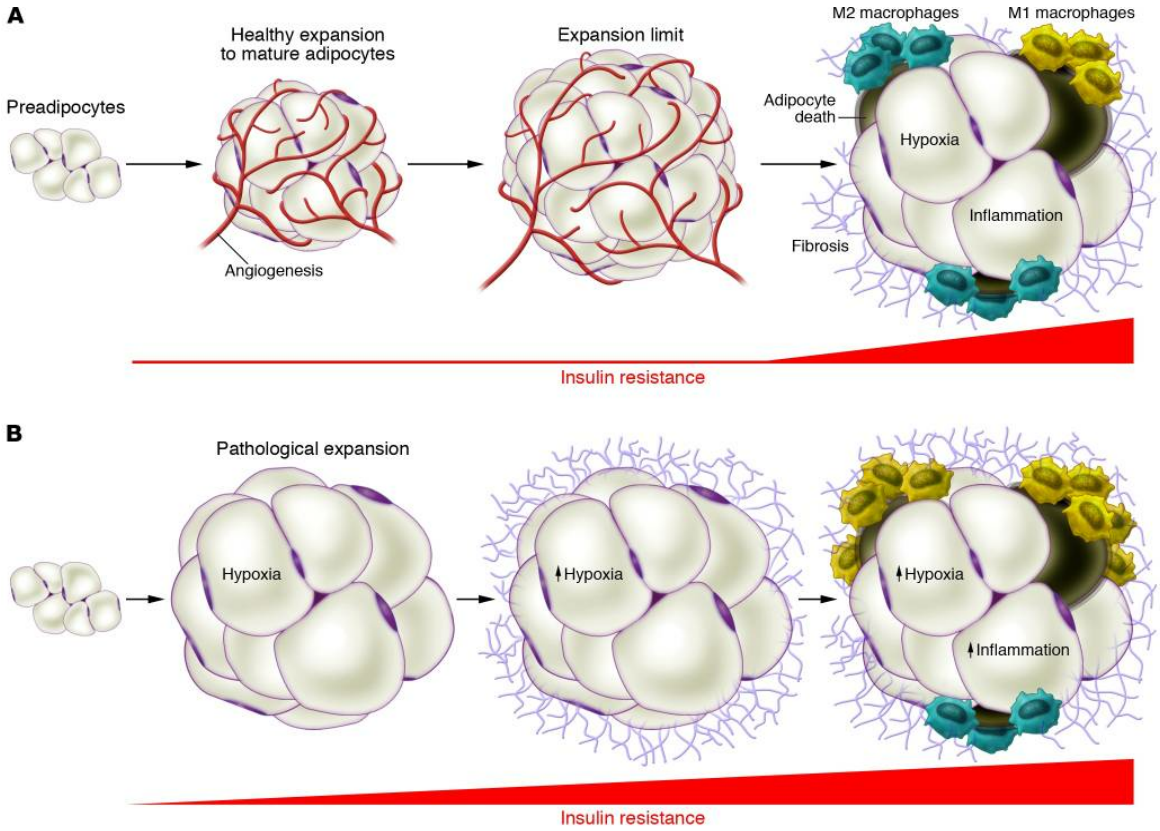

Figure 3 Healthy and unhealthy AT expansion.

The normal AT growth is through the preadipocyte recruitment and the interplay between adipocyte expansion and concomitant angiogenic support (A); However, pathological AT expansion lead to adipocyte hypotrophy and hypoxia, also angiogenesis is limited (B) [39].

1.5.2.1 VEGF

In mammals, there are five structurally related VEGF ligands (A, B, C, D and placenta growth factor), which are highly involved in the regulation of EC survival, proliferation and vascular permeability [48]. VEGFB was also shown to mediate fatty acid transport and insulin sensitivity [49]. As a major angiogenic inducer, VEGFA has been widely investigated in previous studies. It is not only required during the initial EC development in angiogenesis but also plays a key role in EC survival in the healthy tissue [48]. The expression of VEGFA is dependent on its sensitivity to hypoxia and HIF is a potent regulator of VEGF levels [50]. In mice, VEGF overexpression is associated with greater number and size of vessels. It also contributes to improved insulin sensitivity and glucose tolerance, which suggests a protective role of VEGF-induced vascular growth in high fat diet-induced obesity and insulin resistance [51]. In humans, VEGF levels in AT were positively correlated with insulin sensitivity [52], while the failure to trigger VEGF-induced angiogenesis is an important cause of AT capillary rarefaction (low capillary density), hypoxia and inflammation in SAT [41]. However, the protective effect of VEGF-induced angiogenesis is still debatable. In rodents, VEGF protein secretion and gene expression were the highest in OAT compared to other depots [53]. Human adipocyte derived from OAT showed significantly higher VEGF mRNA expression, in contrast to SAT [37]. However, despite greater expression of VEGF, adipocytes in OAT still exhibited more inflammatory and hypoxic characteristics [37].

1.5.2.2 NRP-1

NRPs are transmembrane glycoproteins with multiple functions in neuronal and cardiovascular developments [54]. There are two known homologues of NRP, NRP-1 and NRP-2, which are both involved in tissue angiogenesis. During tissue growth, NRP-

1 is preferentially localized in the arteries while NRP-2 is more expressed in the veins [55]. NRPs are important receptors for VEGF ligands. NRP-1 especially is the co-receptor for VEGF receptor 1 and 2 [56]. In ECs, NRP-1 primarily interacts with VEGFR2, enhancing proliferation, survival, migration, and permeability (**Figure 4**) [57]. NRP-1 knockout mouse embryos displayed a series of vascular defects, suggesting the critical role of NRP-1 in mediating neovasculature formation [58]. Therefore, normal NRP-1 expression is essential for angiogenesis in addition to VEGF expression.

The role of NRP-1 in AT angiogenesis is unclear. In rat white AT, NRP-1 was found mainly in vascular smooth muscle cells (VSMCs) and ECs of arteries. Adipocytes also showed NRP-1 expression [59]. In human fatty bone marrow, higher NRP-1 expression was detected in adipocytes in contrast to hematopoietic and stromal cells [60]. These data suggest a possible NRP-1 involvement in AT angiogenesis.

1.5.2.3 Adipokines

The AT is increasingly being recognised as a crucial endocrine organ, associated with the synthesis and secretion of several hormone-like molecules, adipokines. Among them, the most prominent ones are leptin and adiponectin [12].

Leptin is an adipokine involved in the regulation of appetite and energy expenditure in the central nervous system (CNS). Peripherally, it also plays a role in inducing angiogenesis. In mice, leptin induced angiogenesis synergistically with VEGF, but failed to do so in *ob/ob* mice [61]. In humans, leptin showed angiogenic effects by binding to its functional EC receptors and stimulating the EC tube formation [62]. In response to AT hypoxia, both leptin mRNA expression and protein secretion were elevated, and the elevation was dependent on oxygen concentration [63].

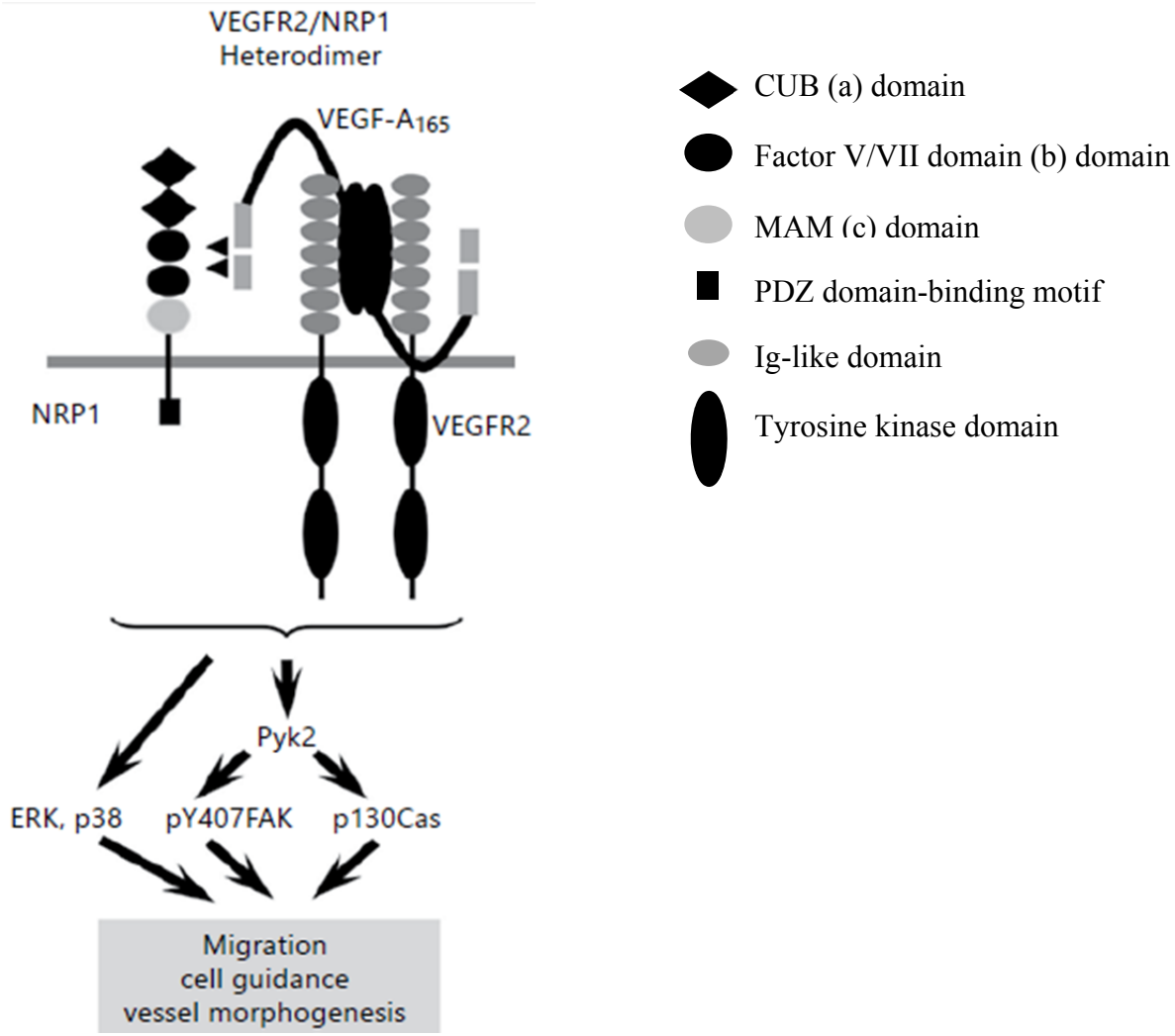

Figure 4 VEGF signalling via NRP-1 [57]

VEGF-A_{165} promotes complex formation by binding to NRP-1. Carboxy-terminal PDZ domain binding motif of NRP-1 associates with PDZ protein synectin, which is considered as an important factor mediating NRP-1 effect in VEGFA signalling pathway via VEGFR2. VEGFR2/NRP-1 complex formation is highly involved in signalling mediated by p38 kinase, ERKs1/2, and Pyk2 pathway, which lead to p130Cas tyrosine phosphorylation and consequently EC migration, guidance and vessel morphogenesis.

Adiponectin, as a protective anti-inflammatory adipokine, is also involved in AT angiogenesis. In lean healthy individuals, adiponectin is one of the most abundant proteins in the circulation. However, these levels are reduced significantly in obesity, perhaps due to the AT hypoxia [63, 64]. The angiogenic effect of adiponectin is still under investigation. In a mouse tumour model, adiponectin showed an anti-angiogenic effect by inducing endothelial cell apoptosis [65]. In human coronary arteries, adiponectin suppressed the VEGF-induced endothelial cell migration by increasing cellular cyclic adenosine monophosphate (cAMP) levels and protein kinase A (PKA) activity, thus protecting vessels from atherosclerosis [66]. However, adiponectin also exhibits pro-angiogenic effects in mouse mammary tumour growth [67]. Furthermore, in human umbilical veins adiponectin promoted EC migration and differentiation into capillary-like structures [68].

1.5.2.4 Depot-specific difference in angiogenesis

Very few studies have directly compared the angiogenic capacity of SAT and OAT. Also the data from the four currently reported studies all appear contradictory. One rodent study and one human study demonstrated greater angiogenesis in OAT by showing that there was higher VEGF mRNA expression and protein secretion from this depot [37, 53]. However, in another human study, SAT explants incubated in Matrigel showed more capillary sprouts compared to OAT even after normalization to the SAT initial capillary density [69]. Moreover, the later study demonstrated that there was no significant angiogenic difference between the two depots after normalizing the vessel number to the number of adipocytes [70].

However, the hypoxic and inflammatory environment in OAT cannot be explained by its normal or even higher angiogenic capacity. It is interesting to see that not only adipocytes but also ECs from OAT were more hypoxic and inflammatory [37], thus it is

doubtful whether the function of neovasculature formed by those inflammatory ECs is preserved.

1.5.3 AT vasoreactivity

1.5.3.1 AT microcirculation: definition and function

The microcirculation is defined as "*all those arterial vessels that respond to increasing pressure by a myogenic reduction in the lumen diameter*", which also include the capillaries and venules [71]. The major function of the microcirculation is to supply nutrients and oxygen for tissue growth and repair. In addition, it also plays an important role in stabilizing the hydrostatic pressure and determining the peripheral resistance [72]. The *in vivo* microvascular function in lean healthy individuals and obese patients has been examined in a few studies [73]. In the basal state and during physiological systemic hyperinsulinemia, obese patients displayed higher systolic blood pressure (SBP), impaired insulin sensitivity and capillary recruitment compared to lean individuals, Thus, the alteration of microvascular function in obesity may not only contribute to the increased peripheral resistance, but also affect glucose and insulin metabolism [73].

1.5.3.2 Regulation of vasoreactivity in AT

Ion channels, endothelium-derived vasoactive molecules, and neuronal transmitters regulate vasoreactivity. In addition, the microvasculature embedded in AT is also directly regulated by adipokines released from adipocyte, as well as the perivascular adipose tissue (PVAT) [74]. Thus alterations of AT cellular and hormonal components and vascular structure may be associated with the compromised vascular function in obese patients.

Potassium and calcium channels (K^+ and Ca^{2+} channels)

The interplay between K^+ and Ca^{2+} channel is an important determinant of vascular tone [75]. K^+ channels are critical regulators of VSMC membrane potential. The activation of K^+ channel increases the efflux of K^+, causing cell membrane hyperpolarisation, closure of Ca^{2+} channel, decrease of intracellular Ca^{2+} and vasodilatation. In contrast, the inhibition of K^+ channel causes cell membrane depolarisation, the voltage-activated Ca^{2+} channel opening, elevated intracellular Ca^{2+} concentration and vasoconstriction (**Figure 5**) [75]. Accumulative evidence suggests vascular K^+ channel alteration is involved in major cardiovascular diseases, such as hypertension and diabetes [75], which are highly prevalent in obese patients.

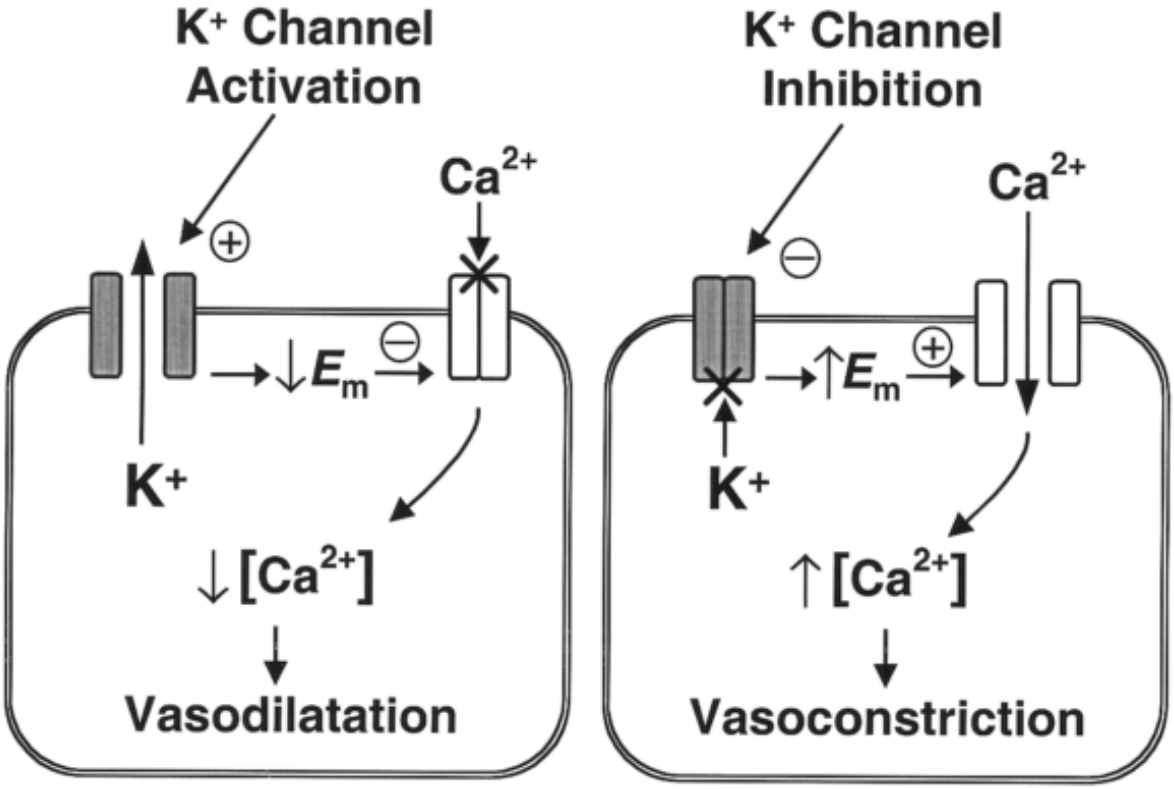

Figure 5 Vascular tone regulated by K^+ channel activation and inhibition [75]

Left: opening of a K^+ channel (grey) in the cell membrane causes an efflux of intracellular K^+ and cell membrane hyperpolarisation, which consequently inhibits voltage-activated Ca^{2+} channels (white) and decreases intracellular Ca^{2+} levels, resulting in vasodilatation.

Right: Reversely, closure of a K^+ channel decreases an efflux of intracellular K^+, leading to cell membrane depolarization and opening of Ca^{2+} channels. Influx of Ca^{2+} increases intracellular Ca^{2+} levels, resulting in vasoconstriction.

Endothelium

The endothelium is not only the monolayer covering the internal lumen of vessels, but also a key factor regulating vascular homeostasis [76]. In healthy ECs, a delicate balance between EC-derived vasodilators [nitric oxide (NO), prostacyclin (PGI_2) and endothelial-derived hyperpolarizing factor (EDHF)] and EC-derived vasoconstrictors [endothelin-1(ET-1), angiotensin II (Ang II) and thromboxane A_2 (TXA_2)] maintains the normal vasoreactivity and vascular permeability [77].

As the most important EC-derived vasodilator, NO is synthesized from L-Arginine catalysed by a family of NO synthases (NOS), NO mediates vasodilatation by activating guanylate cyclase to increase intracellular cyclic guanosine monophosphate (cGMP) levels. Because of the short half-life of NO, it cannot be synthesized and stored in advance, therefore, production of NO highly relies on the activity of endothelial NO synthase (eNOS) [77].

ET-1, as the counterpart of NO, plays an important role in regulating vasoconstriction. ET-1 induces vasoconstriction by binding its G-protein-coupled receptors (GPCR, ET_A and ET_B) on VSMCs and ECs. ET_A is involved in the recruitment of phospholipase C (PLC), which leads to the intracellular Ca^{2+} increase and vasoconstriction [78], while ET_B was also shown to be involved in pulmonary angiogenesis through modulating vascular monocyte adhesion [79].

Obesity is closely associated with endothelial dysfunction, which is characterized by the impaired endothelium-dependent vasodilatation [80]. Impaired vascular relaxation in AT may also compromise insulin-mediated capillary recruitment, therefore leading to insulin resistance [73].

Insulin

To maintain the homeostasis of microvascular system, insulin regulates both vasodilatation and vasoconstriction (**Figure 6**). Insulin mediates vasodilatation by activating eNOS via insulin receptor substrate-1 (IRS-1), phosphatidylinositol 3-kinase (PI3-kinase) and protein kinase B (Akt) pathway [81]. In contrast, insulin induces vasoconstriction by stimulating ET-1 production. ET-1-induced vasoconstriction is elevated following the infusion of insulin [82].

In the postprandial state, insulin mediates microvascular blood flow redistribution from non-nutritive to nutritive vessels, thus enhancing insulin and substrates supply to insulin sensitive organ (capillary recruitment) [83]. In healthy individuals, there is a subtle balance between insulin-mediated vasoconstriction and vasodilatation, so the net effect on vascular tone is negligible [77]. However, obesity-related vascular dysfunction is associated with an alteration of this balance with upregulation of ET-1 and impaired NO bioavailability and bioactivity [84].

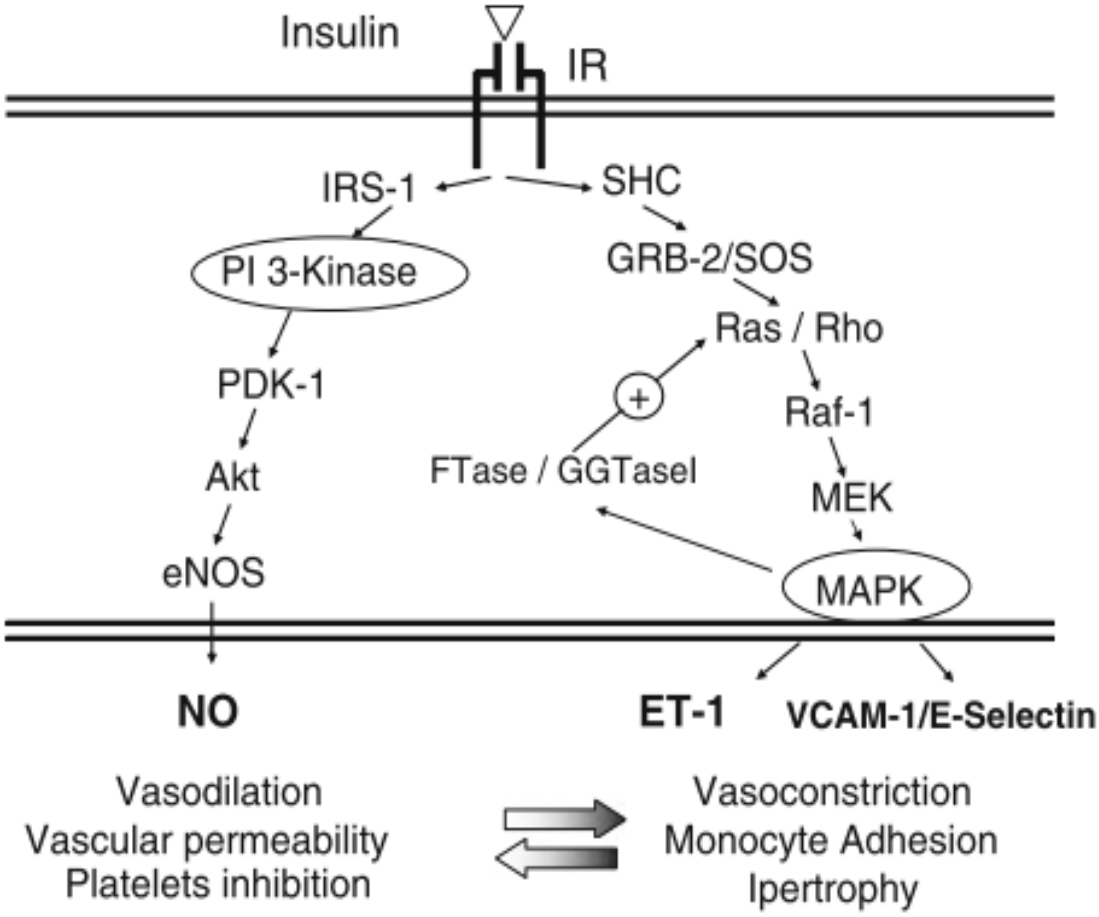

Figure 6 Pathways involved in the insulin-induced vascular tone [77]

Left: insulin binds and activates insulin receptor, consequently activating insulin receptor substrate-1. Downstream from that, PI3-kinase phosphorylates PDK-1 and Akt, leading to eNOS phosphorylation and NO production.

Right: insulin also regulates synthesis and secretion of ET-1 via mitogen-activated protein kinase (MAPK) branch. Signalling includes tyrosine phosphorylated SHC binding to SH2 domain of growth factor receptor-bound protein 2 (GRB2), activation of the pre-associated guanine nucleotide exchange factor (SOS), removal of GDP from Ras and initiation of a kinase phosphorylation cascade including Raf-1, MAPK/extracellular signal-regulated kinases (MEK), and MAPK.

Adipokines

AT is an important endocrine organ associated with the production of pro-and anti-inflammatory adipokines. These adipokines not only regulate AT metabolism and functions, but also are involved in the regulation of vascular tone [12, 85].

Leptin is a crucial adipokine, which regulates appetite and energy metabolism. It also shows vasoactive effects mediating both vasodilatation and vasoconstriction [86, 87]. Leptin at physiological concentrations mediates vasodilatation through AMP-activated Akt signalling pathway, leading to eNOS activation via Ser1177 phosphorylation [88]. However, elevated leptin levels have been shown in obesity [89], and hyperleptinemia is considered as a key factor contributing to the vascular tone dysregulation and hypertension. Centrally, the vasocontractile effect of leptin is through activation of the sympathetic nervous system [90]. Peripherally, leptin increased both ET-1 secretion and ET_A expression, which are tightly associated with EC dysfunction, NO depletion and reactive oxygen species (ROS) elevation [91, 92]. Furthermore, leptin stimulates the secretion of pro-inflammatory adipokines from macrophages, which may further increase vasoconstriction and blood pressure [93].

Adiponectin is a cardioprotective adipokine [94]. The vasodilatory effect of adiponectin has been shown both *in vivo* and *in vitro*. In rats, adiponectin is involved in both NO- and K^+ channel-mediated vasodilatation [95, 96]. In humans, adiponectin activates eNOS and increases NO production by binding to adiponectin type 2 receptor or T-cadherin on EC surface [74] , and adiponectin levels in circulation positively correlated with endothelium-dependent vasodilatation [97].

Both IL-6 mRNA expression and protein levels are elevated in AT of obese patients [98]. The vasoactive effect of IL-6 is time dependent. Acute exposure to IL-6 *in vitro* leads to the aorta relaxation by elevating the production of prostacyclin in VSMCs [99],

while the long-term chronic increase of plasma IL-6 impaired endothelial function by stimulating Ang II-mediated ROS synthesis and reducing eNOS gene expression [100]. TNF-α is associated with chronic inflammation in obesity. Macrophage infiltration into the AT in obesity leads to elevated TNF-α mRNA expression, observed both in rodents and human [89]. It has been reported that TNF-α mediates endothelium-dependent relaxation in cerebral arterioles by elevating iNOS expression [101], it is also involved in the regulation of endothelium-independent vasodilatation via phospholipase A_2 activation and ceramide generation.

PVAT

PVAT is defined as a layer of AT surrounding almost all blood vessels (except cerebral vessels), which is comprised of adipocytes, SVF, macrophages and neuronal networks (**Figure 7**) [102]. There is no anatomic facia to separate this fat depot from vascular adventitia, which facilitates the direct access of the factors secreted from PVAT into the vascular system [103]. Recent data suggest that PVAT shows an anti-contractile effect in both rodent and human vessels. Several studies have demonstrated that PVAT secreted soluble relaxing factors leading to K^+ channel-mediated vasodilatation [104, 105]. The identity of adipocyte-derived relaxing factor (ADRF) is still under investigation. Adipokines including adiponectin and Ang 1-7 have been considered as potential candidates of ADRF because of their vasodilatory effect [96, 104]. In human arterioles, adiponectin mediates vascular relaxation by improving NO bioavailability, while blockade of adiponectin binding to its type 1 receptor completely abolished the anti-contractile effect of PVAT [74]. Ang 1-7 induced vasodilatation via the endothelium-dependent pathway stimulating NO release, as well as endothelium-independent pathway involving H_2O_2-mediated activation of soluble guanylate cyclase [106].

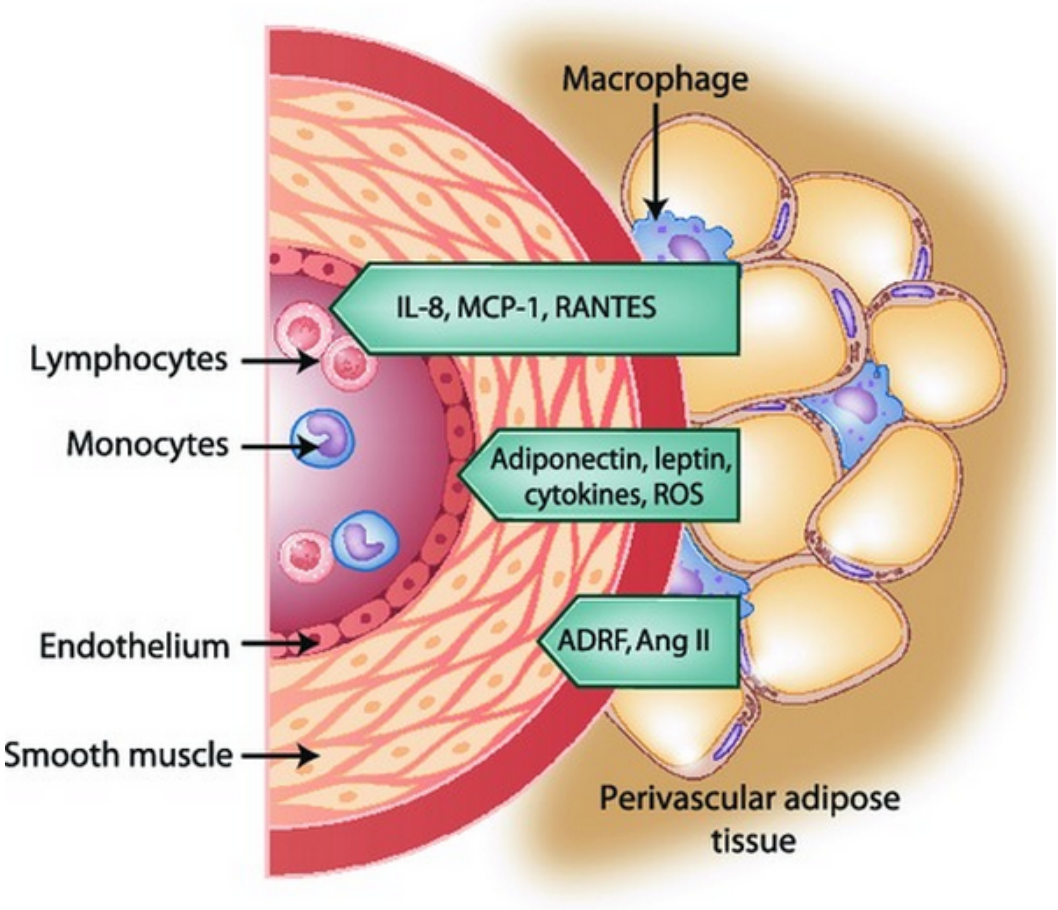

Figure 7 Interaction between PVAT and vasculature [102]

PVAT interacts with vascular endothelium, smooth muscle, and immune cells and the mediators are involved.

ADRF adipocyte-derived relaxing factor; Ang II angiotensin II; IL-8 interleukin-8; MCP-1 monocyte chemoattractant protein 1; ROS reactive oxygen species

Like other AT depots PVAT also expands during the development of obesity and becomes more inflammatory [107]. Significant macrophage infiltration has been observed in PVAT of obese animals accompanied by the decrease of anti-inflammatory adipokines, such as adiponectin [102]. Evidence suggests that local inflammation abolished anti-contractile properties of PVAT in obese patients [74] and the altered paracrine effect of PVAT may be an important risk factor associated with vascular dysfunction and insulin resistance [108].

Prostanoids

Prostanoids are synthesized from the substrate arachidonic acid catalysed by cyclooxygenase 1 and 2 (COX-1/COX-2). The endothelium-derived prostanoids include vasoconstrictors (TXA_2) and vasodilators [prostaglandin E2 (PGE_2) and prostacyclin (PGI_2)]. Rat and human adipocytes are also capable of synthesizing prostanoids, which suggest that prostanoids may play a role in regulation of the vasculature in AT [109]. Increased production of TXA_2 was found in the aorta and carotid arteries of obese mice [110]. This response was fully blocked by non-selective COX inhibitors but not COX-2 selective inhibitors, which suggests that COX-1-dependent vasoconstrictor synthesis may contribute to the enhanced vasoconstriction in obesity [110, 111]. Also evidence suggests that obesity-linked hyperinsulinemia may inhibit the stimulatory effect of adrenergic agonists on the synthesis of PGE_2 and PGI_2, thus contributing to the increased peripheral resistance and hypertension in obesity [112].

Neuronal transmitters

Noradrenaline (NA) is a classic neuronal molecule synthesized and released from sympathetic neurons and peripheral tissues. A series of enzymes are involved in NA synthesis, the most important ones are tyrosine hydroxylase (TH, catalysing the first

step of the reactions), L-aromatic amino acid decarboxylase and dopamine-ß-hydroxylase (DBH).

In obese individuals, the adrenergic effect on AT metabolism mainly includes the stimulation of lipolysis and glucose uptake [113]. Additionally, ß-adrenergic agonists induced IL-6 and inhibited leptin release from AT both *in vitro* and *in vivo* [114]. However, the adrenergic regulation on AT microvasculature is less clear. The effect of NA on vascular tone is achieved by binding to its functional adrenoceptors α and ß. Stimulation of α1-adrenoceptors activates the PLC and inositol 1, 4, 5-trisphosphate (IP3) pathway, causing Ca^{2+} mobilization from organelles into cytoplasm and VSMC contraction. In contrast, stimulation of ß-adrenoceptors increases intracellular cAMP by activating adenylate cyclase (AC), leading to the activation of PKA, elevation of K^{+} influx and vasodilatation [115].

Obese patients have increased sympathetic activity. Compared with lean healthy individuals, obese patients showed higher renal NA spillover [116]. Greater systemic NA levels were observed in hypertensive obese patients compared to normotensive patients, which implicated a pathological role of NA elevation in obesity-associated hypertension [117]. Recent data points to AT as a new source of NA. Both NA and NA synthetic enzymes were found in rodent adipocytes [118]. Microvasculature embedded in the AT may be directly regulated by NA released from adipocytes, but the adrenergic effect on microvascular tone within AT between different depots is still to be investigated.

Neuropeptide Y (NPY) is a 36-amino acid peptide derived from the brain and sympathetic nerves [119]. In the central nervous system, it participates in the regulation of energy homeostasis by increasing food intake and decreasing physical activity [120]. Peripherally, NPY is stored and released along with NA from sympathetic nerve terminals [121]. Both human and animal studies confirmed the cooperation between

NPY and NA in the regulation of vascular tone [122]. NPY potentiated NA-induced vasoconstriction particularly via sensitizing α1 adrenergic vasoconstriction [123]. Elevated activities of NPY and its receptors have been observed in experimental obesity [124]. However, its effect on the AT vascular tone is not known.

Collagen deposition

The AT expansion in obesity is accompanied by considerable tissue remodelling, which is characterized by increased macrophage infiltration, tissue fibrosis and increased extracellular matrix (ECM) components [125]. The accumulation of ECM in AT may be a consequence of chronic inflammation and hypoxia. ECM synthesis was enhanced in adipocyte precursors after treatment with conditioned media with secretions from macrophages [126], while inhibition of HIF-1α expression significantly prevented AT fibrotic response [127].

Elevated ECM protein and gene expression have been observed in AT in obesity [128]. Particularly, collagen type VI is elevated in SAT and associated with insulin resistance [129, 130]. Fibrosis may also affect the vasculature in AT. Abundant collagen staining was seen around vessels in OAT, and collagen gene expression was elevated in SVF compared to adipocytes [128]. These data implicate the deposition of collagen in AT as altering vascular structure and function. Collagen type I and type III are predominant in cross-banded fibrils of vessel wall, which provide tensile strength [131]. In obese patients, both of them were increased in AT [128]. Increased collagen deposition in the vascular wall directly causes vascular fibrosis and arterial stiffening and contributes to atherosclerosis and hypertension [132].

Data from rodents suggest NA may be a potent regulator of ECM in liver and lung [133, 134]. NA induced hepatic fibrosis in mice by modulating the leptin action, while 72 hrs of NA infusion significantly induced pulmonary fibrosis and vascular hypertrophy

detected in lung histology [134]. However, whether NA shows similar fibrotic effects in AT and AT vasculature is unknown.

1.5.3.3 Depot- and diabetes- specific differences in vasoreactivity

In previous studies, structure and function of large- and medium-size vessels have been widely investigated in obese patients. The pathological alterations include increased vascular stiffness [135], decreased compliance and distensability [136], and endothelial dysfunction [137]. However, the microvasculature in AT is less well studied. One study compared microvascular structure and function in obese patients with healthy lean individuals using arterioles from SAT. Increased media thickness, vessel stiffness and impaired endothelium-dependent vasodilatation were found in the obese compared with lean group [138].

OAT, compared with SAT, is more associated with increased risks of metabolic and cardiovascular diseases in obesity [17, 139], the direct comparison between SAT and OAT in obesity is helpful to understand the intrinsic depot difference and to what extent these two depots contribute to obesity-related complications. Two studies have been reported, mainly focused on the endothelium-dependent vasodilatation [140, 141]. Both studies suggest the vasodilatory impairment in OAT caused by the endothelial dysfunction. In addition, even SAT NO-mediated vasodilatation was compromised in obese patients with Type II diabetes [141].

However, vasoconstriction, as a counterpart of vasodilatation, is also involved in AT metabolism and remodelling [142]. Very few studies that compare the depot difference in AT microvascular contractile function have been reported. Only one study investigated the NA-mediated vasoconstriction in SAT, and concluded that NA-mediated vasoconstriction in SAT was enhanced in obese patients with and without Type II diabetes compared to the lean controls [141].

1.6 Aims of the thesis

The aims of this thesis were to investigate in:

Study 1: the depot- and diabetes-specific differences of noradrenaline (NA) synthesis, NA-mediated vasoconstriction and tissue fibrosis in abdominal SAT and OAT of morbidly obese patients.

Study 2: the depot- and diabetes-specific differences of capillary density, angiogenic capacity and angiogenesis-related mRNA and protein expression.

Study 3: the adipokine production of PVAT of the saphenous vein (SV) and internal thoracic artery (ITA).

Chapter 2

Methods and Materials

2.1 Study population

2.1.1 Patient recruitment

Morbidly obese patients undergoing laparoscopic bariatric surgery (gastric bypass, gastric sleeve, or gastric band) were recruited from the pre-operative clinic (North London Obesity Surgery Service, Whittington Hospital, London, UK). Morbid obesity was define as BMI $\geq$ 40 $kg.m^{-2}$ or BMI $\geq$ 35 $kg.m^{-2}$ with significant co-morbidities [143]. Patients with coronary artery disease, uncontrolled hypertension, malignancy or terminal illness, connective tissue disease or other inflammatory conditions likely to affect cytokine levels, immuno-compromised subjects and those with substance abuse or other causes for poor compliance were excluded. The study was approved by the National Ethics Committees and written informed consent was obtained from all participants.

2.1.2 Demographic and anthropometric data

Weight (kg) and height (m) were measured in pre-clinic assessment and BMI was calculated. Blood pressure and pulse were measured using digital monitor (Datex-Ohmeda Patients Monitor, GE Healthcare, UK). Patient information including demographic data (date of birth, gender, ethnicity), surgery type (gastric bypass, gastric band, gastric sleeve), co-morbidities, current medication, weight loss history, smoking habits and alcohol consumption were recorded from hospital notes.

2.1.3 Blood and AT sample collection

Blood samples, following an overnight fast, were drawn from an ante-cubital vein on the day of the operation immediately after anaesthesia. After centrifugation (3000 rpm, 15 minutes, 25^{o}C), the plasma or serum was collected and stored at -80 ^{o}C until analysis.

AT from the abdominal subcutaneous and intra-abdominal greater omental depots was obtained during the surgery (~5g each) and quickly transported in serum-free medium (Cellgro, Mediatech Manassas, VA) to the laboratory.

2.2 Adipokine study

2.2.1 AT organ and EC culture

0.05 g AT from each depot was dissected and incubated in 500 µl Cellgro serum-free media (Mediatech Manassas, VA) with 5% penicillin-streptomycin overnight (37 ^{o}C, 95% O_2 / 5% CO_2). Following incubation the medium was collected and stored at -80^{o}C until later assessment of adipokines secretion.

HUVECs and HCAECs, obtained from TCS Cell Works (Buckingham, UK), were cultured in endothelial basal medium (EBM; Lonza, Nottingham, UK) supplemented with gentamycin-ampicillin, epidermal growth factor and bovine brain extract (Singlequots; Lonza) and 10% (v/v) foetal bovine serum (FBS) (complete EBM). Cells were harvested when they reached 80-90% confluence, and then stored in -80^{o}C for subsequent total RNA extraction.

2.2.2 Insulin and adipokine ELISAs

Serum insulin level was measured by specific insulin ELISA (Mercodia, Sweeden). Insulin sensitivity was determined by the Homeostasis Model Assessment Index-Insulin Resistance (HOMA-IR). HOMA-IR was calculated from the fasting glucose (mmol/l) and insulin levels (mU/L) using the equation HOMA-IR=(insulin *glucose)/22.5 [144].

Adipokine levels in serum and tissue culture supernatant including total adiponectin, leptin and MCP-1 were measured by commercially available two-site ELISAs (R&D Systems, UK). Briefly, standards and samples were pipetted into the 96 wells of microplates pre-coated with antibody against the target protein. After incubation, target

protein was bound to the antibody pre-coated on the bottom of the well. The unbound substance was then washed away, followed by adding a detecting enzyme-linked antibody specific for the target protein. After washing, to remove the unbound antibody-enzyme reagent, the substrate was added and colour development in proportion to the amount of target protein bound was observed. Colour development was stopped at set times as per manufacturer's instructions and the intensity of the colour measured by the microplate reader (Opsys MR, Dynex, UK), as absorbance at 450 nm, with correction at 540 nm.

2.3 Histochemistry and immunohistochemistry

2.3.1 Estimation of adipocyte number, size and capillary density

0.3 g tissue from each depot was fixed in 10% formalin for 24 hours at room temperature and then transferred to 50% ethanol at +4 ^{o}C prior to being embedded in paraffin. 3 μm sections were deparaffinised and dehydrated in Xylene (Sigma-Aldrich, UK) for 20 min, followed by 100, 90, 80, 70, and 60% ethanol. The sections were incubated for 30 minutes in a dark moist container with the staining solution containing lectin fluorescein isothiocyanate (FITC) conjugate (from Griffonia simplicifolia [GS], 25 μg/ml, Sigma-Aldrich), lectin tetramethylrhodamine isothiocyanate conjugate (from Ulex europaeus [UEA], 10 μg/ml, Sigma-Aldrich), and 4',6-diamidino-2-phenylindole, dihydrochloride (DAPI, 0.3 μg/ml, Sigma-Aldrich). The GS lectin stains the plasmalemma, UEA stains the capillaries [145], and DAPI stains nuclei [146]. Sections were rinsed with 0.1M sodium phosphate buffer (PBS, pH 7.4) for 40 min and then mounted on glass slides with water-soluble mounting medium (Cardinal Health, Dublin). Images of the stained sections were captured with a Zeiss Axioplan 2 upright microscope (Intelligent Imaging Innovations, Denver, USA) using a Photometrics CoolSnap HQ CCD camera and a Sutter Lambda LS 175W Xenon arc lamp.

Images were then analyzed by ImageJ software (National Institutes of Health, USA). Adipocyte number per section was counted by numbering all the adipocytes on the picture (**Figure 8A**). Damaged or incompletely displayed adipocytes were excluded. Adipocyte size was measured by tracing the pixel area (**Figure 8B**). For tracing the pixel area, "Free Hand" function was selected in ImageJ and the border of each adipocyte was traced manually. Capillaries shown as orange spots or lines were also counted and expressed as capillary number per section (**Figure 8C**).

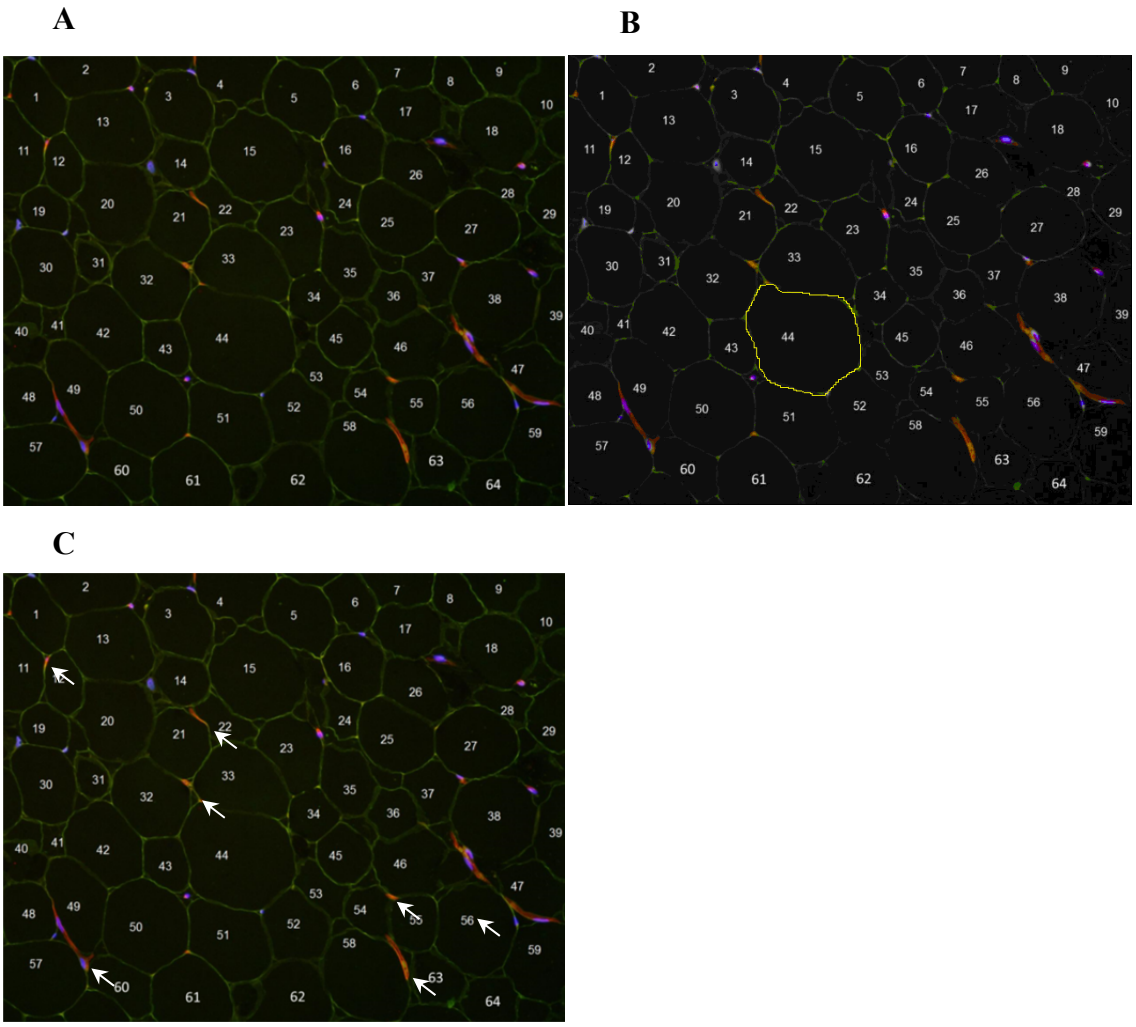

Figure 8 Calculation of adipocyte number (A), area (B) and capillary number (C)

A: All adipocytes on each section were counted and numbered.

B: Area of each adipocyte was measured by tracing the border manually.

C: Capillaries were labelled by UEA staining, and then counted manually.

2.3.2 Macrophage staining

Slides were washed in Tris buffered saline for 2 min and blocked at room temperature for 5 minutes in DAKO peroxidase blocking solution and 10% horse serum. CD68 affinity purified rabbit anti-human polyclonal antibody (Sigma-Aldrich, UK), as a macrophage marker, was added and incubated for 60 minutes at room temperature and secondary antibody (1:1000 dilution of anti-rabbit IgG peroxidase conjugated antibody, Sigma-Aldrich, UK) for 45 minutes. Detection was by standard Avidin Biotin Complex (ABC)/DAB method.

2.3.3 Estimation of endothelial markers and catecholamine synthetic enzyme

AT sections were immunostained for EC markers, CD31 and CD34, as well as for TH (marker of catecholaminergic fibres). Slices were washed in 0.1M PBS for 30 minutes and permeabilized and blocked with 0.1% Triton in 10% FBS for 60 minutes. Tissue was then incubated overnight at 4^{o}C in anti-CD34 antibody, or anti-CD31 antibody or sheep anti-TH antisera (1:250, Abcam, UK). Sections were washed and subsequently incubated in 488 Alexa Fluor rabbit anti-sheep (1:1000) for 1 hour. Slices were cover-slipped with Vectashield HardSet mounting medium (Vector Laboratories, USA) with DAPI. Images were captured and analysed using ImageJ software. TH stained area was selected using threshold function to filter the DAPI staining (**Figure 9A&B**), and then images were transformed into 8 bit (**Figure 9C**). TH-immunoreactive fibre density was estimated by measuring grey density of TH stained areas with the gel analysis function, the grey density was shown as the area under the curve (**Figure 9D**) and calculated by "Wand tool" function. The data was expressed as number of bits per section.

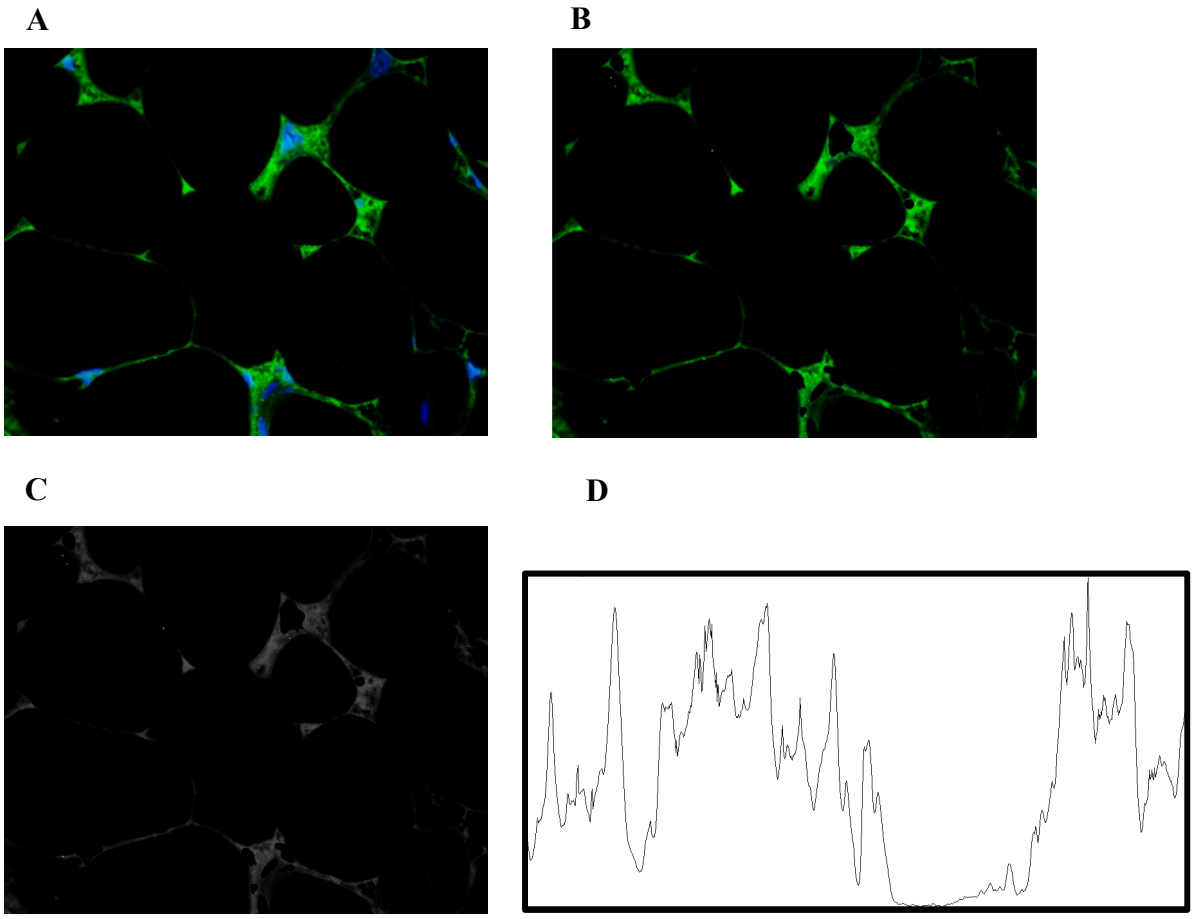

Figure 9 Analysis of TH immunoreactive fibre densities

A: TH was immunostained by TH antibody shown as green and nucleus was stained by DAPI shown as blue.

B: Nucleus staining area was filtered by Image J "threshold" function.

C: Image was transformed into 8-bit format.

D: The grey density of TH staining area was measured by gel analysis function shown as the area under the curve.

2.3.4 Estimation of collagen deposition

Sections were deparaffinized and hydrated to distilled water, followed by incubating in Verhoeff's hematoxylin for 30 minutes. After washing, sections were differentiated in 2% ferric chloride solution for elastic fibre staining. Then slides were rinsed and iodine was removed. Finally sections were counterstained in Van Gieson's for 5 minutes and then dehydrated and coverslipped. For collagen deposition analysis, as elastic fibre staining (black) was filtered using ImageJ threshold function (**Figure 10A&B**) and the collagen staining area (pink) was transformed into 8 bit format (**Figure 10C**), the staining area was calculated using "Analyse Particles" function . The data was expressed as the pixel area of the collage deposition.

2.3.5 Adiponectin and leptin derived from PVAT

For immunohistochemical identification of leptin and adiponectin, frozen transverse sections of vessels with intact PVAT were prepared as previously described [147]. Solvent that would dissolve the fat was avoided. 15 μm transverse sections were thaw-mounted, post-fixed for 10 min in 4% formal saline and stored at -80^{o}C until use. Standard immunohistochemistry was performed using the Vectastain ABC-AP kit (Vector Labs, Burlingame, CA, USA). Leptin was identified using a polyclonal anti-rabbit antibody (Santa Cruz Biotechnology Inc, Santa Cruz, CA, USA) and adiponectin using a polyclonal anti-rabbit antibody, (Aviva Systems Biology, UK), at dilutions 1:25 to 1:100 in PBS and processed following the manufacturer's instructions. Negative controls were prepared in the absence of primary antibody. In some cases CD31 (1:100 in PBS; DAKO labs, Glostrup, Denmark) immunostaining of paraffin sections was performed for the identification of ECs. Vector red substrate was used to develop the colour, sections were counterstained with haematoxylin, viewed under an Olympus BX 50 microscope and representative photographs taken.

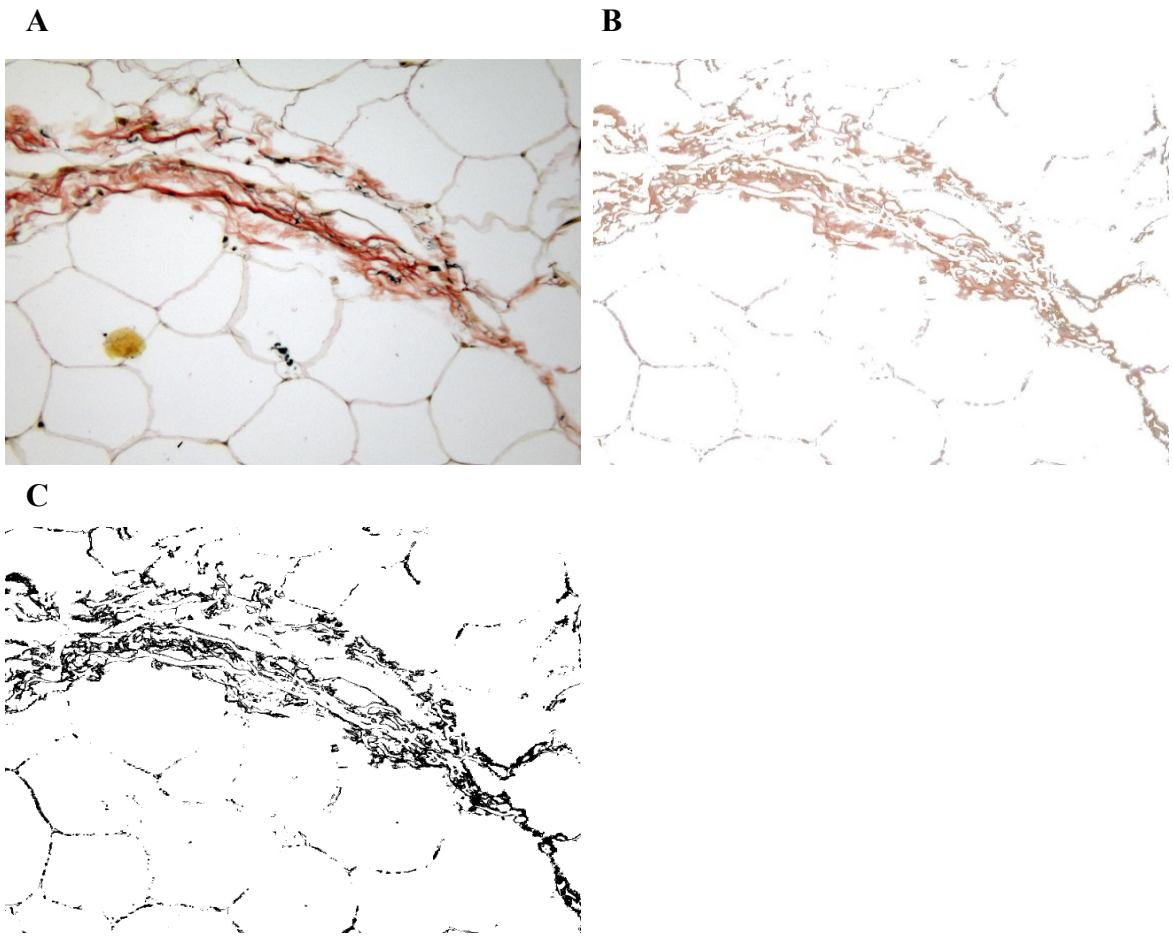

Figure 10 Analysis of AT collagen deposition

A: Collagen deposition in AT was stained by EVG staining, collagen was shown as pink and elastin was shown as black.

B: Elastin staining area was filtered by Image J "threshold" function and collagen staining area was isolated.

C: Collagen staining area was transformed into 8-bit format for further particle measurements.

2.4 AT gene expression

2.4.1 Whole tissue and cell RNA extraction

~0.15 g AT was ground in liquid nitrogen using a pestle and mortar. Tissue powder or cells were collected and homogenized in TRIzol reagent (Invitrogen, Life Technologies, UK). Then chloroform was added and mixed thoroughly (0.2 ml chloroform per 1ml TRIzol). After centrifugation (3200 rpm, 15 minutes, 4 ^{o}C), the mixture was separated into a lower red phenol-chloroform phase, an interphase, and a colourless upper aqueous phase, the upper phase containing total RNA was transported into a new eppendorf. Equal volume of 100% isopropanol was added and mixed gently. The sample was then incubated at -20^{o}C for 1.5 hour. After another round of centrifugation (3200 rpm, 15 minutes, 4^{o}C), the RNA pellet was formed on the bottom of the eppendorf. The pellet was washed twice in 75% ethanol [ethanol for molecule biology (Sigma-Aldrich, UK); nuclease-free water (Invitrogen, Life Technologies, UK)] and dissolved in 40 µl nuclease-free water [148].

The purity and yield of total RNA were determined spectrophotometrically (NanoDrop-1000 Spectrophotometer, Thermo Scientific, USA). The concentration of RNA was measured as absorbance at 260 nm. The purity was determined by the ratios between 260 nm and 280 nm (260/280) and between 260 nm and 230 nm (260/230). 260/280 and 260/230 ratios within 1.7-2.0 were accepted purity for RNA.

2.4.2 cDNA synthesis

For first strand cDNA synthesis 500 ng of total RNA was added into reverse transcription reaction mixture containing MultiScribe Reverse Transcriptase (1.25 Unit/µl), dNTP (ATP, CTP, GTP, UTP, 500 µM each), Oligod(T)$_{16}$ (which ensures the transcription of only mRNA but not rRNA or tRNA, 2.5 µM), RNase inhibitor (0.4

Unit/µl), $MgCl_2$ (5.5 mM) and reaction buffer (Taqman Reverse Transcription Reagents, Roche, New Jersey, USA). The sample was then incubated in the thermal cycler (Genius, Techne, UK) for 60 minutes at 42°C, 15 minutes at 72 °C and holding at 4°C. After the incubation, cDNA was stored at -20 °C until use.

2.4.3 Real-Time Polymerase Chain Reaction (Real-Time PCR)

Target gene transcription was measure by Taqman Real-Time PCR. Primers of β-actin (housekeeping gene), collagens type 1α1, NRP-1, adiponectin and leptin were purchased from Qiagen Company, UK. Reaction was carried out in triplicate in 284-well microtitre plates using 5 µl total volume per well from 25 µl mixture [12.5 µl SYBR-green solution, 2.5 µl primer, 10 µl cDNA (25 ng) with nuclease-free water]. PCR cycle was 50 °C for 2 minutes, 95 °C for 15 minutes, followed by 40 cycles of 94 °C for 15 seconds, 56 °C for 30 seconds and 76°C for 30 seconds in ABI Prism 7900HT Sequence Detection System (Applied Biosystems, UK).

Cycle threshold value (the number of cycles required for the fluorescent signal to cross the threshold, Ct value) was used to quantify the gene expression. Data was expressed as the Ct ratio of β-actin / target gene.

2.5 AT protein expression

2.5.1 Protein extraction and quantification

Protein lysate was prepared by using ~150 mg AT homogenized in 500 µl RIPA buffer (Sigma-Aldrich, UK). The total protein concentration was estimated using bicinchoninic acid (BCA) protein Assay (Novagen, EMD Chemicals, CA, USA). Briefly, the standard curve was built by using diluted bovine serum albumin as the standard (Sigma-Aldrich, UK, concentration: 0, 25, 125, 250, 500, and 1000 µg/ml). 25µl standards and samples were loaded into a 96-well plate followed by 200µl BCA working reagent (1 portion of

4% Cupric Sulfate plus 50 portions of BCA solution). The plate was incubated at 37 ^{o}C for 30 minutes. Cu^{2+} was reduced to Cu^{1+} by protein in alkaline solution and then reacted with BCA producing a purple colour with absorbance at 562 nm [149] in proportion to the protein concentration.

2.5.2 Western blot

2.5.2.1 Sample preparation and electrophresis

Sample was prepared by mixing AT protein extracts with NuPAGE LDS Sample Buffer and NuPAGE Sample Reducing Agent (Invitrogen, UK). Each 10µl sample mixture contained 5 mg total protein, 2.5 µl LDS Sample Buffer and 1 µl Sample Reducing Agent. Then sample mixture was heated at 70^{o}C for 3 minutes to denature the protein and break protein complexes.

10µl samples and protein ladder (Spectra Multicolor Broad Range Protein Ladder, Thermo Science, UK) were loaded into the pre-cast polyacrylamide gels (NuPAGE, Novex 4-12% Bis-Tris Gels, 1.0 mm, 15 well, Invitrogen, UK). Gel was run at 200 Volt in a running buffer (NuPAGE MOPS SDS Running Buffer, Invitrogen, UK, 20x diluted in distilled water to 1x,) until the bromophenol blue dye front has reached the bottom.

2.5.2.2 Transfer

The gel was removed from the cassette and placed in the transfer buffer (NuPAGE Transfer Buffer, Invitrogen, UK, 50 ml 20x stock diluted with 850 ml distilled water and 100 ml methanol) to equilibrate. Two filter papers (from PVDF/Filter Paper Sandwich, 0.45 µm pore size, 8.5 cm x 13.5 cm, Invitrogen, UK) were placed in transfer buffer and the PVDF membrane soaked in methanol. When saturated, it was rinsed in water and then soaked in the transfer buffer. Six sponges were saturated with transfer buffer for later use. The transfer "sandwich" was assembled by three sponges, first filter

paper, gel, PDVF membrane, second filter paper and the other three sponges. The electrophoretic gel transfer was carried out in the transfer blotting module (XCell II Blot Module, Invitrogen, UK) at a constant voltage of 35 Volt for 1.5 hour. The membrane was subsequently blocked in 20 ml blocking solution (5% marvel non-fat milk in PBS with 0.1% Tween 20) for 1 hour at room temperature.

2.5.2.3 Antibody incubations and chemiluminescence

The membrane containing the transferred proteins was incubated in 5 ml of primary antibody (diluted in blocking solution, 1:1000 dilution) at 4^{o}C overnight, followed by washing and secondary antibody incubation (horseradish peroxidase conjugated, 1:10000 dilution) at room temperature for 1 hour. Following further washes, the membrane was incubated with Amersham ECL western blotting detection reagent (75μl reagent A plus 3ml reagent B, GE Healthcare, UK), which generates a chemifluorescence signal. The membrane was then exposed to an autoradiography film (Amersham Hyperfilm ECL, GE Healthcare, UK) for variable periods depending on results. The grey density of the blots was analysed by ImageJ gel function and data was expressed as the grey density ratio of target protein / β-actin.

2.6 Determination of vascular reactivity

2.6.1 Vascular tissue distinction and dissection

The first step of vessel preparation was to distinguish artery from vein. There were 3 major differences between artery and vein in human AT: (1). the branch of the artery is seen as “V shaped: while the branch of the vein was “U-shaped”; (2) the lumen size of artery is apparently smaller compared to the vein; (3) the blood flow was faster in artery versus vein (**Figure 11**). For ensuring the vessel luminal diameter within the range of 200-400 μm, normally the second to third branch of artery was dissected. After

carefully dissecting the surrounding AT, arterioles were isolated under a dissecting microscope and cut into segments (~2 mm long).

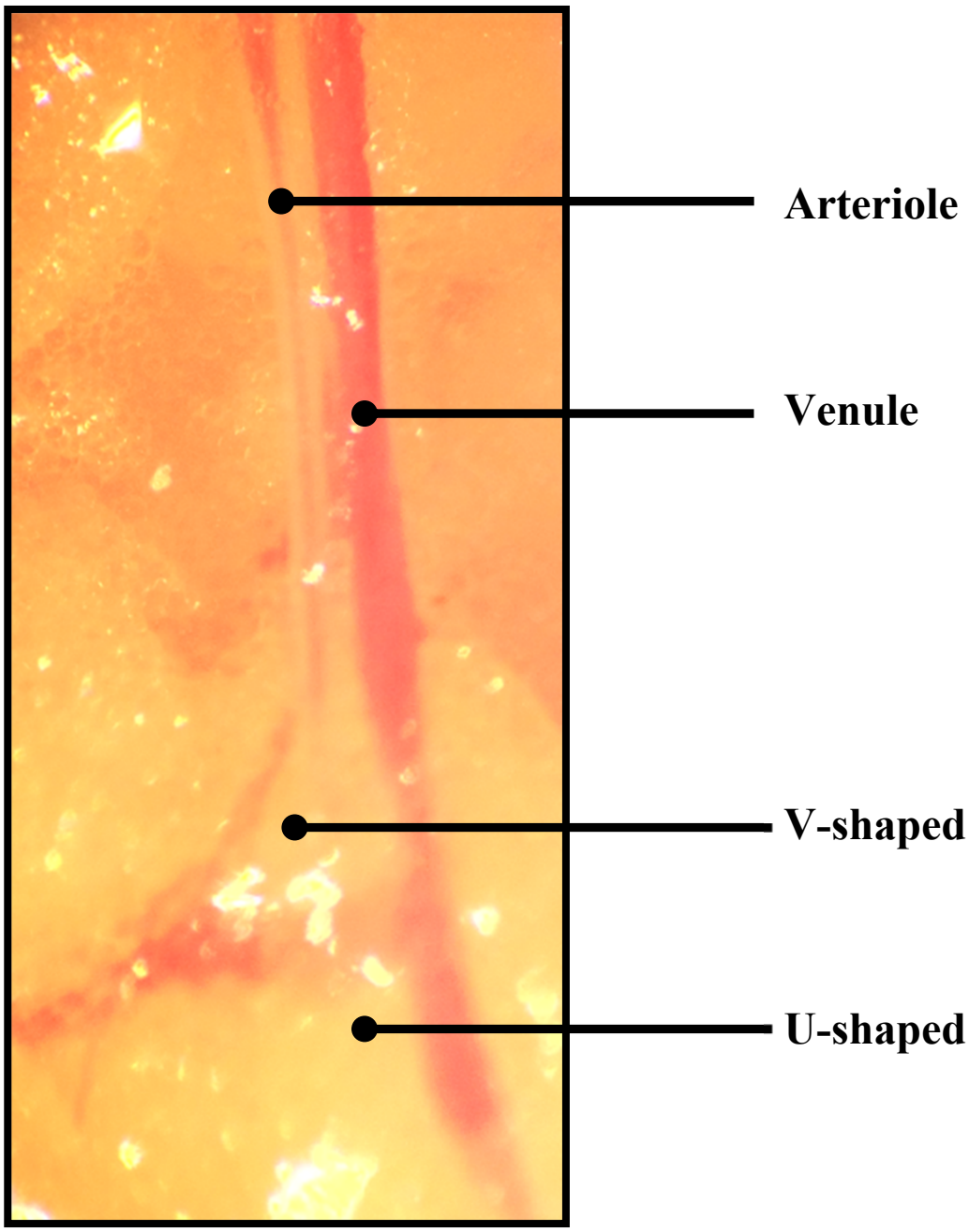

Figure 11 The major differences between artery and vein

The Lumen of arteriole is smaller with a “V-shaped” branch while venule has larger lumen size with a “U-shape” branch.

2.6.2 Vessel mounting

They were then mounted on wires (40 μm diameter) in an auto dual wire myograph system (510 A; JP Trading, Aarhus, Denmark) containing normal physiological salt solution (NPSS). The NPSS contained (in mM) 112 NaCl, 5 KCl, 1.8 $CaCl_2$, 1 $MgCl_2$, 25 $NaHCO_3$, 0.5 KH_2PO_3, 0.5 NaH_2PO_3, and 10 glucose (gassed with 95% O2/5% CO2 to pH 7.4). During the mounting procedure, further dissection was carried out to clean the connective tissue surrounding the vessels which may restrict the vessel relaxation. **Figure 12** showed how the arteriole was mounted onto the wire attached on jaws. Firstly, the luminal entrance of the vessel was opened by gently squeezing the vessel wall, normally lumen was opened by the blood spilling out, the first wire was then threaded through the whole segment, the arteriole performed as its own guide being pulled along the wire and fixed on the wire between the two jaws (**Figure 12A&B**). After that, the second wire was threaded through the artery very slowly and carefully avoiding any scratching on the inner layer of the vessel, this ensured the intactness of endothelium (**Figure 12C**). Finally, the second wire was attached onto the right jaw (force transducer). In preparation for the next step of normalization, the two wires were then slightly separated to make them just barely touching each other to finish the mounting procedure (**Figure 12D**).

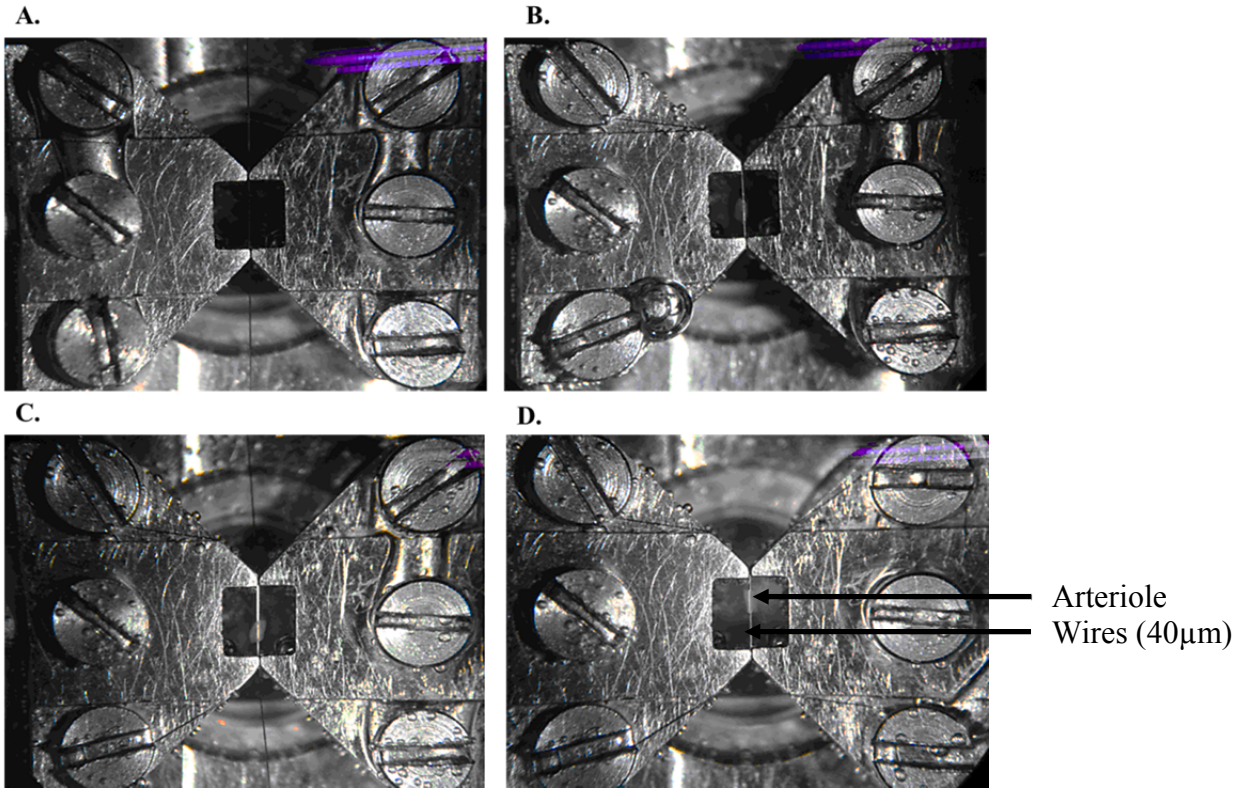

Figure 12 Vessel mounting in myography

A: Place the first wire between the jaws, then screw the jaws together to clamp the wire.

B: A segment of vessel was mounted onto the first wire.

C: The second wire was threaded through the lumen carefully.

D: Vessel was mounted on two wires and ready for normalization.

2.6.3 Vessel normalization

The vessels were continuously aerated at 37 °C followed by the normalization. The aim of the normalization procedure is to stretch the segment to achieve the normalized internal circumference, which was defined as the internal circumference when vessel fully relaxed with a specified transmural pressure. For human arterioles the transmural pressure was typically 100 mm Hg (13.3 kPa). The lumen diameter of each segment was calculated by the myograph system automatically. An equilibration period of at least 1 h was allowed during which time tissues were contracted with KCl (100 mM) to optimize tissue response.

2.6.4 Vasoconstriction measurement

Following equilibration, vasoconstriction was assessed by constructing cumulative concentration-response curves for NA (10^{-9}–$10^{-5.5}$ M), and TXA_2 analogue U46619 (10^{-9}–10^{-6} M). Where possible, two dose–response curves were obtained in the same preparation separated by a washout period of 30–60 min. With this protocol, there was no apparent time-dependent change in the response to any of the vasoconstrictors. Myography data were recorded and analysed using Myodaq and Myodata (Danish. Myotech, Aarhus, Denmark). Under each dose, peak value of vessel tension was collected; tension increase was calculated by peak value for each dose minus basal vessel tension (mN), and then adjusted by lumen diameter (mN/μm).

2.7 Assays

Plasma glucose concentration was assayed with glucose hexokinase reagent (Roche, CA, USA). Serum specific insulin levels were determined by ELISA (Mercodia, UK). Serum triglycerides, total, low density lipoprotein (LDL-) and high density lipoprotein (HDL-) cholesterol were assayed with commercial reagents (total-cholesterol:

Boehringer-Mannhein, Sussex, UK and triglycerides: Roche Diagnostics, Herts, UK). LDL-cholesterol was calculated using the Friedwald formula [150]. All lipid assays were performed by Dr David Wickens (Chemical Pathology, Whittington Hospital, London, UK). Insulin resistance was calculated using the HOMA where HOMA = (glucose in mmol/L x insulin in mIU/L)/22.5 [144].

2.8 Statistical Analysis

Data were analysed using SPSS version 14 for Windows (Statistical Package for the Social Sciences, SPSS UK Ltd, Chertsey, UK). Normality of distributions was tested with the Kolmogorov-Smirnov test. Data are shown as mean (SD), or for non-normally distributed data as median (interquartile range), in text and in tables. Comparison of depots was by paired t-tests or by Wilcoxon test. Pearson or Spearman rank correlations were used for the bivariate analysis. Significance was defined as $p \leq 0.05$.

Chapter 3

NA Synthesis, NA-mediated vasoconstriction and collagen deposition in abdominal AT

3.1 Introduction

3.1.1 Sympathetic nerve activation in abdominal obesity and diabetes

Abdominal obesity is associated with increased sympathetic nerve activity [151, 152]. The AT over-expansion in abdominal area includes SAT and OAT depots, consequently leading to subcutaneous and visceral obesity. However, the two obesity phenotypes may not be similar in their association with the sympathetic nerve activation. Compared to non-obese individuals, subcutaneous obese patients showed no significant elevation in muscle sympathetic nerve activity [153], while obese patients with high proportions of OAT showed higher muscle nerve burst compared with those with less OAT accumulation [151]. Moreover, in obese patients with Type II diabetes, the sympathetic nerve dysfunction was further exaggerated, shown as higher sympathetic nerve burst, decreased plasma NA clearance, and lower neuronal reuptake [152].

3.1.2 Local NA synthesis by AT

The major measurements of adrenergic activity in obesity are by testing the muscle sympathetic nerve burst or systemic NA level [151, 152]. However, the local NA synthesis is less investigated. AT, as an endocrine organ, is innervated by sympathetic nerves [154] and adrenergic regulation is highly involved in AT metabolism and adipokine secretion [114, 154]. Data from rodents also show that adipocytes *per se* may be a new source of NA synthesis [118], which points to local adrenergic regulation of AT and its vasculature via autocrine and paracrine pathways.

3.1.3 Adrenergic regulation on vascular tone

The adrenergic system is an important regulator of vascular function via activation of α and β adrenoceptors. As a part of GPCRs, adrenoceptors mediate the functional effect of NA. Adrenergic dysfunction has been observed in obesity, which could be due to AT

expansion, hyperleptinemia, and hyperinsulinemia, [155]. However, the adrenergic effect on local vascular function within AT is less investigated. Microvasculature embedded in AT directly mediates tissue growth, remodelling, metabolism and oxygenation [42]. It is also involved in the regulation of peripheral resistance. In obesity, due to the sympathetic nerve overreaction, there are a series of pathological alterations in vascular structure including tissue fibrosis, narrowed lumen diameter and increased wall thickness (reviewed in [156]). Whether the vascular function is also compromised is still being investigated. Previous data have reported endothelium-dependent vasodilatation while NA-mediated vasoconstriction is less studied [73, 138].

3.1.4 Adrenergic effect on tissue fibrosis

NA is a potent regulator of ECM deposition, inducing both tissue and vessel fibrosis in liver and lung in rodents [133, 134]. In humans, there is greater AT fibrosis in obese patients compared with lean individuals, and more collagen deposition surrounding vessels in OAT than SAT [128]. While it is probable that the vascular tone was altered by the accumulation of collagens around the vessels, direct evidence for this in human adipose microvessels is not currently available.

3.1.5 Aims

The aims of this study were to investigate, in human SAT and OAT:

1. The depot- and diabetes-specific difference in NA production,
2. NA-mediated vasoconstriction, and
3. NA-induced collagen gene expression.

3.2 Methods

Morbidly obese patients were recruited and characterised as described in **Section 2.1**. Adipocyte size and macrophage infiltration were estimated using the methods described in **Section 2.3.1** and **2.3.2**.

NA synthetic enzyme-TH was investigated using immunohistochemistry. The staining and analysis have been described in **Section 2.3.3**

Tissue explants and protein lysates were prepared as described in **Section 2.2.1** and **2.5.1**.

Local NA concentration in AT explant and protein lysate was measured using NA ELISA (Labor Diagnostika Nord, Germany). Briefly, NA in samples was extracted using a cis-diol-specific affinity gel, acylated to N-acyladrenaline and then converted enzymatically. Antigen is pre-coated to the solid phase of the microtiter plate. Acylated catecholamine from the sample and solid phase-bound catecholamine compete for a fixed number of antiserum binding sites. When the system is in equilibrium, free antigen and free antigen-antiserum complexes were removed by washing. The antibody bound to the solid phase was detected by anti-rabbit IgG-peroxidase conjugate using TMB as a substrate.

Vascular tone mediated by NA and TXA_2 analogue U46619 was investigated using dual wire myography system. Details were described in **Section 2.6**.

Tissue collagen deposition was studied by EVG staining. The staining protocol and analysis were described in **Section 2.3.4**.

For testing whether NA can induce AT collagen mRNA expression, 0.05 g of AT was minced and incubated for 6 hours in 500 μl serum-free medium (Cell-gro, Mediatech, VA, USA) with or without 1μM NA. The tissue was then stored in -80 ^{o}C for later total RNA extraction and real-time PCR.

Collagen type1α1 gene expression was investigated using total RNA extracted from whole AT and real-time PCR technique described in **Section 2.4**.

Data were analysed using SPSS version 14 for Windows (Statistical Package for the Social Sciences, SPSS UK Ltd, Chertsey, UK). Normality of distributions was tested with the Kolmogorov-Smirnov test. Data are shown as mean (SD), or for non-normally distributed data as median (interquartile range), in text and in tables. Comparison of depots was by paired t-tests or by Wilcoxon test. Pearson or Spearman rank correlations were used for the bivariate analysis. Significance was defined as $p \leq 0.05$.

3.3 Results

3.3.1 Patients' characteristics

Patient characteristics are shown in **Table 1 (**n=44**,** 85% female**)**. Compared to the non-diabetic group, diabetic patients were older. The majority of the non-diabetic obese patients studied were normoglycaemic, but at the expense of hyperinsulinaemia. A sub-set remained normoinsulinaemic and were excluded from these studies (n=3).

Medication regimen: None of the 44 patients were treated with ß-blockers. In the non-diabetic group only 5 out of the 28 patients were taking any medication (thiazolidinedione n=1; statins n=3 and Ang converting enzyme inhibitors n=1). In the 16 diabetic patients the main hypoglycaemic therapy was metformin (n=11) and one was on diet alone. 2 patients were on insulin and 2 on thiazolidinediones. Additional medication included statins (n=6), Ang converting enzyme inhibitors (n=5) and Ang-2 receptor antagonists (n=2).

Despite treatment the diabetic patients had higher fasting plasma glucose, but, lower insulin concentrations. Levels of HOMA-IR, serum lipids and blood pressure were all comparable between the two groups.

Variables	Non-diabetic(N=28)	Diabetic(N=16)	*p* value
Age (year)	39.9(12.3)	48.4(8.4)	0.01
BMI ($kg.m^{-2}$)	47.7(8.9)	45.0(7.8)	0.41
SBP (mmHg)	131.4(16.3)	136.4(20.1)	0.54
DBP (mmHg)	79.2(9.1)	76.4(11.8)	0.59
MABP (mmHg)	96.6(10.1)	96.4(13.6)	0.76
FPG (mmol/L)	5.1(1.0)	7.7(3.2)	<0.01
Insulin (mIU/L)	11.3(8.1-16.1)	7.1(5.7-14.4)	0.04
HOMA-IR	2.5(1.7-3.9)	2.7(1.3-5.5)	0.66
TG (mmol/L)	1.8(1.2-2.3)	1.1(0.8-2.4)	0.12
Total-chol (mmol/L)	4.2(1.2)	3.8(1.1)	0.35
LDL-chol (mmol/L)	2.6(1.3)	2.2(1.0)	0.16
HDL-chol (mmol/L)	0.9(0.2)	1.0(0.2)	0.10

Table 1 Patients' characteristics.

Data shown as mean (SD) or median (interquartile range); BMI: body mass index, SBP, systolic blood pressure, DBP, diastolic blood pressure; MABP: mean arterial blood pressure; FPG, fasting plasma glucose, HOMA-IR, homeostasis model assessment of insulin resistance; TG: triglycerides; Total-, LDL-, HDL-chol, Total-, LDL-, HDL-cholesterol

3.3.2 Tissue NA synthesis

In order to test the hypothesis that chronically elevated locally synthesized NA in the OAT and in diabetic patients may lead to vessel insensitivity to the catecholamine, the expression of the rate-limiting NA synthetic enzyme, TH, as well as tissue and explant levels of NA were determined.

TH immunoreactivity was associated with the adipocytes as well as with the vasculature (**Figure 13A&B**). Lower TH density was apparent in SAT compared to that of the OAT depot in non-diabetic group (SAT non-diabetic: 98904 [79403-128929] arbitrary unit [AU], N=14 versus OAT non-diabetic: 117088 [100115-139084] AU, N=13, p= 0.04, **Figure 13C**). However, no such depot-specific difference of TH staining was found in the diabetic tissue (SAT diabetic: N=6, 154348.5 [125651.5-167425.25] AU; OAT diabetic: N=6, 171109 [153441-197658.75] AU, p=0.17).

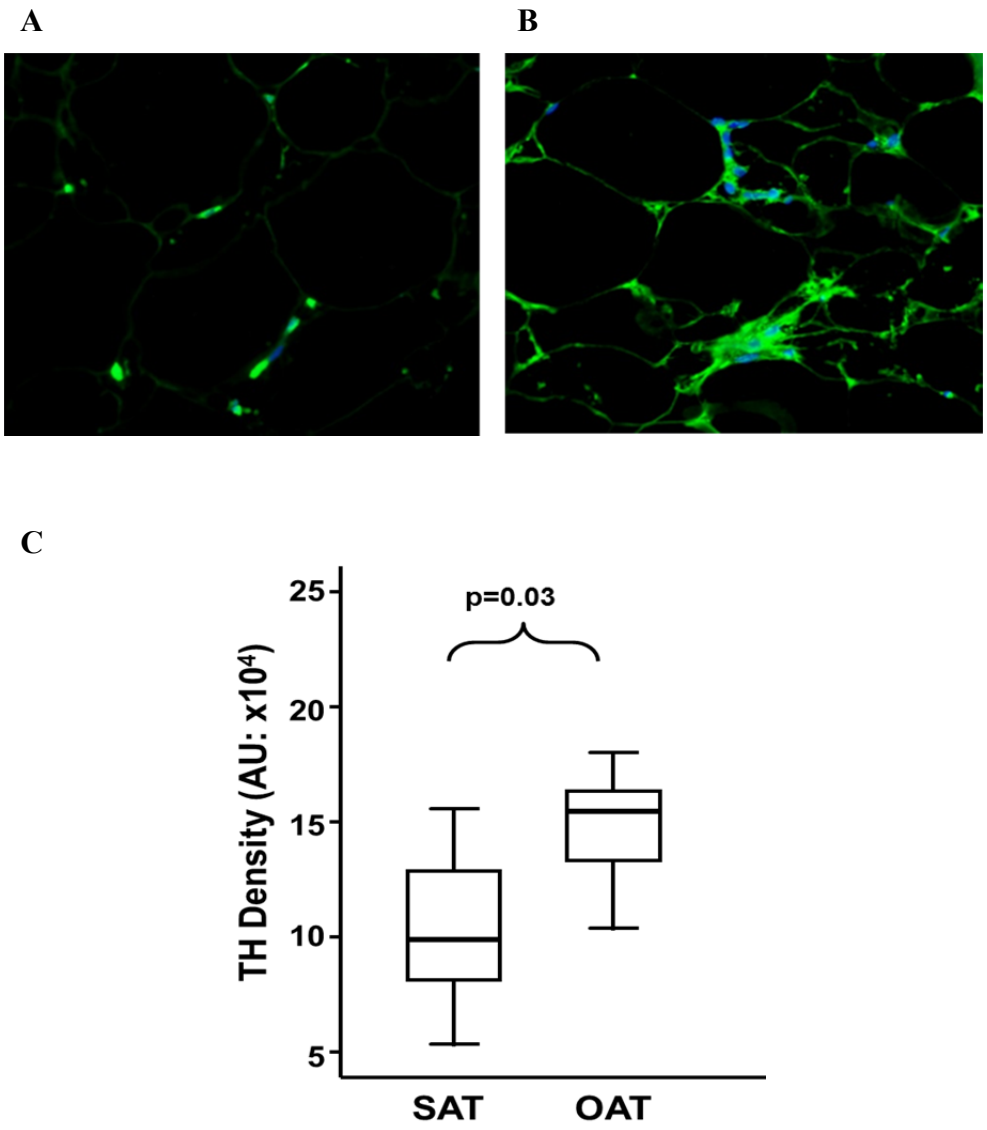

Figure 13 Depot- and diabetes-specific differences in TH density

TH positive staining (green) was apparent around the adipocytes of both SAT (**A**) and OAT (**B**). In tissue from non-diabetic subjects TH staining was significantly less in SAT than OAT (**C**, p=0.03). Within the diabetic group there were no significant differences in TH staining between the depots (p=0.17).

Tissue NA levels were significantly lower in SAT compared to OAT in all patients (SAT versus OAT: 19.4[1.1-500.4] versus 335.6 [4.3-1921.5] pg/mg total protein, N=12, p=0.01).

As shown in **Figure 14**, it was only in the non-diabetic group that this depot-specific difference was apparent (SAT versus OAT: 6.1 [0.8-563.6] versus OAT: 534.8 [2.2-2819.2] pg/mg total protein; N=6, p=0.03), perhaps explaining the greater sensitivity of the vessels from this depot to its vasoconstrictive effect. In diabetic patients, the tissue NA was comparable in the two depots. (SAT: 194.7 [1.4-529.7] versus OAT: 335.6 [6.4-3457.7] pg/mg total protein; N=6, p=0.17).

Very low concentrations of NA were detected in explant medium of both SAT and OAT (<1.0 pg/ml), suggesting a mainly autocrine/paracrine, rather than endocrine, effect.

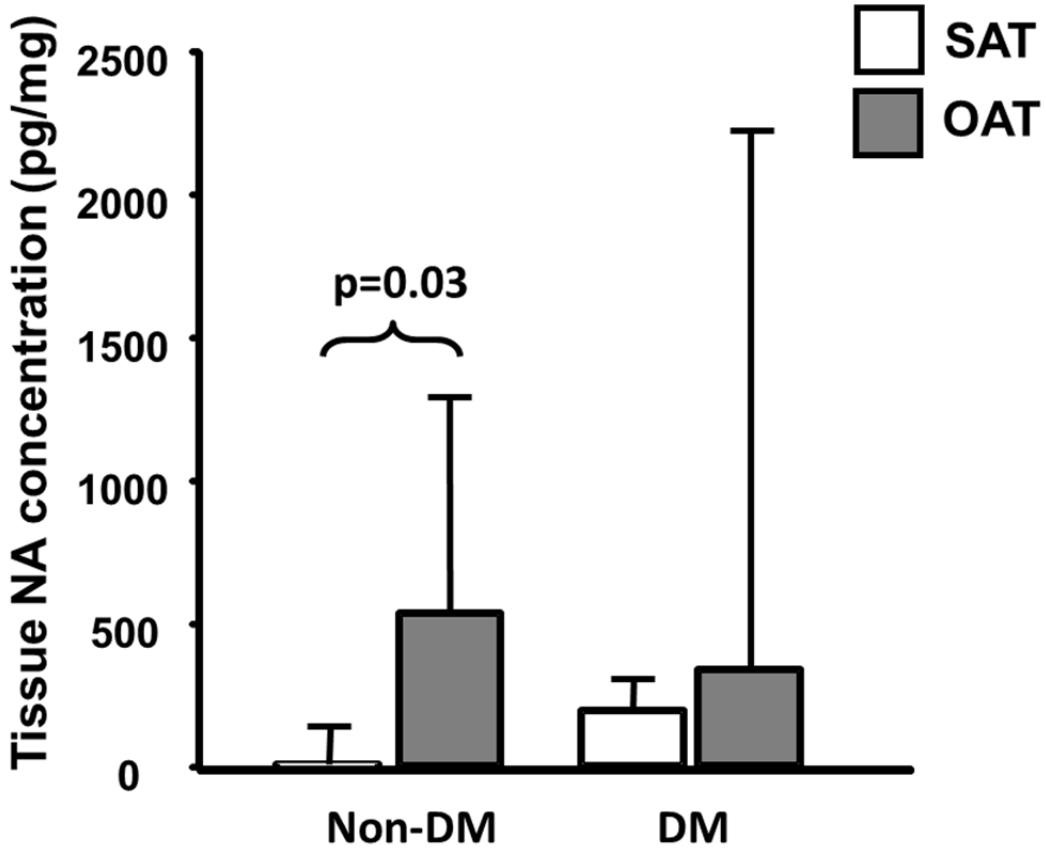

Figure 14 Depot- and diabetes-specific difference in tissue NA concentration

Local NA levels was significantly higher in OAT compared to SAT in non-diabetic while no depot-specific difference was found in diabetes.

Non-DM: non-diabetic obese patients; DM: diabetic obese patients.

3.3.3 NA- and TXA_2 (U44419) - mediated vasoconstriction

In all subjects the vasocontractile function of arterioles with comparable lumen sizes were investigated (non-diabetic: SAT 306.9 [215.9-440.0] μm and OAT 335.1 [233.4-430.4] μm, N_{SAT}=14, N_{OAT}=16, p=0.73; diabetics: SAT 278.8 [179.4-442.5] μm and OAT 330.8 [181.1-592.8] μm, N_{SAT}=8, N_{OAT}=8, p=0.72).

In the non-diabetic patients, there was a significant depot-specific difference in both the sensitivity to NA-mediated vasoconstriction and the maximal contractile response (**Figure 15A&C**). The arterioles from the SAT showed vasoconstriction at lower, near physiological doses of NA (at dose 10^{-8} M, p=0.01; dose $10^{-7.5}$ M, p=0.02; Log EC50: SAT versus OAT, -7.3[0.6] versus -6.2[0.6]). However, the maximal contractile response of the OAT vessels was higher compared to those from SAT (OAT: 0.021 [0.011-0.039] mN/μm versus SAT: 0.013 [0.004-0.022] mN/μm, p=0.05).

No depot specific differences in the sensitivity or vessel tension were seen in the diabetic patients (**Figure 15B&D**, Log EC50: SAT versus OAT, -6.4[0.7] versus -6.4[0.8], SAT versus OAT maximal vessel tension, p=0.83).

Furthermore, the SAT arterioles from non-diabetic patients showed greater sensitivity to NA at physiological doses compared to those from the diabetic patients (10^{-8} to$10^{-7.5}$ M, p=0.01 and 0.03 respectively).

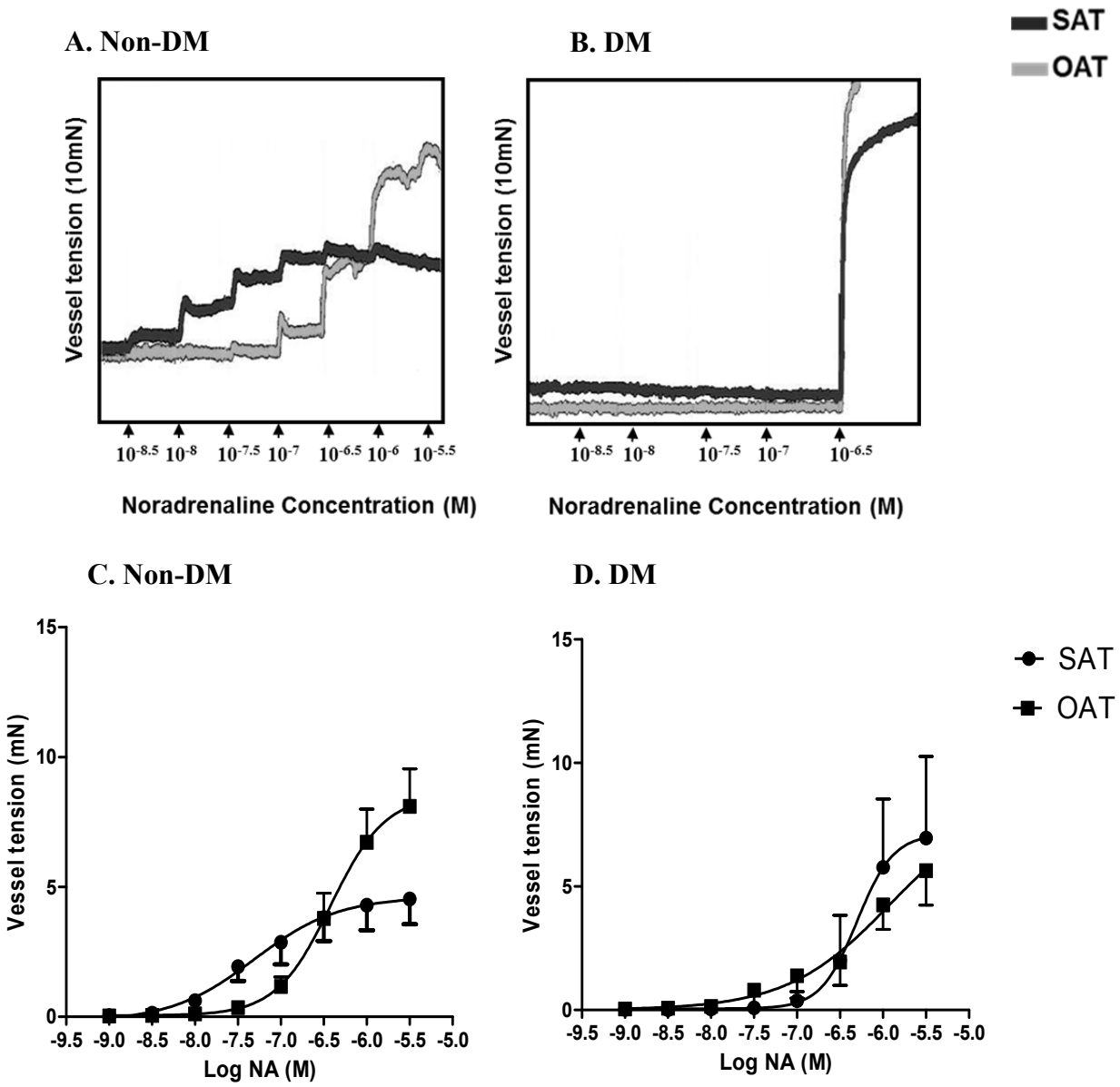

Figure 15 Depot- and diabetes-specific differences in NA-mediated vasoconstriction (I)

A&B: Images captured from the representative myography trace in single experiment of one non-diabetic and one diabetic obese patient. Vessel NA sensitivity was only apparent in SAT of non-diabetic group, while abolished in OAT and diabetes.

C&D: Overall analysis of vasoconstriction in non-diabetic and diabetic obese patients, it confirmed the depot- and diabetes-specific difference in NA-mediated vasoconstriction. Data was expressed as mean and mean of standard error.

Non-DM: non-diabetic obese patients; DM: diabetic obese patients.

Data was also expressed as median and interquartile range (**Figure 16**), it confirmed that SAT in non-diabetic group is the only depot showing greater sensitivity to NA-mediated vasoconstriction within the physiological range (10^{-8}-$10^{-7.5}$, $p<0.05$).

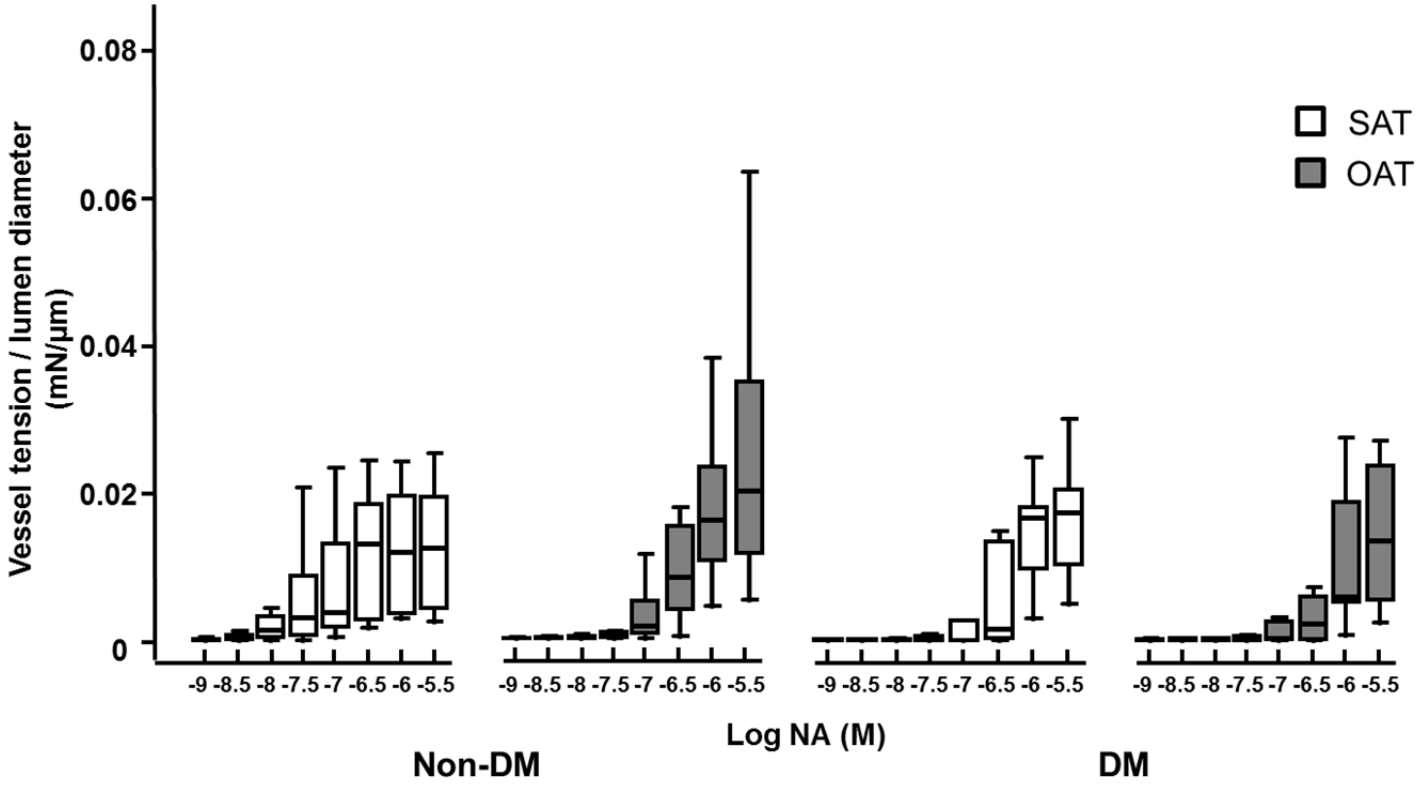

Figure 16 Depot- and diabetes-specific difference in NA-mediated vasoconstriction (II)

Data was expressed as median and interquartile range, which confirmed the depot- and disease-specific difference in NA-induced vasoconstriction, significant increase in vessel tension was only observed in SAT of non-diabetic group from 10^{-8}-$10^{-7.5}$ M compared to OAT of non-diabetic group and both depots of diabetic group.

Non-DM: non-diabetic obese patients; DM: diabetic obese patients.

To examine if other vasoconstrictor also elicits a similar depot-specific difference in response, U46619, a TXA_2 mimic and a powerful vasoconstrictor, was tested in arterioles from tissue from the non-diabetic group. No difference in sensitivity to U46619 mediated vasoconstriction was apparent between SAT and OAT derived arterioles (Log EC50: SAT versus OAT, -6.3[1.0] versus -6.8[0.7], p=0.29, **Figure 17A**). However, at supra-pharmacological doses OAT arterioles exhibited greater vasoconstriction (10^{-6}-$10^{-5.5}$M, p=0.02).

Furthermore, in the comparison between U46619- and NA-mediated vasoconstriction in non-diabetic group, the vasoconstriction mediated by U46619 were significantly lower compared with those mediated by NA in SAT (10^{-8} M to $10^{-6.5}$ M, $p<0.05$, **Figure 17B**), while there were no such differences detected in OAT, which suggests an NA-specific vessel sensitivity in SAT of non-diabetics.

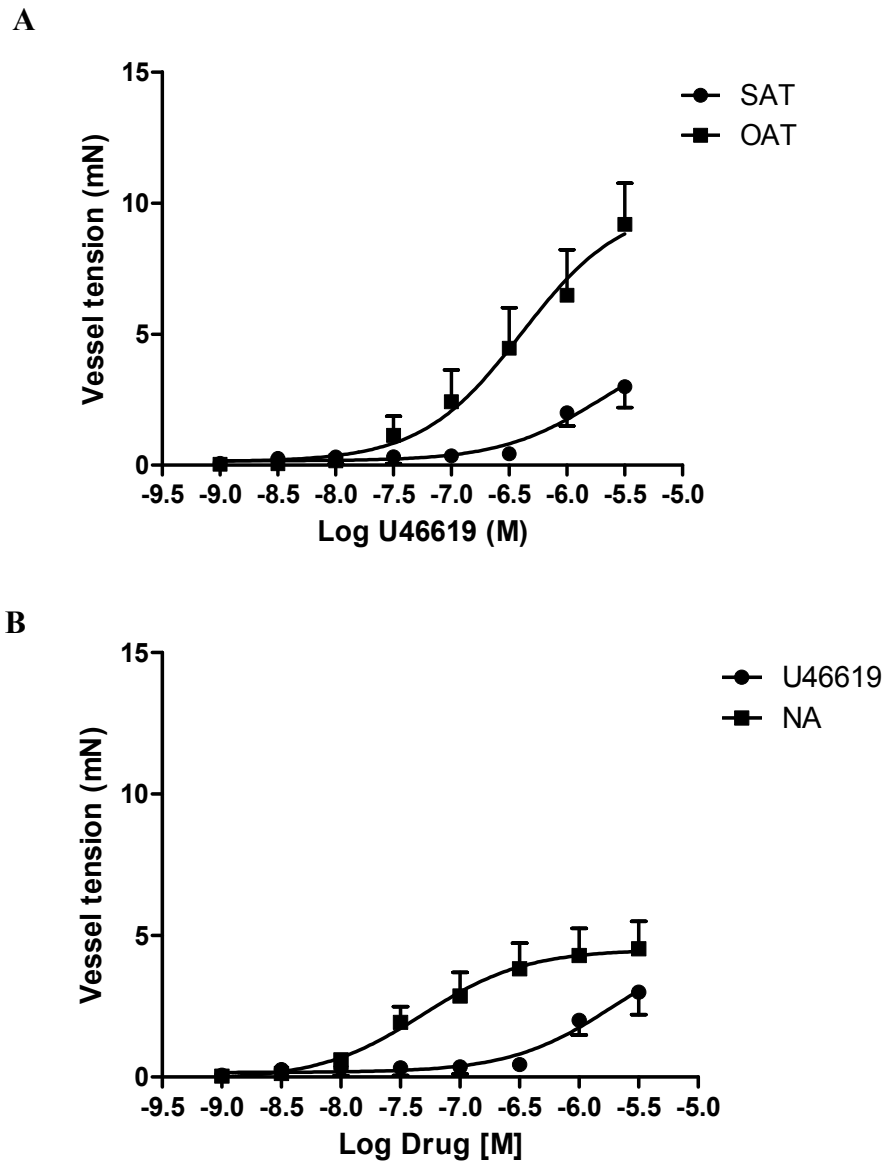

Figure 17 Vasoconstriction mediated by TXA_2 mimic U46619 and comparison of vasoconstriction mediated by U46619 and NA in SAT of non-diabetics

A: No significant sensitivity difference was shown in U46619-mediated vasoconstriction between SAT and OAT, while maximal vessel tension was significantly higher in OAT compared with SAT in non-diabetic group ($p=0.02$).

B: NA mediated vasoconstriction was significantly higher compared to that mediated by U46619 in SAT of non-diabetic group (10^{-8} M to $10^{-6.5}$ M, $p<0.05$).

3.3.4 Collagen deposition and gene expression

In SAT of the non-diabetic group, low levels of collagen deposition were observed both surrounding the vessels and dispersed within the rest of the tissue (**Figure 18Ai&ii**), while OAT showed significantly higher collagen staining which was mostly near the vessels but also throughout the tissue (**Figure 18Aiii&iv**). Greater tissue fibrosis was observed in diabetic tissues. In SAT, collagen staining was observed around the vessels and widely dispersed within the tissue, which suggests tissue fibrosis and consequent vessel stiffness (**Figure 18Av&vi**). Similar results were also found in OAT of this group (**Figure 18Avii&viii**). This finding was confirmed by collagen pixel area analysis and gene expression data. SAT of non-diabetic subjects displayed the lowest collagen deposition compared to OAT of non-diabetic group and both depots of diabetic group ($p<0.05$, **Figure 18B**).

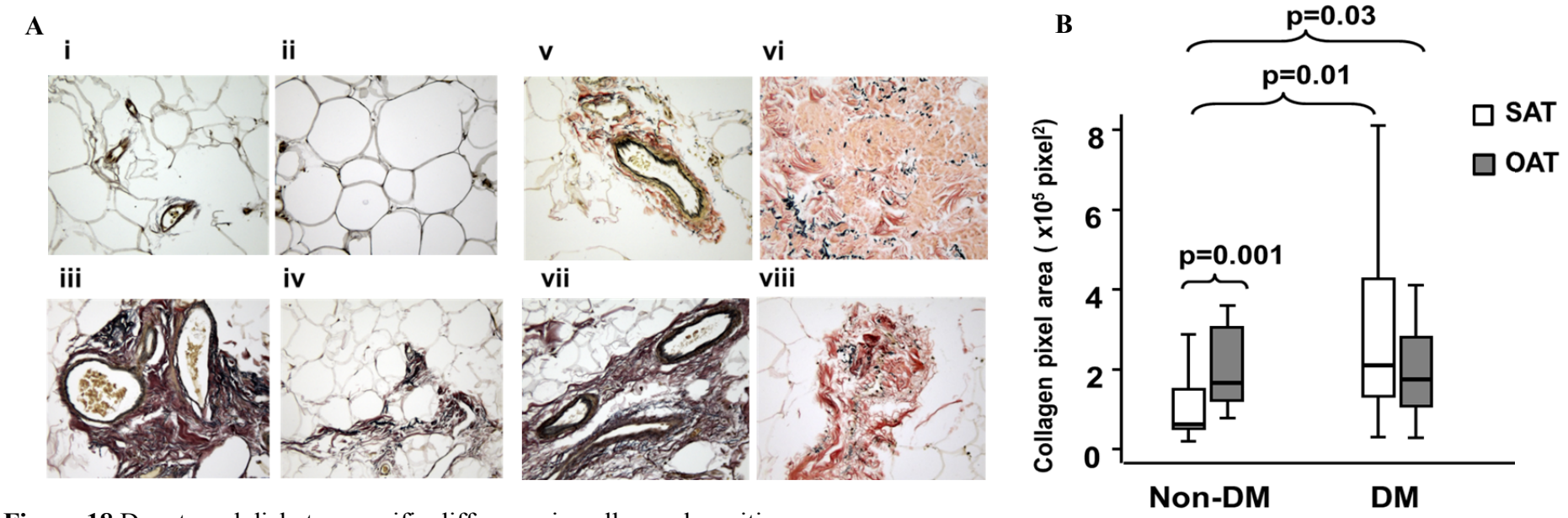

Figure 18 Depot- and diabetes-specific difference in collagen deposition

Collagen was stained as pink and elastin was stained as black. Representative images were selected to show the collagen deposition surrounding the vessels and within the rest area of the tissue. In non-diabetic group, SAT showed very low levels of collagen staining both within the vessel area(**Ai**) and the other part (**Aii**), while abundant collagen deposition was shown in OAT wrapping the vessels(**Aiii)** and in the rest part of the tissue (**Aiv**).

More collagen deposition was observed in the diabetic compared to non-diabetic group. In SAT, it was not only around the vessels (**Av**) but also widely dispersed within the tissue (**Avi**). OAT showed the similar collagen distribution and comparable collagen quantity (**Avii&viii**). Collagen staining analysis showed the least collagen deposition in SAT of non-diabetic patients compared to OAT of non-diabetics and both depots in diabetes (**B**). Non-DM: non-diabetic obese patients; DM: diabetic obese patients.

Collagen gene type Iα1 expression also showed the same trend, with SAT of non-diabetic patients having the lowest mRNA gene expression compared to OAT in non-diabetic group and both depots in the diabetic group (**Figure 19A**).

Significant elevation of collagen type Iα1 mRNA expression was observed in AT incubated with 1μM NA compared with the control [NA: 0.67(0.64-0.68) versus Control: 0.62(0.61-0.65), n=6, p=0.03, **Figure 19B**], which implicates a direct fibrotic effect of NA on AT.

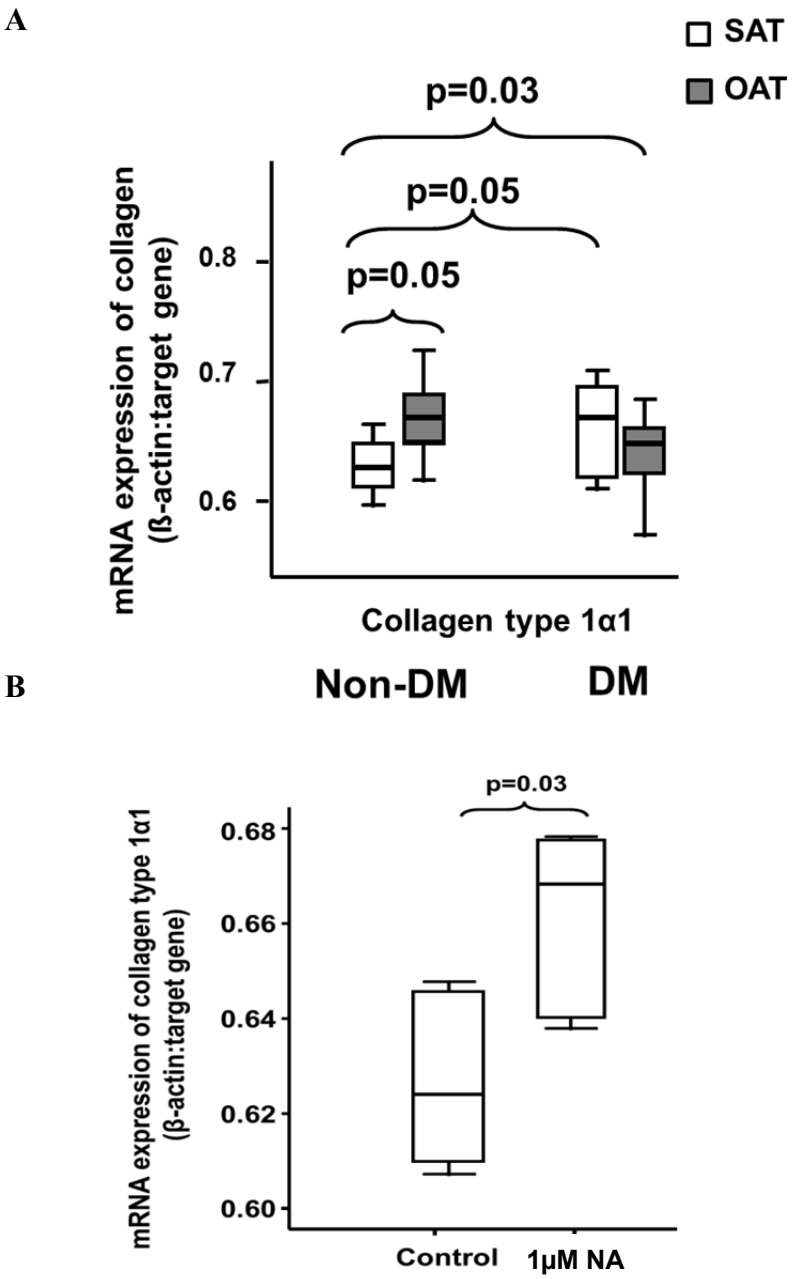

Figure 19 Depot- and diabetes-specific differences of collagen mRNA expression and collagen gene up-regulated by NA

Collagen type 1α1 mRNA was less expressed in SAT of non-diabetic group compared to OAT and both depots in diabetics (**A**). Furthermore, AT collagen gene type Iα1 was upregulated by 1μM NE incubation (**B**)

Non-DM: non-diabetic obese patients; DM: diabetic obese patients.

3.3.5 Adipocyte size and macrophage infiltration

Adipocyte area was assessed by manually tracing the pixel area (**Figure 20**). Smaller adipocytes were observed in OAT compared to SAT in both groups, while adipocyte in SAT were bigger in diabetic than non-diabetic patients. Moreover, SAT and OAT of diabetic patients displayed larger adipocytes compared to those in non-diabetic patients (upon the dotted line), which suggests tissue hypertrophy

In the non-diabetic subjects, OAT, compared to SAT, showed significantly smaller adipocytes (SAT: N=260, 2.7[1.8-3.9] $x10^4$ $pixel^2$, OAT: N= 286, 2.1[1.5-3.1] $x10^4$ $pixel^2$, $p<0.001$).

The SAT depot of diabetic patients had larger adipocytes compared to that of non-diabetic patients (diabetic SAT: 3.1 [2.0-4.5] $x10^4$ $pixel^2$ versus non-diabetic SAT: 2.7[1.8-3.9] $x10^4$ $pixel^2$, $p=0.04$). However, in the OAT these differences were not significant (diabetic OAT: 2.2 [1.3-3.2] $x10^4$ $pixel^2$ versus non-diabetic OAT: 2.1[1.5-3.1] $x10^4$ $pixel^2$, $p=0.9$).

Low levels of AT macrophage infiltration were observed in both SAT and OAT and there was no significant difference between the depots and groups (data not shown).

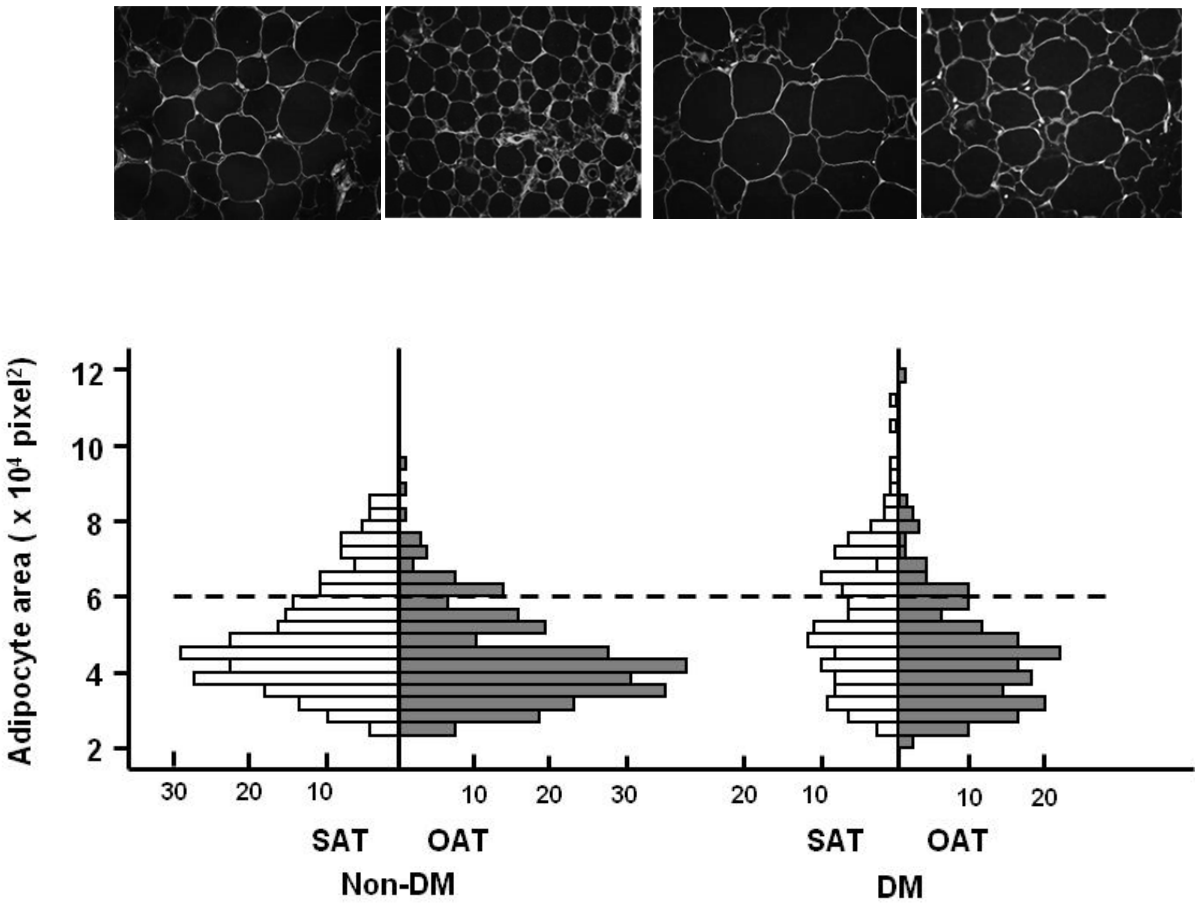

Figure 20 Depot- and diabetes-specific difference in adipocyte number and size.

More smaller adipocytes were observed in OAT compared to SAT in both groups, while adipocytes in SAT were larger in diabetic than non-diabetic patients. Moreover, SAT and OAT of diabetic patients displayed more large adipocytes compared to those in non-diabetic (upon the dotted line), which suggest tissue hypertrophy.

Non-DM: non-diabetic obese patients; DM: diabetic obese patients.

3.4 Discussion

3.4.1 Local NA synthesis in AT

In this study, the depot- and diabetes-specific differences in AT NA synthesis, NA-mediated micro-vasoconstriction, collagen gene expression and deposition and adipocyte morphology were investigated.

Adipocytes from rodents were recently shown to synthesize catecholamine [118]. In this study, TH, a key enzyme involved in NA synthesis, was found in the human AT, and specifically located surrounding the adipocytes, which suggested the capability of human AT to synthesize NA. It was still not clear whether the TH was derived from adipocytes, peripheral sympathetic nerves, macrophages or other components within the tissue. No significant depot-specific difference in macrophage infiltration, examined by CD68 staining, was seen between SAT and OAT in the non-diabetic group and TH density was analyzed by measuring the whole staining area. Thus the depot-specific difference of TH density may be not caused by a sole component difference within the tissue. Furthermore, NA was detectable in protein extracts from whole tissue but not in explant medium, these data suggest AT-derived NA is synthesized and stored within the tissue instead of being directly released into the circulation. Thus, NA from AT may achieve its effect through autocrine/paracrine, rather than endocrine, mechanisms and microvasculature embedded in the AT might be directly affected by AT-derived NA.

3.4.2 NA-mediated vasoconstriction

In the non-diabetic group, there was a depot-specific difference in NA-mediated arteriolar vasoconstriction displayed as a more sensitive response in SAT compared to OAT at lower NA concentrations, however this difference was absent in diabetic obese patients. Meanwhile, TH density and local NA concentration were significantly lower in SAT than OAT in non-diabetics but were elevated and comparable in the depots in

Type II diabetes. These data imply that the vessel sensitivity to NA-mediated vasoconstriction was preserved only in SAT of non-diabetic patients, perhaps due to the low level of tissue NA content and synthesis, whereas the arterioles in the OAT of non-diabetics and both depots of diabetic group were desensitized by long-term exposure to local chronic elevated NA concentration, which has been shown in other studies [157, 158]. In addition, this phenomenon was only apparent in NA-mediated vasoconstriction, TXA_2 is a potent vasoconstrictor synthesized by EC and adipocyte, in response to physiological concentration of TXA_2 mimic U46619, no significant difference was observed between SAT and OAT in non-diabetic group, both depots showed weak but comparable vasoconstriction, which suggests that the sensitivity difference to NA between depots is specific. A recent study demonstrated that arteriolar vasodilatation was impaired in AT of morbidly obese patient, while the current study showed that the vasoconstriction was also compromised. Both vasodilatation and vasoconstriction are involved in functional microcirculation, which is critical for maintaining the homeostasis of blood pressure and transporting oxygen to prevent tissue hypoxia. This finding has also been supported by the very recent study of AT blood flow [113]. After intravenous adrenaline infusion, there was a significant increase in microvascular volume of SAT in non-diabetic group while this response was abolished in diabetes, which could also be explained by the NA desensitization in SAT arterioles of diabetic patients.

Insulin mediated capillary recruitment required functional vasoconstriction and vasodilatation to transport insulin from insulin-insensitive to insulin-sensitive organs. Evidence showed glucose-mediated vasodilatation was abolished via beta-adrenergic mechanisms [159]. Current data suggests that obese patients with diabetes also showed resistance to NA-mediated vasoconstriction. Thus, the abortion of microvascular tone may be an important risk factor of tissue hypoxia and insulin resistance.

3.4.3 AT collagen deposition and its effect on vasoreactivity and adipocyte morphology

Tissue fibrosis could be another consequence of local NA elevation. Following NA increase in OAT of non-diabetic group and both depots of diabetic group, there was accordant increase of collagen deposition within these depots. This could be a consequence of local NA elevation, since evidence showed fibrotic response was up-regulated by NA in several organs and vessels [133, 134]. Current data also suggests that collagen mRNA expression was elevated by NA incubation.

In addition, AT hypoxia may also contribute to collagen deposition. AT incubated in HIF-1α displayed significant increase of collagen synthesis (reviewed in [39]). Thus, collagen deposition could be a hallmark of AT hypoxia and dysfunction. It is noteworthy that SAT in non-diabetics showed the lowest extent of fibrosis while OAT in non-diabetics and both depots of diabetic patients had elevated and comparable collagen deposition. This implies that SAT in non-diabetics may preserve its function and oxygenation, perhaps explained by its vascular sensitivity to NA. Higher collagen deposition surrounding adipocytes in OAT and diabetes may increase the mechanic stress and lead to adipocyte necrosis and inflammation.

Transforming growth factor-β (TGF- β) could be another factor involved in vessel fibrosis. TGF- β is a multifunctional regulator involved in cell division, differentiation, migration, adhesion, organization and promoting ECM production [160]. There are three different TGF- β isoforms, TGF- β1, TGF- β 2 and TGF- β 3, among which TGF-β1 plays an important role in cardiovascular system. It has been found in ECs, VSMCs, macrophages, myofibroblasts and other hematopoietic cells [161]. In ECs, VSMCs and fibroblasts, TGF- β enhances α-smooth muscle actin and collagen type I expression via mediating ED-A fibronectin expression. In addition, TGF- β decreases collagenase production and stimulates the expression of tissue inhibitor of metalloproteinases

(TIMP), further exaggerates tissue fibrosis [162] . Previous study in mice showed, in response to high-fat diet, there was an up-regulation of TGF- β protein expression in both aorta and AT, which was associated with increased vessel stiffness [163]. Human TGF- β expression and secretion levels were higher in AT of morbidly obese patients compared with lean control [164]. Further study is required to identify the depot- and diabetes-specific difference in AT TGF- β levels as well as its effect on local collagen deposition.

The abundant collagen surrounding the vessels in the tissue might restrict the vasoreactivity. In addition, collagen type 1α1 was highly expressed in OAT of non-diabetic patients and in diabetes. Collagen type 1 was the major component of vessel wall by synthesizing cross-banded fibrils, which provided tensile strength [131]. Increased collagen in vessel wall may greatly increase vessel stiffness and decrease vessel sensitivity, but it may also explain why there was a maximal tension difference between SAT and OAT in non-diabetic group.

3.4.4 Conclusion

Thus SAT in non-diabetic obese patients preserved its adrenergic sensitivity to NA-mediated vasoconstriction due to low levels of local NA synthesis, meanwhile the lower collagen deposition also meant the vascular structure is less restricted. However, the high levels of NA in OAT and diabetes may lead to a vessel desensitization and elevated collagen deposition.

3.4.5 Study limitations.

During this study, AT was collected from morbidly obese patients under variety of treatments. While all the medication has been documented (mentioned in the text), the experimental interference could not be excluded. Also most of the patients were female, the gender effect on the results still needs to be investigated.

Chapter 4

Depot- and diabetes-specific differences in abdominal AT angiogenesis

4.1 Introduction

4.1.1 The importance of AT angiogenesis.

Angiogenesis is crucial to AT growth and remodelling. The adipose plasticity is dependent on constant alterations of numbers and functions of microvasculature to support and regulate AT metabolism [31]. Sufficient and functional vascular network ensures the delivery of oxygen, insulin and other nutrients to the tissue, thus maintaining AT normoxia and functions. In morbidly obese patients, capillary rarefaction (low capillary density) has been reported to be associated with AT hypoxia and insulin resistance [38].

4.1.2 Depot-specific difference of AT angiogenesis

Central obesity is the abdominal AT expansion including SAT and OAT. The depot-specific difference of angiogenesis between SAT and OAT may directly determine the abdominal fat distribution. The angiogenic difference between SAT and OAT has been investigated mainly in three studies, but the results were conflicting. A human AT endothelium study showed that angiogenesis-related genes were more highly expressed in ECs in OAT compared to SAT [37]. However, AT angiogenesis study *in vitro* showed different results. The SAT explant incubated in Matrigel displayed higher capillary density and angiogenic capacity than OAT [69]. In addition, the third study concluded that there was no significant difference of capillary density between SAT and OAT after normalizing the capillary number to the adipocyte number [70].

4.1.3 Regulation of AT angiogenesis

AT angiogenesis is regulated by a series of factors, among which NRP-1 plays an important role as a co-receptor for VEGF receptors. In rat white AT, NRP-1 was found mainly in VSMC and ECs of arteries, but adipocytes also showed to be NRP-1 positive

[59]. This finding was confirmed in the human fatty bone marrow. Higher NRP-1 expression was detected in adipocytes in contrast to hematopoietic and stromal cells [60]. However, the expression of NRP-1 in human AT depots and in diabetes has not been reported.

4.1.4 Aims

This study aimed to investigate the depot- and diabetes-specific differences of angiogenesis and angiogenesis-related gene expression between SAT and OAT in non-diabetic and diabetic obese patients.

4.2 Methods

Morbidly obese patients were recruited and characterised as described in **Section 2.1**. SAT was dissected from abdominal area using forceps and scissors, OAT was dissected from intra-abdominal greater omentum using endoscopic linear cutter.

Capillaries were stained by lectin tetramethylrhodamine isothiocyanate conjugate (from Ulex europaeus [UAE], Sigma-Aldrich) then the capillary density was calculated (described in **Section 2.3.1**).

Sections were immunostained for EC markers, CD31 and CD34 (method described in **Section 2.3.3**).

Angiogenic capacity was estimated by AT explant incubated in Matrigel. Briefly, SAT and OAT was cut into ≈ 1 mm^3 pieces and embedded into individual wells of 96-well plates with 50 µl growth factor reduced Matrigel (BD Bioscience, UK). Each well was filled with 200µl EGM2-MV medium (Lonza, UK), and half of the medium was replaced every other day [69]. Incubation ended at day 10 and photographs were captured at 40x magnification using Nikon TMS microscope and ProgResC14 software

(resolution 1300x1030). For each sample, pictures were captured with five sections (whole tissue, up, down, left and right). Image information was then analysed using ImageJ. The pixel area covered by neovasculature was traced manually and adjusted by AT area ($R_{V/A}$). Data was also analysed by particle measurement. Background of image was filtered and capillaries were isolated by ImageJ threshold function. Then capillary quantity was estimated by particle measurement function.

Angiogenic gene regulation was performed using the commercially available RT^2 Profiler PCR array for human angiogenesis (PAHS-024; Qiagen, UK). Total RNA isolated from SAT and OAT of non-diabetic and diabetic patients (n=8) were used in these studies (total RNA extraction was described in **Section 2.4.1**). Briefly, 400ng total RNA was mixed with Genomic DNA Elimination Mixture first to avoid the contamination from any residual genomic DNA contamination in RNA samples before it can be amplified into secondary products that would otherwise cause false positive signals (400ng total RNA / 10µl mixture, incubate at 42^{o}C for 5 minutes, then on ice for at least 1 minute). Reverse transcription was carried out by mixing 10µl decontaminated sample with 10µl reverse transcription mixture (each 10µl contains 4µl Reverse Transcription Buffer, 1µl Primer and External Control Mix, 2µl Reverse Transcriptase Mix and 3µl RNase-free water, incubate at 42°C for exactly 15 min. Then immediately stop the reaction by incubating at 95°C for 5 min). Finally, samples were diluted in RNase-free water, mixed with RT^2 SYBR Green Mastermix prior to proceeding with real-time PCR. The 384-well microarray plate (96x4) contains 4 replicate primer assays for each of 84 pathway- or disease-focused genes and 4 replicate primer assays for each of 5 housekeeping genes. In addition, 4 wells contain genomic DNA controls, 12 wells contain reverse-transcription controls, and 12 wells contain positive PCR controls. Finally, data was formatted and analysed using web-based analysis software of Qiagen (www.SABiosciences.com/pcarraydataanalysis.php). Adjusted data was expressed as

the fold changes of mRNA expression between target group and control group as specified.

The mRNA expressions of NRP-1 were determined by real-time RT-PCR. β-actin was chosen as the house-keeping gene. Data was expressed as the ratio of NRP-1 Ct/β-actin Ct (described in **Section 2.4**). NRP-1 protein levels were investigated using western blot, the method and analysis was described in **Section 2.5.** Data was expressed as the ratio of NRP-1 / β-actin grey density.

Plasma glucose concentration, serum insulin levels, serum triglycerides, total, low density lipoprotein (LDL-) and high density lipoprotein (HDL-) cholesterol were assayed as described in **Section 2.7**. Insulin resistance was calculated using the HOMA where HOMA = (glucose in mmol/L × insulin in mIU/L)/22.5 [144].

Data were analysed using SPSS version 14 for Windows (Statistical Package for the Social Sciences, SPSS UK Ltd, Chertsey, UK). Normality of distributions was tested with the Kolmogorov-Smirnov test. Data are shown as mean (±SD), or for non-normally distributed data as median (interquartile range), in text and in tables. Comparison of depots was by paired t-tests or by Wilcoxon test. Pearson or Spearman rank correlations were used for the bivariate analysis. Significance was defined as $p \leq 0.05$.

4.3 Results

4.3.1 Patients'characteristics

Patient characteristics are shown in **Table 2** (n=60, 85% female)**.** No significant differences were found between the two groups for most parameters except that in diabetic group fasting plasma glucose level is significantly higher ($p<0.001$) despite treatment (thiazolidinediones: 3/20; metformin: 14/20). The other medications were shown on **Table 3**.

Variables	Non-diabetic(n=40)	Diabetic(n=20)	P value
Age	47.1±8.9	48.9±7.9	0.24
BMI (kg.m^{-2})	46.2±8.3	45.0±6.8	0.84
SBP (mmHg)	138.4±23.1	132.8±19.0	0.50
DBP(mmHg)	77.4±12.2	77.2±10.7	0.77
MABP (mmHg)	97.7±14.0	95.7±11.9	0.73
Total-chol (mmol/L)	4.3±1.4	3.7±1.1	0.10
LDL-chol (mmol/L)	2.5±1.3	2.0±1.0	0.12
HDL-chol (mmol/L)	1.0±0.2	1.0±0.2	0.52
TG(mmol/L)	1.5(1.2-2.4)	1.1(0.9-2.3)	0.09
FPG (mmol/L)	5.2±1.1	7.7±3.2	<0.001
Insulin (mIU/L)	8.6(6.0-20.3)	7.1(4.9-19.0)	0.61
HOMA	1.8(1.5-4.5)	2.4(1.3-5.9)	0.61
Se.adipo (μg/ml)	4.2(2.5-7.2)	5.5(3.7-9.6)	0.06
Se.MCP-1 (pg/ml)	272.3(178.0-424.7)	252.3(176.4-336.0)	0.59
Se.IL-6 (pg/ml)	2.4(1.5-4.2)	1.9((1.3-3.0)	0.08
Se.Leptin (ng/ml)	40.2(25.2-51.7)	33.8(23.8-58.7)	0.83

Table 2 Patients' characteristics

Data shown as mean (SD) or median (interquartile range); BMI: boday mass index, SBP, systolic blood pressure, DBP, diastolic blood pressure; MABP: mean arterial blood pressure; FPG, fasting flasma glucose, Total-, LDL-, HDL-chol, Total-, LDL-, HDL-cholesterol; TG: triglycerides; HOMA-IR, homeostasis model assessment of insulin resistance; Se.adipo, serum adiponectin; Se.IL-6, serum interleukin-6, Se.MCP-1, serum monocyte chemoattractant protein-1.

Medication	Non-diabetic group (n=40)	Diabetic group (n=20)
Statins	3/40	8/20
Angiotensin converting enzyme	5/40	7/20
Angiotensin-2 receptor antagonists	0/40	2/20
Aspirin	1/40	3/20
Selective serotonin reuptake inhibitor	8/40	4/20
Tricyclic antidepressant	5/40	1/20

Table 3 Medication regimen in non-diabetic and diabetic group.

4.3.2 Capillary and EC density

In the non-diabetic group, SAT showed significantly less capillary numbers compared to OAT (p=0.01, **Figure 21Ai&ii**), while in the diabetic patients, no significant depot-specific difference in capillary numbers was observed (**Figure 21Aiii&iv**). Furthermore, there was an elevation in capillary numbers in SAT in diabetics compared to non-diabetics (p=0.05, **Figure 21Ai&iii**).

The finding was confirmed by manually counting the capillary numbers in each section, result shown in **Figure 21B.**

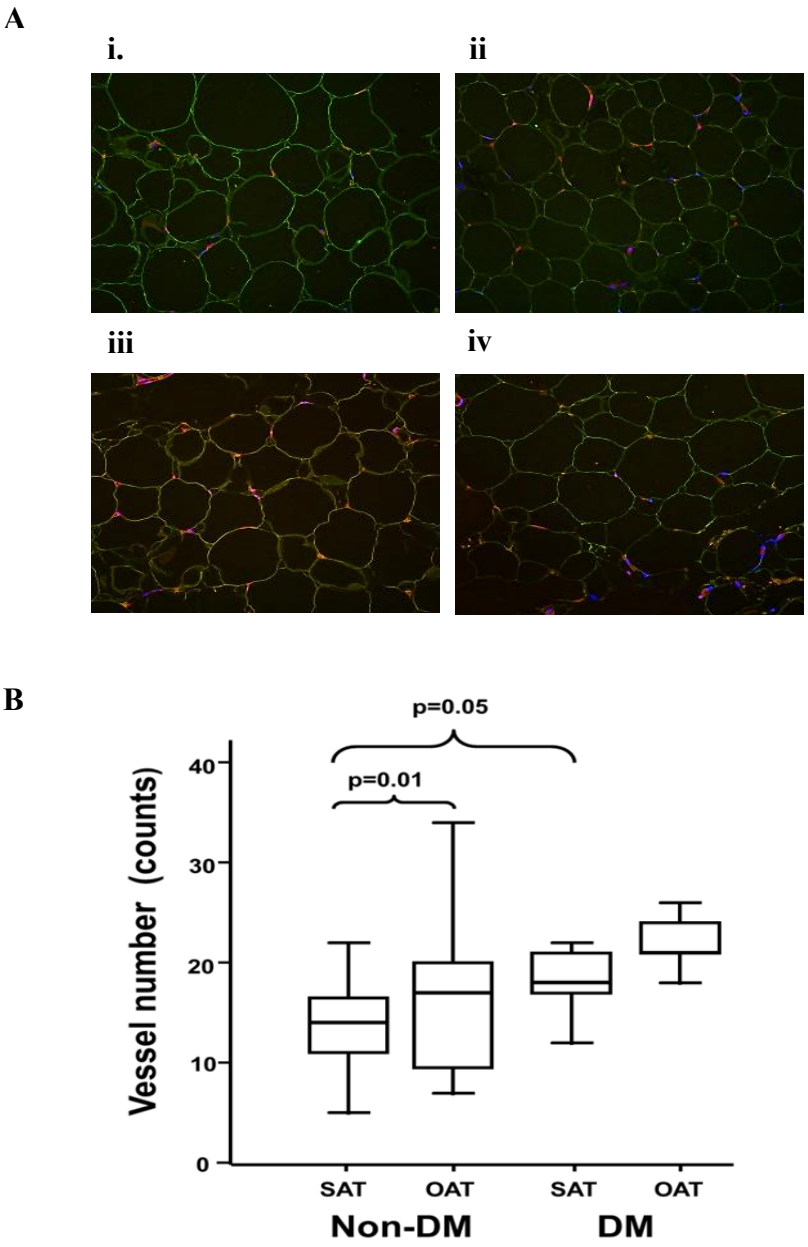

Figure 21 Depot- and diabetes-specific difference in capillary density

Capillary density is significantly lower in SAT (**Ai**) than OAT (**Aii**) in non-diabetic group, while no significant depot-specific difference was observed in diabetic group, SAT (**Aiii**) and OAT (**Aiv**) showed elevated but comparable numbers of capillaries. Nonparametric comparison showed SAT in non-diabetic group has the lowest numbers of capillaries compared to OAT and diabetics (**B**).

Non-DM: non-diabetic obese patients; DM: diabetic obese patients.

Endothelial immunostaining with CD31/CD34 confirmed there was greater number of ECs in the OAT compared with SAT in non-diabetic patients (CD31, **Figure 22 A&B**; CD34, **Figure 22 C&D**). Furthermore, in non-diabetic group, capillary numbers also correlated significantly with both serum adiponectin (SAT: r=0.38, p=0.002; OAT: r=0.44, p=0.008) and serum MCP-1 concentrations (SAT: r=0.51, p=0.002; OAT: r=0.53, p=0.001). These adipokines have previously been shown to induce angiogenesis [165, 166].

A. CD31 **B. CD31**

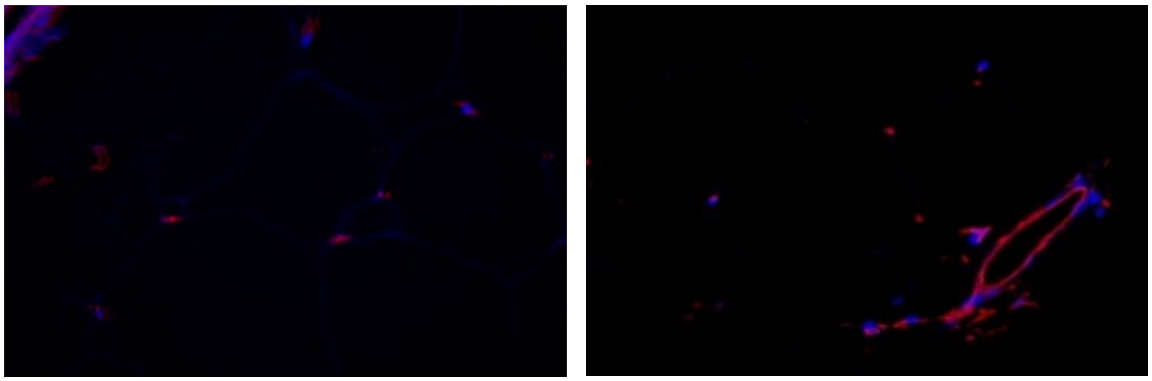

C. CD34 **D. CD34**

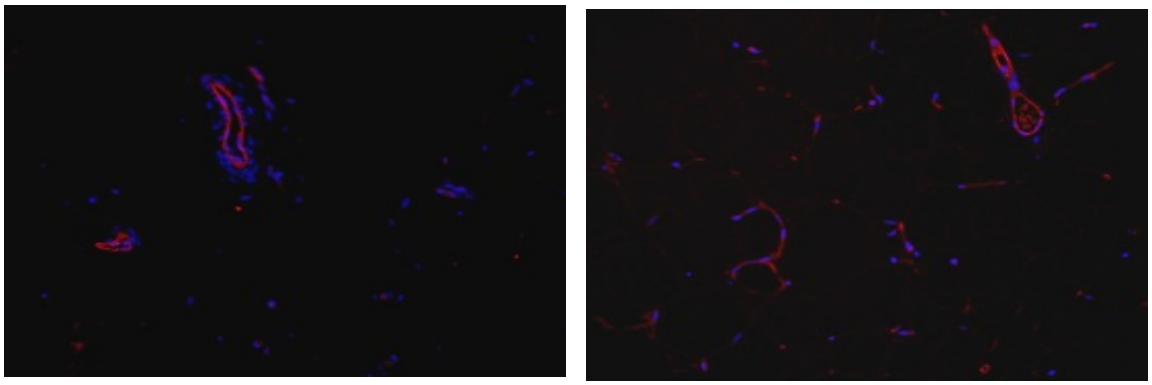

Figure 22 Depot- specific difference in EC quantity by CD31/CD34 staining

The depot-specific difference was confirmed by CD31/CD34 staining. In non-diabetic group, SAT (**A&C**) showed less EC staining compared with OAT **(B&D).**

4.3.3 Angiogenic capacity

In the non-diabetic group, significant depot difference of $R_{V/A}$ was found between SAT and OAT. More capillaries were observed in OAT compared to SAT (SAT: 8.5(8.0-9.5) *versus* OAT: 12.9(8.4-18.9), p=0.03, **Figure 23Ai&ii, B**). Furthermore, diabetic patients displayed higher $R_{V/A}$ in SAT compared to non-diabetics (Non-diabetic SAT: 8.5(8.0-9.5) versus diabetic SAT: 11.5(10.8-11.4), p=0.004, **Figure 23Ai&iii, B**). However, no significant depot difference was found in the diabetic group.

Capillary quantification by particle measurement confirmed the diabetes-specific difference in SAT, which also exhibited the higher capillary quantity in SAT of diabetic group than non-diabetic group.

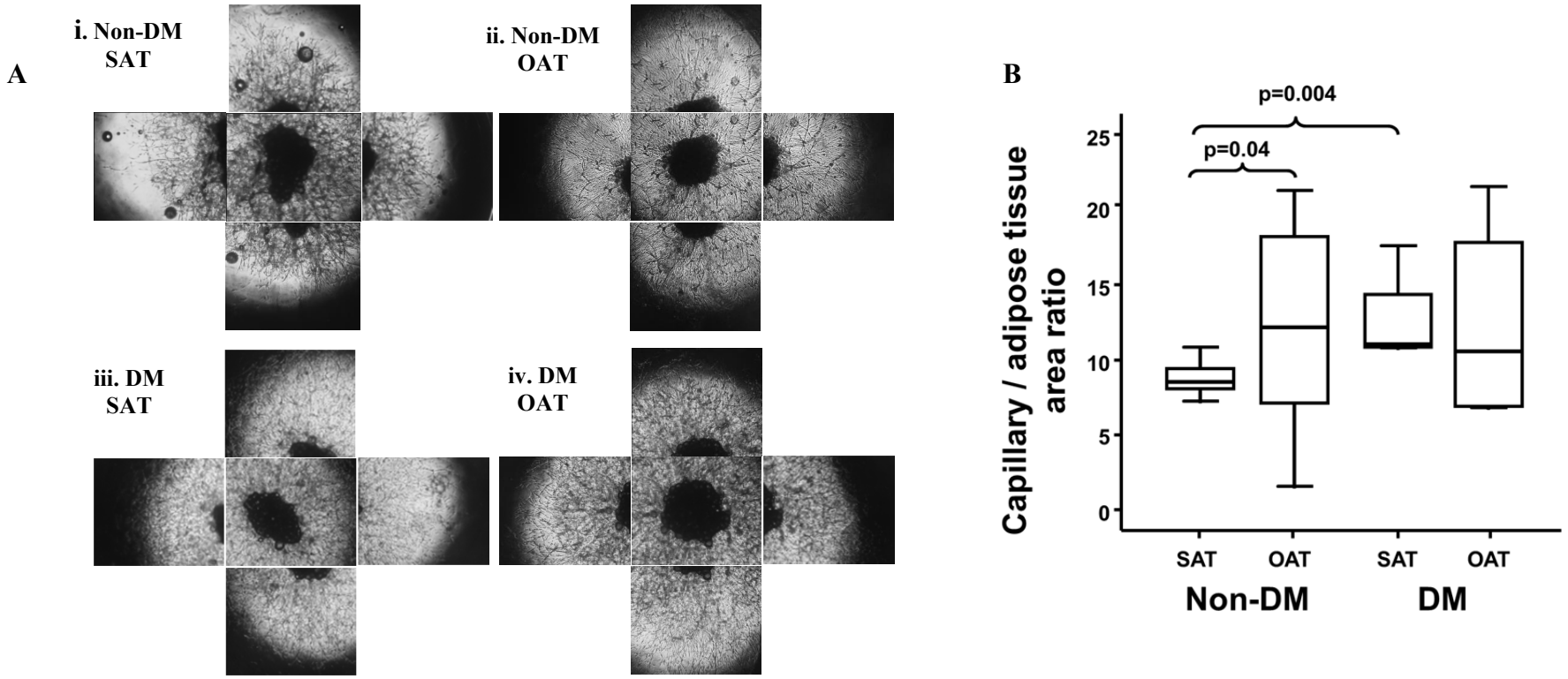

Figure 23 Depot- and diabetes-specific difference in angiogenic capacity

In non-diabetic group, SAT (**Ai**) incubated in matrigel showed less neovasculature expansion compared to OAT (**Aii**), while no significant depot-specific difference was observed in comparison between SAT (**Aiii**) and OAT (**Aiv**) in diabetic group. Furthermore, SAT in diabetic group showed significantly higher angiogenic capacity compared to that in non-diabetic group. This finding was confirmed by nonparametric test that SAT in non-diabetic group showed the lowest angiogenesis compared to OAT and diabetics (**B**). Non-DM: non-diabetic obese patients; DM: diabetic obese patients.

4.3.4 Depot- and diabetes-specific expression of genes regulating angiogenesis

The association between the observed depot- and diabetes-specific differences in capillary density and the expression of genes considered essential to angiogenesis were investigated.

A comparison of the two depots revealed that, in the non-diabetics, among the 84 genes tested, 11, mainly angiogenic genes, were significantly up-regulated while 5 were down-regulated by > 2-fold in OAT compared to SAT. However, in the diabetic patients, only 7 out of the 11 genes were up-regulated and 9 were down-regulated in the OAT compared to SAT (**Fugure 24A**).

Assessment of the effect of diabetes on gene expression in the two depots showed greater number of genes upregulated in the SAT of diabetic, compared to the non-diabetic tissue (**Figure 24B**), especially those of epidermal growth factor (EGF) and NRP-1. However, in the OAT only 4 genes that were mainly chemokines/cytokines were upregulated in the diabetic compared to the non-diabetic tissue, while 3 others were lower in the OAT of diabetics compared to the non-diabetics (**Figure 24C**).

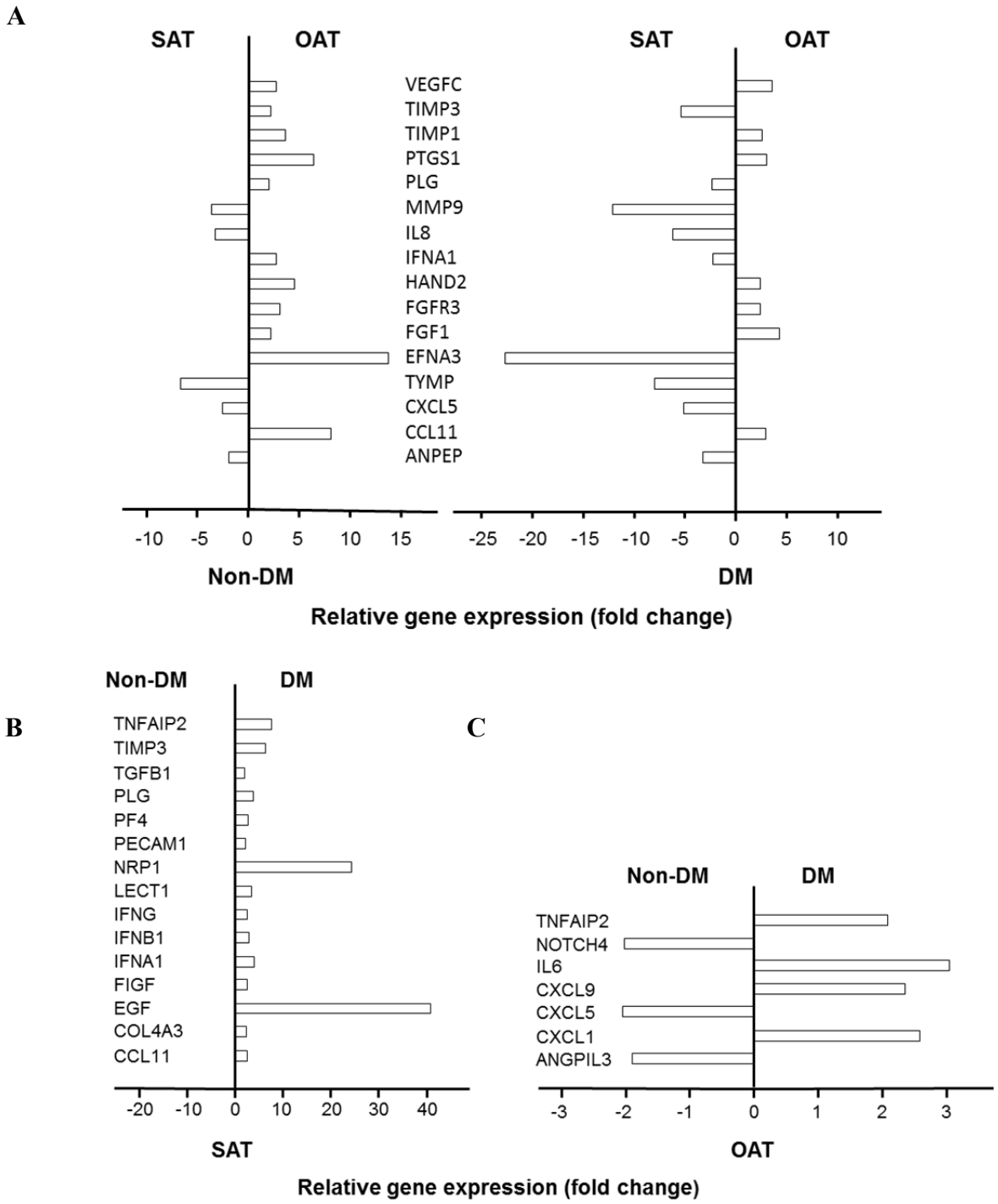

Figure 24 Depot- and diabetes-specific differences in AT angiogenesis-related gene expression

A: In non-diabetic group, most of angiogenic genes were up-regulated in OAT (n=11) compared to SAT (n=5), while diabetic patients showed comparable numbers of gene expression in SAT (n=9) and OAT (n=7).

B: in the comparison between non-diabetic and diabetic group, all gene expression was up-regulated in SAT in diabetes, while no significant diabetes-specific difference was found in OAT.

Non-DM: non-diabetic obese patients; DM: diabetic obese patients; VEGFC: vascular endothelial growth factor C; TIMP: TIMP metallopeptidase inhibitor; PTGS1: prostaglandin-endoperoxide synthase 1; PLG: plasminogen; MMP9: matrix metallopeptidase 9; IFNA1: interferon, alpha 1; HAND2: heart and neural crest derivatives expressed 2; FGFR3: fibroblast growth factor receptor 3; FGF1: fibroblast growth factor 1 (acidic); EFNA3: ephrin-A3; TYMP: thymidine phosphorylase; CXCL: chemokine (C-X-C motif) ligand; CCL: chemokine (C-C motif) ligand; ANPEP: alanyl (membrane) aminopeptidase; TNFAIP2: tumor necrosis factor, alpha-induced protein 2; TGFB1: transforming growth factor, beta 1; PF4: platelet factor 4; PECAM1: platelet/endothelial cell adhesion molecule; LECT1: leukocyte cell derived chemotaxin 1; IFNG: interferon, gamma; IFNB1: interferon, beta 1, fibroblast; IFNA1: interferon, alpha 1; FIGF: C-fos induced growth factor (vascular endothelial growth factor D); EGF: epidermal growth factor; COL4A3: collagen, type IV, alpha 3; NOTCH4: notch 4; ANGPIL3: angiopoietin-like 3.

4.3.5 NRP protein levels in AT

Because NRP-1, a potent mediator of angiogenesis, showed the greatest alteration amongst the genes modulated by diabetes in the SAT, this was further investigated at the protein level.

In this study, two isoforms of NRP-1 were found in human AT. The expression of primary bands (~130 kDa) was relatively lower compared with the secondary ones (>200 kDa), but it was interesting to see that, in the non-diabetic group, more primary bands were observed in OAT (n=5) than SAT (n=1). Furthermore, the protein expression of the primary band was elevated in both SAT and OAT in diabetic patients versus non-diabetics. The secondary band, with a molecular weight of >200 kDa showed to be more highly expressed in OAT than SAT in both non-diabetic and diabetic groups. (**Figure 25**).

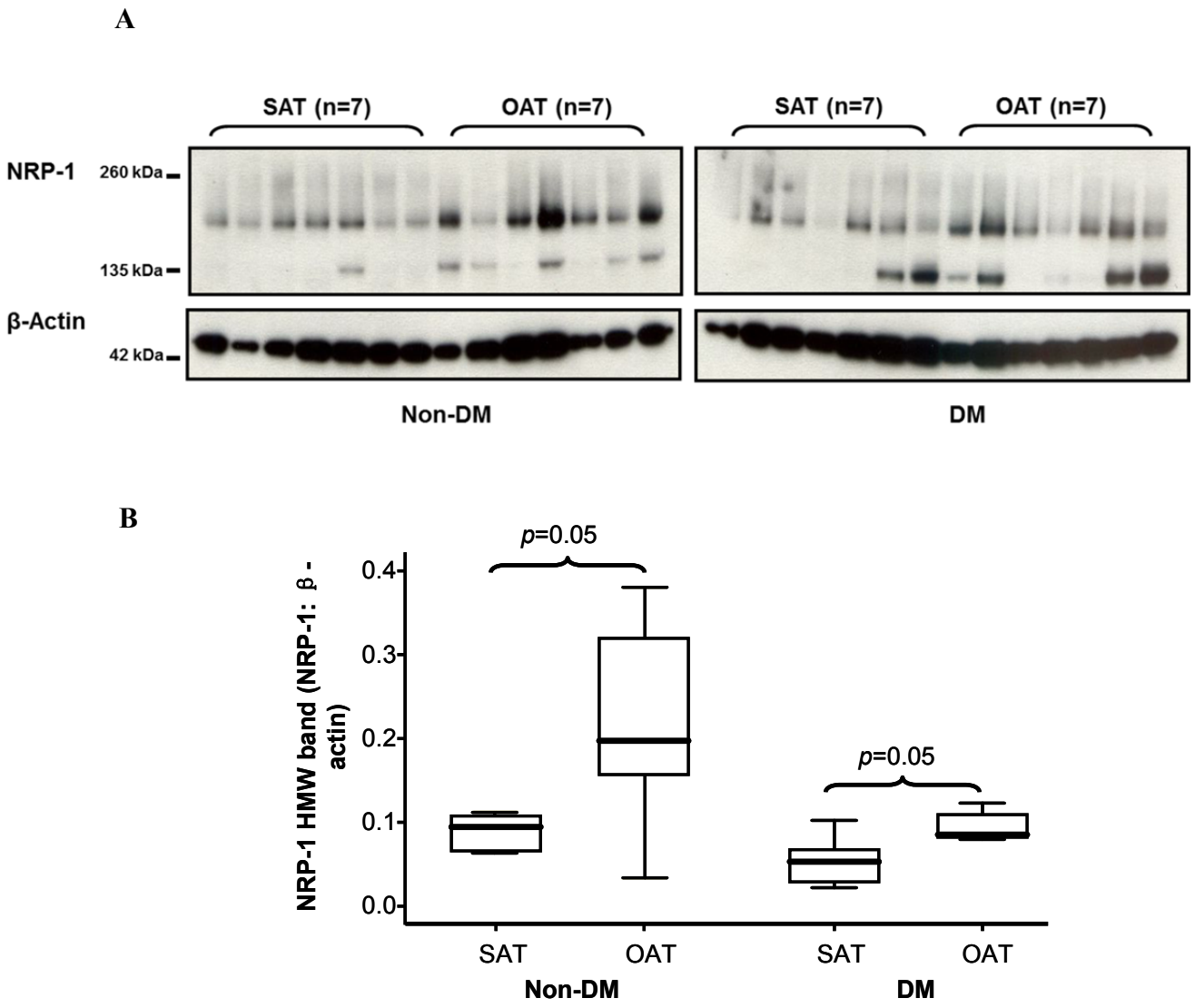

Figure 25 NRP-1 protein levels between depots and in diabetes.

Western blot showed 2 isoforms of NRP-1, larger bands with higher molecular weight (>200kDa) were more highly expressed in OAT compared to SAT in both non-diabetic and diabetic group, while smaller bands with lower molecular weight (~130 kDa) were up-regulated in diabetic compared to non-diabetic group (**A**). Data was analysed by Image J and expressed as grey density ratio between NRP-1 and β-actin (**B**).

Non-DM: non-diabetic obese patients; DM: diabetic obese patients; HMW: high molecular weight.

4.4 Discussion

4.4.1 Paradox between high angiogenesis and inflammation in OAT

This study investigated the depot- and diabetes-specific differences in human AT capillary density, angiogenic capacity and angiogenesis-related gene expression. AT angiogenesis has been shown to be beneficial in rodent samples, sufficient angiogenesis may prevent tissue hypoxia and reverse insulin resistance [51]. In this study, non-diabetic obese patients showed greater capillary numbers and angiogenic capacity in OAT than SAT. Meanwhile, most of angiogenic genes were upregulated in OAT versus SAT. However, paradoxically OAT still displayed more inflammatory and hypoxic micro-environment [37], which perhaps indicates that increased capillary numbers and angiogenesis are not efficient to counter the local AT hypoxia. This could be attributed to the vascular tone dysfunction, since convincing data demonstrated that the vasodilation was impaired in OAT but preserved in SAT [140]. In addition, data in **Chapter 3** suggests vasoconstriction was also compromised due to the NA desensitization. Vascular tone dysfunction may directly restrict local AT blood flow and contribute to the local hypoxic environment.

4.4.2 Angiogenesis was upregulated in obese patients with Type II diabetes

There was also elevation of capillary number and angiogenic capacity in SAT of diabetic compared to non-diabetic subjects. The effect of hyperglycemia and diabetes on angiogenesis is conflicting. In retinopathy, nephropathy, and antherosclerotic plaque, there was excessive angiogenesis, while the neovascularisation was decreased in wound healing and myocardial perfusion [167]. In this study, SAT vessels in the diabetic group was more angiogenic compared to that of non-diabetics, and the microarray data

suggests this increase could be caused by the elevation of a series of angiogenic factors, including VEGF and NRP-1.

The investigation of NRP-1 protein expression in AT showed a new high molecular weight isoform of this molecule. This could be the NRP-1extracellular domain modified by addition of chondroitin sulfate-glycosaminoglycan (CS-GAG) moiety at Ser^{612} in the protein backbone. CS-GAG-linked NRP-1 has been found in HCASMC and some tumour cells [54], while its effect in AT needs further investigation.

Full-length non-GAG NRP-1 was found to be up-regulated in both depots in diabetics compared to the non-diabetics. Data from human epithelial ovarian carcinoma cells showed absence of NRP-1 after 48hr incubation in glucose free medium, suggesting NRP-1 protein expression is glucose dependent [168]. The elevation of NRP-1 in diabetes could be a consequence of hyperglycemia. Also, increased NRP-1 protein expression may, at least partly, explain the higher angiogenic capacity and capillary density in OAT and diabetes.

4.4.3 Technical limitations

In neovasculature measurement, two different methods were used to identify the capillary quantity in each depot. Both of them showed a significant difference in SAT between non-diabetic and diabetic individuals, but only area measurement showed a depot-specific difference. This could be due to the limitation of the threshold function, which may exclude part of the vessels along with the background and loss of sensitivity to detect the depot difference. Furthermore, this chapter displayed two types of capillaries, one is the pre-existing capillary within AT stained by UEA, the other is the neovasculature sprout from AT. However, the maturation of vasculature includes the EC tube structure formation and VSMC recruitment, current data can not identify the association between these two types of vessels, future study needs to focus on the

vascular morphogenesis, also EC and SMC markers may be required to fully identify the components of neovasculature.

The microarray was used for the identification of depot- and diabetes-specific difference in AT angiogenesis-related gene expression. It showed a series of mRNA expression involved in AT angiogenesis, and the sensitivity is reliable, which has been confirmed by western blot. However, the expense of the microarray plates and related reagents may restrict its utilization in studies with larger sample sizes.

NRP-1 was selected to validate the microarray and two isoforms were observed. Although previous study proved that the high molecular weight band is a glycosylated form of NRP-1, we did not confirm that in AT due to the technical limitations. Future study is required to fully investigate the different isoforms of NRP-1 as well as how to inhibit the glycosylation of NRP-1 in AT.

4.4.4 Conclusions

Adipose capillary density and angiogenic capacity are lower in SAT in non-diabetic obese patients compared with OAT and diabetics, but AT function is preserved in these vessels as seen by its normal vascular tone (described in **Chapter 3**). The overexpression of a series of angiogenesis-related genes may explain the higher angiogenesis in OAT and in diabetes, perhaps a consequence of local inflammation and hypoxia.

Chapter 5

The protective effect of PVAT and endothelium-derived adiponectin

5.1 Introduction

Blood vessels comprise three distinct layers, the intima, media and the outermost layer, the adventitia, that within medium to large vessels, are surrounded by a cushion of PVAT. PVAT comprises discrete adipocytes containing a network of capillaries and nerve fibres as well as a variety of other cell types. Leptin and adiponectin, as two of the most abundant adipokines in the circulation, are critical in the development of metabolic disorders and cardiovascular diseases. High levels of leptin and low levels of adiponectin are associated with adverse cardiovascular events [169]. Recent studies have described the endothelium-dependent vasodilatory effects of adiponectin and leptin [88, 170]. PVAT is considered a major source of vasoactive adipokines and, since no fascia separates this fat depot from the vessel adventitia, it facilitates the access of PVAT-derived adipokines to the vessel wall [103]. Recently, adiponectin has been shown to be expressed and secreted by human renal tubular epithelial cells [171], suggesting that adiponectin may not be produced by adipocytes solely. In addition, significant levels of adiponectin have been found in injured vascular walls [172], implicating a vascular source of adiponectin production. Apart from PVAT-derived adiponectin, vascular and endothelial sources have not been fully investigated.

To test the hypothesize that human vasculature and endothelium are associated with adipokine production independent of PVAT both adiponectin and leptin levels were measured in:

1) Saphenous vein (SV) and the internal thoracic artery (ITA) dissected free of surrounding PVAT.

2) Isolated PVAT removed from SV and ITA.

3) Local subcutaneous adipose depots (SAT, SV=calf/thigh; ITA = sternum).

Adiponectin and leptin mRNA expression was also determined in cultured human coronary artery endothelial cells (HCAECs) and umbilical vein endothelial cells (HUVECs).

5.2 Methods

Patients undergoing CABG were recruited from Orebro University Hospital, Sweeden. SV and ITA samples (n=6) were obtained at surgery with PVAT being isolated from graft material. In addition, 'local' subcutaneous fat (SV=calf/thigh; ITA = sternum) was collected (~0.05g). A separate segment of vessel with PVAT intact was also removed for subsequent immunohistochemistry. All samples were then transferred to UK and stored at -80^{o}C until use. The study was approved by local ethical committee and patients gave written informed consent.

Total protein was extracted from vessels, PVAT, and SAT, and the total protein concentration was estimated using BCA protein Assay (described in **Section 2.5.1**). Adiponectin and leptin levels were measured by commercially available two-site ELISAs (described in **Section 2.2.2**). Final adipokine concentration was adjusted for total protein concentration.

Total RNA was extracted from HUVECs and HCAECs (cell culture described in **Section 2.2.1**). The mRNA expressions of adiponectin and leptin were determined by real-time PCR (described in **Section 2.4**). β-actin was selected as house-keeping gene. Data was expressed as a ratio of target gene Ct / β-actin Ct.

Data were analysed using SPSS version 14 for Windows (Statistical Package for the Social Sciences, SPSS UK Ltd, Chertsey, UK). Data are shown as mean (SEM), or for mRNA expression data as median (interquartile range), in text and in figures. Comparison of mRNA expression data was by Mann-Whitney test. Significance was

defined as $p \leq 0.05$.

5.3 Results

5.3.1 Tissue levels of adiponectin and leptin

As shown in **Figure 26**, Leptin (A) and adiponectin (B) levels measured by ELISA in isolated vessels (V); perivascular adipose tissue (PVAT) and subcutaneous adipose tissue (SAT) of SV (vein) and ITA (artery).

In the ITA, there were low levels of leptin both in the vessels and the surrounding PVAT when compared to the local SAT (vessel: 0.08(0.02), PVAT: 0.13(0.04) *versus* local SAT 0.59(0.23), pg/μg total protein). Isolated SV samples showed similar low leptin levels with detectable concentrations in the surrounding PVAT (vessel: 019(0.15), PVAT: 0.27(0.09) *versus* local SAT 0.72(0.25), pg/μg total protein, **Figure 26A**).

Interestingly, while the vessel and PVAT adiponectin levels were similar, both were higher when compared to SAT (ITA vessel: 0.36(0.14) *versus* local SAT: 0.31 (0.15); SV vessel: 0.29(0.04) versus local SAT: 0.20(0.07), ng/ μg total protein, **Figure 26B**).

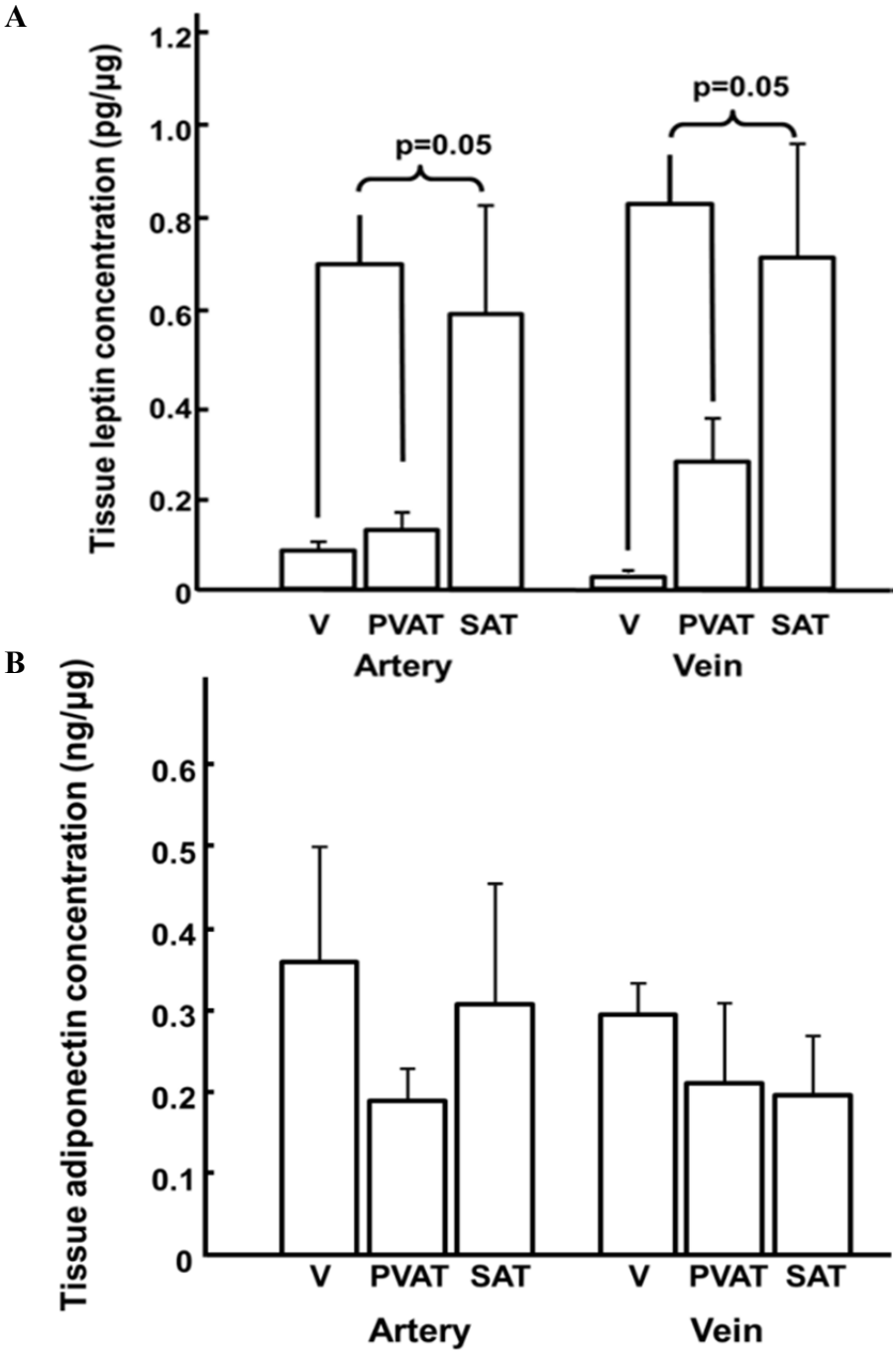

Figure 26 Adipokine levels of vessels, PVAT and SAT

Leptin (**A**) and adiponectin (**B**) levels measured by ELISA in isolated vessels (V); perivascular adipose tissue (PVAT) and subcutaneous adipose tissue (SAT) of SV and ITA. Significant differences are apparent for the SAT compared to either V or PVAT for leptin. No significant differences between V, PVAT or SAT was seen for adiponectin.

5.3.2 Adiponectin and leptin in PVAT and endothelium

A more pronounced cushion of PVAT was observed surrounding the SV than the ITA. Apart from adipocytes the ITA was encapsulated in connective tissue, muscle and brown adipose tissue. **(Figure 27**).

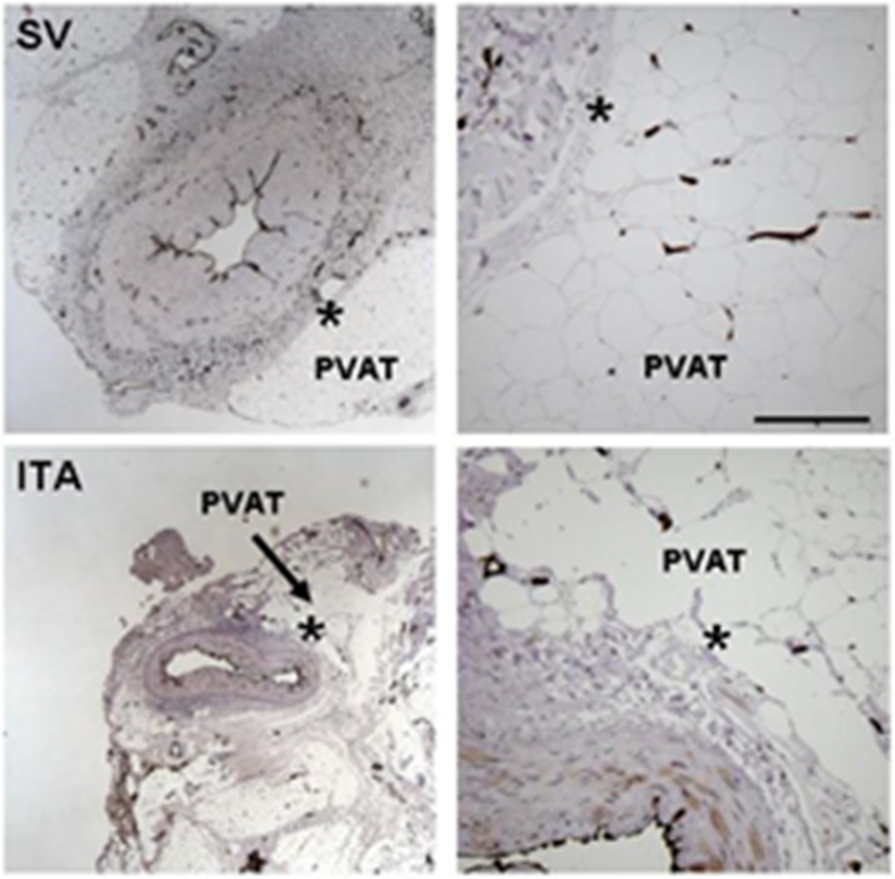

Figure 27 Vessel and PVAT morphology.

Transverse, H&E-stained sections of SV and ITA at low (left) and high (right) magnification, * indicates the region of left panels shown at higher magnification on the right. Scale bar = 2mm for left and 0.5 mm for right panels.

Furthermore, both adiponectin and leptin staining was abundant surrounding adipocyte in PVAT from SV and ITA **(Figure 28A&B),** which again suggests a protective, anti-contractile effect of PVAT in maintenance of normal vascular function as described in previous study [173].

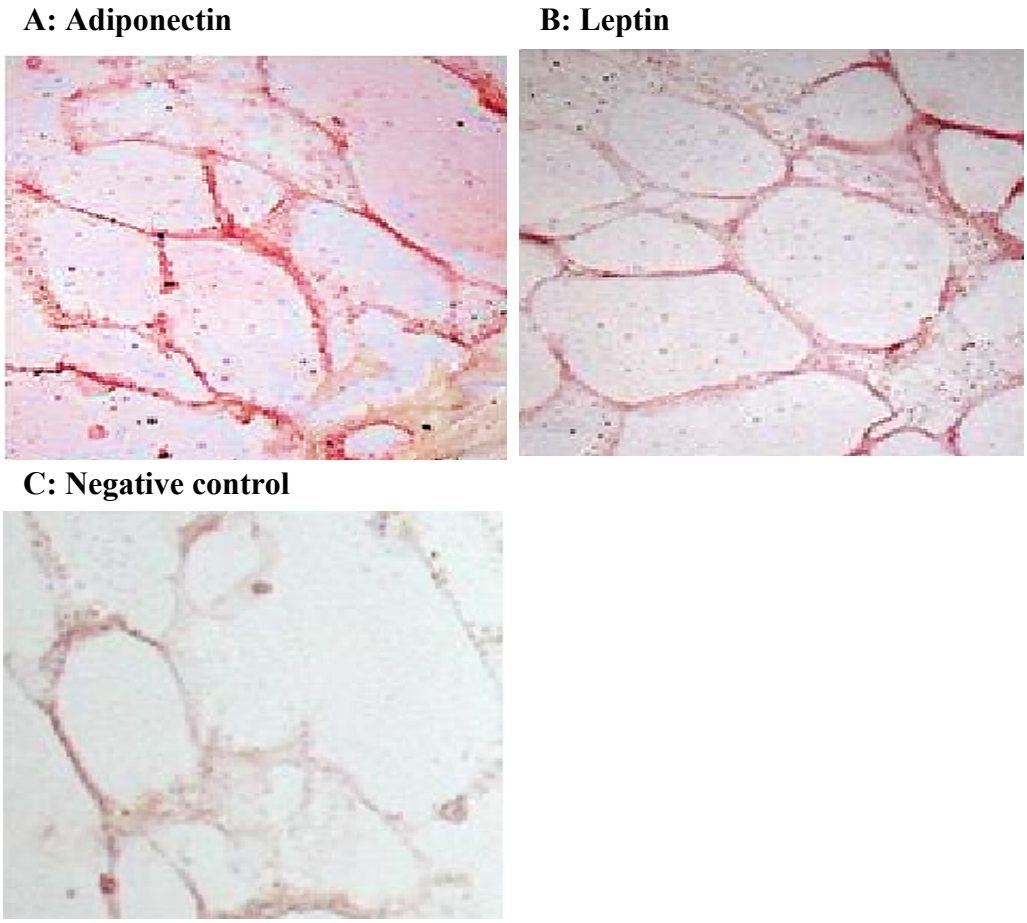

Figure 28 Adiponectin and leptin staining in PVAT

A: PVAT adiponectin staining;

B: PVAT leptin staining;

C: Negative control.

Although there was no adiponectin immunostaining in either vessel wall, discrete staining was associated with endothelial cells lining the lumen of both the artery and the vein as well as those of the vasa vasorum and capillaries embedded in PVAT (**Figure 29A&B**), while no evidence of leptin staining was found associated with endothelial cells lining the vessel lumen (**Figure 29C**), the vasa vasorum or capillaries (not shown).

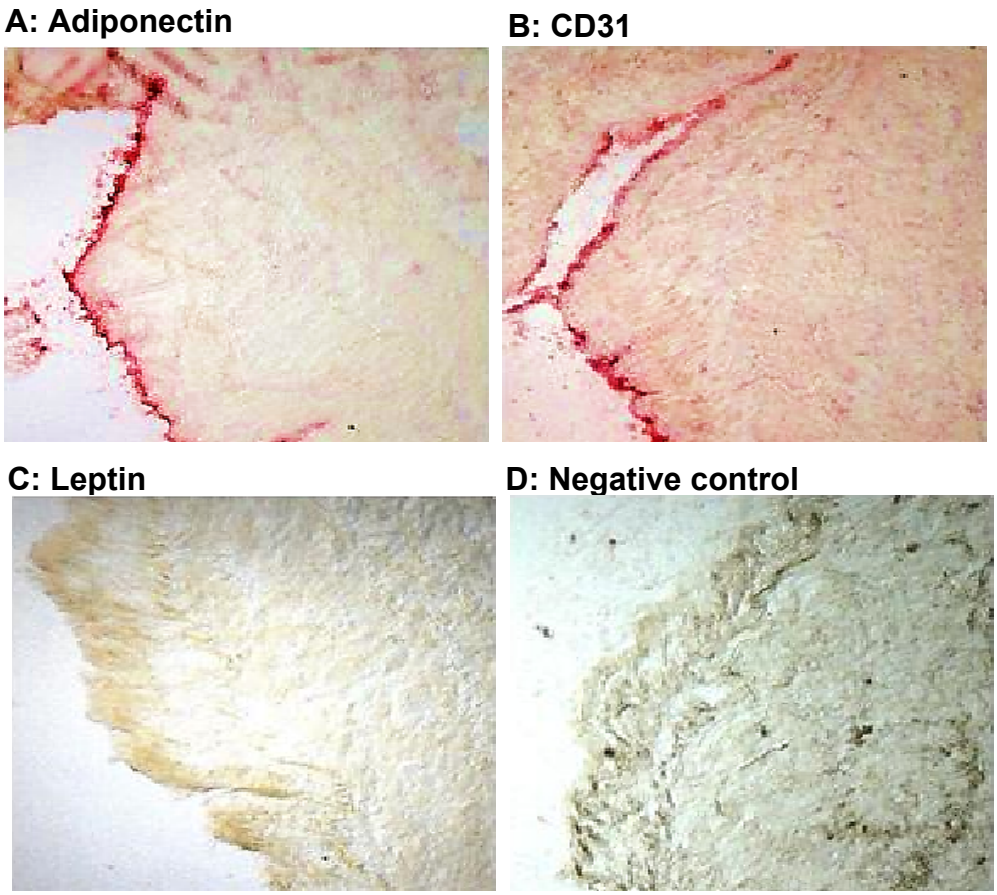

Figure 29 Adiponectin and leptin staining in SV endothelium

A: SV endothelial adiponectin staining;

B: Endothelium identified using CD31;

C: No endothelial leptin staining;

D: Negative control.

5.3.3 Adiponectin and leptin mRNA expression in ECs

Adiponectin mRNA expression is abundant in both HCAECs and HUVECs, while no leptin mRNA expression was detectable. Furthermore, the adiponectin expression is significantly higher in HCAECs than HUVECs (Ct ratio, artery: 0.59(0.59-0.60) *versus* vein 0.54(0.53-0.55), p=0.03, **Figure 30**).

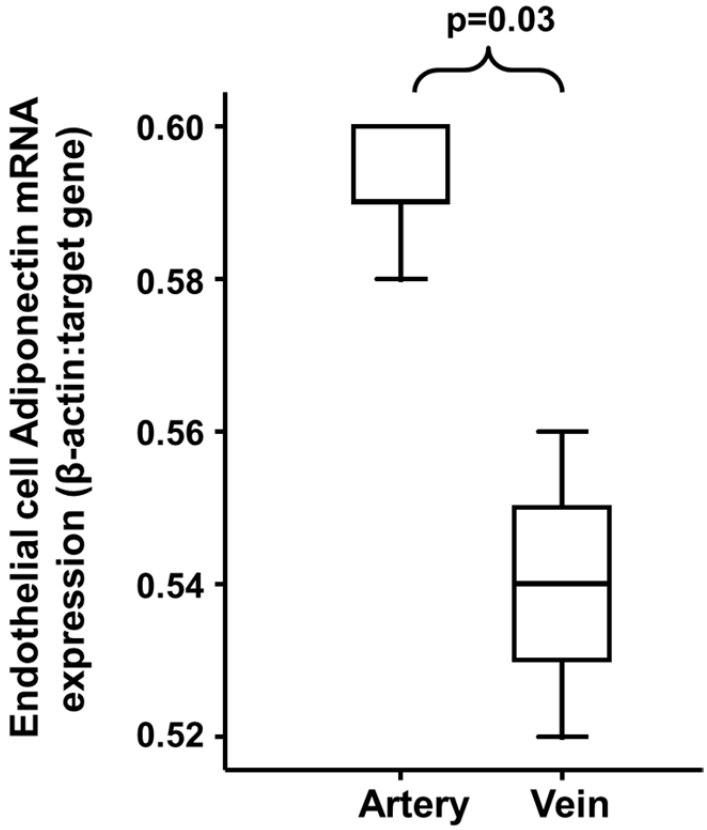

Figure 30 Artery/vein difference of adiponectin mRNA expression in ECs

Adiponectin mRNA expression is abundant in both HCAECs and HUVECs, and it is more highly expressed in artery compared to the vein ($p<0.05$). Data expressed as Ct ration between β-actin and adiponectin.

5.4 Discussion

The main finding of this chapter is the first identification of endothelial adiponectin expression in human vessels used as bypass grafts in patients undergoing CABG. This source of adiponectin expression and production is independent of PVAT.

The interplay between AT and the vasculature has been the focus of a number of studies. Both AT-derived SVF and adipocytes can induce angiogenesis and alterations in vessel structure, suggesting adipocytes and vascular cells may share the same progenitor [46]. Furthermore, a preadipocyte marker has been detected in ECs, implicating the endothelial origin of certain adipocytes [47]. This data suggests that ECs may differentiate from adipocyte progenitors and display a similar secretory ability to adipocytes in terms of adiponectin production, while the leptin secretion was diminished, a finding supported by the recent study showing adiponectin expression in mouse aortic endothelial cells [174].

The mechanisms associated with adiponectin production from the endothelium are unclear, although data showing that EC adiponectin mRNA expression is elevated in cells exposed to supra-physiological levels of insulin was obtained (data not shown). Since circulating adiponectin levels show a positive correlation with insulin sensitivity [175], this data implies that adiponectin production in the endothelium may be also influenced by the metabolic status of the patients.

Although the effects of endothelium-derived adiponectin are unknown, adiponectin is generally accepted as a protective molecule with anti-inflammatory, anti-diabetic and anti-atherogenic effects [176]. In addition, adiponectin is a vasodilator inducing vasorelaxation by elevating eNOS bioavailability and enhancing NO production [74]. Abundant adiponectin was shown in the endothelium and PVAT in this study. In conventional CABG preparations the SV graft is stripped of PVAT, leading to a loss of

PVAT-derived adiponectin as well as a potential reduction of endothelial sources. It has been reported that SVs harvested by the 'no-touch' technique, with intact PVAT and endothelium, provide superior grafts compared with those prepared by conventional CABG [177]. This improvement may be, at least in part, due to the protective effects of adiponectin in the intact PVAT and endothelium. Moreover, the higher adiponectin mRNA expression in the HCAECs may explain the arterial superiority as a bypass graft [178].

Although the current study did not reveal the functional importance of endothelium-derived adiponectin, previous data from rabbits demonstrated that local adiponectin elevation in intima significantly suppressed mRNA expression of atherosclerotic adhesion molecules and reduced atherosclerotic plaque area in vivo. Furthermore, adiponectin transferred from adventitia showed a similar effect, which implicates luminal (endothelium-derived) and exogenous (PVAT-derived) adiponectin may equally contribute to preventing atherosclerosis in cardiovascular system [179]. Future investigation is required to determine whether endothelial adiponectin concentrations can be up-regulated and contribute to either the atheroprotective and/or vasodilatory capacities of grafted vessels.

Chapter. 6

Discussion and conclusion

6.1 Heterogeneity of the patients

The initial aim of this thesis was to identify the AT metabolic and secretory features of MHO individuals, thus individuals recruited in this thesis were all morbidly obese with significant AT expansion. Previous studies compared obese with lean individuals and showed a series of obesity-related dysfunctions due to the excess AT deposition [180-183]. However, there are no significant metabolic differences between MHO and lean healthy individuals, which cannot be explained by the AT expansion. Thus, AT dysfunction, rather than fat mass per se, may contribute to metabolic disorders in obesity. Comparison between different subtypes of morbidly obese patients may be more important to reveal the mechanisms behind MHO individuals, rather than comparing obese and lean phenotypes. Additionally, the advantage of this patient cohort is a good homogeneity in most other parameters between the two groups, which facilitates the investigation of the AT- and diabetes- specific differences between groups. Nevertheless, the limitation of this patient cohort is the lack of healthy, insulin-sensitive, control individuals. Although data showed SAT in non-diabetic obese patients has greater NA sensitivity, lower levels of NA synthesis, collagen deposition and angiogenesis compared to OAT and diabetes, it is still not clear whether healthy individuals display similar vascular features.

6.2 Adrenergic effect on AT glucose/lip metabolism and blood flow

In **Chapter 3**, the adrenergic effect on AT vasoconstriction was investigated. The major finding is the vessel desensitization in OAT and diabetes caused by local chronic NA elevation. Sympathetic nerves innervate AT and the nerve ending reaches the adipocyte and vasculature [154, 184]. Thus, the local NA synthesis and release in AT facilitate a direct adrenergic regulation of AT metabolism and vasculature via paracrine and

autocrine, rather than endocrine signals. Furthermore, under adrenergic regulation, there is close interplay between glucose/lipid metabolism, vascular tone and AT blood flow (ATBF), which is discussed below.

6.2.1 Glucose and lipid

In lean, insulin sensitive individuals, in response to oral glucose ingestion, there was catecholamine elevation concomitant with vasodilatation and elevated ATBF [185]. This effect was abolished by β-adrenoceptor antagonist [159], which implicates the adrenergic regulation in glucose-mediated AT vasodilatation. However, glucose-mediated vasodilatation was impaired in glucose-intolerant individuals even at the very early stages [186]. Additionally, an *in vivo* human study showed that AT glucose uptake in non-diabetic obese individuals was elevated after the stimulation of α1 adrenoceptor, independent of insulin, while this effect was also abolished in obese patients with insulin resistance [187, 188]. Thus, vascular tone regulated by NA may play a role in AT glucose metabolism, while compromised vasodilatation and desensitized vasoconstriction may be important factors leading to hyperglycaemia.

The lipolytic effect of the sympathetic nervous system in AT has been extensively investigated (reviewed in [154]). Catecholamine-mediated AT lipolysis is dependent on the balance between lipolysis stimulated by the β_2 adrenoceptor activation and anti-lipolytic effect of α_2 adrenoceptor activation [189]. A recent study compared SAT lipolysis induced by NA in overweight non-diabetic and diabetic individuals. NA infusion significantly increased non-esterified fatty acid (NEFA) output in both groups, but the elevation was delayed in the diabetic group. The non-diabetic subjects also showed lower NEFA levels in post-NA infusion compared with pre-NA infusion stage, while that in diabetic individuals post-NA NEFA remained higher than the pre-infusion values [113]. These data demonstrated that the adrenergic dysregulation may be associated with increased lipolysis but decreased NEFA clearance, which could

contribute to the elevation of circulating NEFA and increase the risk of ectopic AT accumulation. Interestingly, the adrenergic effect on vascular tone is coordinated with AT lipolysis. Thus, α_2 adrenoceptor stimulation leads to vasoconstriction and suppression of lipolysis, while β_2 adrenoceptor stimulation promotes vasodilatation as well as lipolysis [190]. Therefore, the delayed excess release of NEFA could be, at least partly, due to the impaired vasoconstriction leading to suppression of lipolysis.

Nevertheless, in this thesis, SAT α adrenoceptor mRNA expression was found to be higher in diabetic compared to non-diabetic group (β-actin/α-adrenoceptor Ct ratio, Non-diabetic *versus* Diabetic: α1: 0.60[0.57-0.63] *versus* 0.63[0.60-0.69], p=0.04; α2: 0.71[0.69-0.73] *versus* 0.77[0.72-0.80], p=0.01), which cannot explain why the NA sensitivity is abolished in diabetes. Further studies are required to show the vascular adrenoceptor expression at the protein levels.

6.2.2 Vascular tone and ATBF

Most of previous studies focused on the NA spillover from heart and kidney, while AT *per se* is less investigated. Furthermore, studies have mainly focused on the endothelium-dependent vasodilatation and the effect of weight reduction on vascular function [138, 141, 191]. There is only one study investigating the NA-mediated vasoconstriction in SAT comparing non-diabetic and diabetic obese individuals [141]. This study reported higher vasoconstriction in the diabetic compared to non-diabetic group but failed to show the increased SAT NA sensitivity of the non-diabetic vessels within the physiological range. In **Chapter 3**, local NA synthesis in AT and adrenergic regulation on vascular tone was demonstrated, and reporting for the first time, the difference in depot- and diabetes-specific NA sensitivity. These data suggest that even in the context of obesity-related hyperinsulinemia and sympathetic activation, SAT in non-diabetic individuals retain normal vascular function by preserving local NA sensitivity (the potential mechanism is further discussed in **Section 6.3**&**6.4**). However,

due to the technical limitations, we could not fully clarify the cellular source of NA. A recent rodent study showed NA production from adipocytes [118], but here it cannot be excluded that NA may also be derived from adrenergic fibres and macrophages.

Adequate blood flow is a direct reflection of normal vascular function. It has been reported that fasting blood flow is lower in insulin-resistant/obese patients compared to lean healthy individuals [192]. Furthermore, there is a regional difference shown as higher basal ATBF in abdominal area compared with femoral depot [193]. However, up to date, there is no direct comparison of ATBF between SAT and OAT. A recent human study showed that physiological levels of NA infusion in abdominal SAT significantly increased the microvascular volume and stimulated the capillary recruitment in non-diabetic overweight individuals but no changes were observed in diabetics [113]. This could be partly explained by the impaired vasodilatation in SAT of diabetic individuals [141]. However, the mechanism as to why microvascular volume was not changed in SAT in diabetics is still unclear. Our data suggest that SAT microvasculature of non-diabetic obese individuals is more responsive to physiological concentrations of NA; the coordination between vasoconstriction and vasodilatation may generate a "pumping" effect to regulate the re-distribution of ATBF, whereas this effect is abolished in OAT and diabetes due to the impairment of both vasoconstriction and, the previously reported vasodilatation.

6.3 The potential mechanism of sympathetic nervous activation in obesity

6.3.1 AT expansion, depot-specific difference

One potential drive of sympathetic activation is elevated adipose mass. Increased abdominal AT is associated with sympathetic nerve activation. Especially, the OAT expansion, compared with SAT, is more correlated with sympathetic nerve overreactivity [151]. A study in humans showed that there was no significant

sympathetic nerve activation in subcutaneous obesity [153], which could be also attributed to the low levels of local NA synthesis and preserved NA sensitivity in this depot. In contrast, multiple factors may be involved in OAT-induced sympathetic nerve activation, which includes elevated non-esterified fatty acid, leptin, macrophages and other inflammatory cells [155].

6.3.2 Hyperinsulinemia

As described in **Chapter 3**, the non-diabetic obese group maintained normoglycemia by hyperinsulinemia. The hyperinsulinemia-mediated NA spillover has been investigated in several studies. Under acute exposure to hyperinsulinemia, there is an elevated plasma concentration of NA, mainly from muscle and AT [194, 195]. Interestingly, this is contradictory to that seen in nonobese individuals experiencing modest weight gain, which is associated with increased sympathetic nervous activity but no changes in insulin concentration [196]. Therefore, it cannot be concluded that sympathetic nervous activation is only triggered by hyperinsulinemia. Furthermore, NA spillover mediated by acute elevation of insulin may not represent the physiological condition *in vivo*, while our data focused more on the chronic elevation of NA in OAT and diabetes, as well as its effect on vascular tone and collagen deposition. It suggests that vascular function may be compromised due to the long-term exposure to elevated local NA rather than the acute stimulation.

6.4 The potential mechanism of vessel desensitization to NA

The phenomenon of vessel desensitization by NA was firstly described thirty years ago [157]. Rat aortic ring incubated in Krebs solution was exposed to 800 $ng \cdot kg^{-1} \cdot min^{-1}$ NA. The vessel desensitization was exhibited as a significant elevation of EC_{50}. Furthermore, the desensitization was abolished when the vessel NA uptake was blocked, implicating

the desensitization of adrenoceptors caused by the accumulation of intracellular NA. Furthermore, blockade of catchol-O-methyltransferase (an enzyme degrading NA) significantly enhanced desensitisation, which suggests that the desensitization is induced by NA rather than its metabolite.

Although the mechanism of vessel desensitization in AT is still unclear, in cirrhotic patients vascular hypocontractility was induced by the desensitization of GPCRs [197]. GPCRs are a large family of integral membrane receptors transducing information from extracellular stimuli into intracellular secondary messenger via G-protein and its downstream regulation [198]. One of the best characterised GPCRs is α adrenoceptor. Normally NA activation of its functional α1 adrenoceptor disassociates G-protein α subunit from the β/γ subunits and subsequently regulates intracellular Ca^{2+} and vasoconstriction. As a negative feedback, activation of GPCRs also recruits β-arrestin-2 protein mediated by G-protein-coupled receptor kinase 2 (GRK-2), thereby hindering the intracellular vasocontractile pathway. However, due to the high-intensity or long-term exposure to stimuli, there is an elevation of either GRK-2 or β-arrestin-2 protein, leading to the vessel desensitization [197]. The vessel desensitization observed in OAT and diabetes perhaps shares a similar mechanism, which is worth further investigation.

6.5 AT fibrosis mediated by sympathetic nervous activation

Multiple factors may contribute to tissue fibrosis. Previous studies mainly investigated the inflammation- and hypoxia-mediated AT fibrosis, HIF-1α was suggested as a major initiating factor for fibrosis induction (reviewed in [39]). Interestingly, chronic hypoxia is associated with sympathetic excitation, which has been shown in individuals with obstructive sleep apnoea (OSA) and chronic obstructive pulmonary disease [199]. However, direct adrenergic regulation of collagen deposition is less documented. Accumulating data demonstrate that catecholamine modulates tissue remodelling by

elevating collagen gene/protein expression [134, 200], and the local adrenergic effect on fibrosis was mainly investigated in heart and kidney [201, 202]. Our data suggest AT-derived NA may also mediate local fibrotic response in AT via autocrine or paracrine signals. Although current data is not adequate to identify the specific subtypes of collagen in AT, abundant collagen gene type Iα1 was detected in AT, which was also up-regulated by NA incubation. In both rat and human studies, the imbalance between collagen type I deposition and degradation is associated with myocardial fibrosis and essential hypertension [203, 204]. It has been reported that human collagen type I production in VSMCs was stimulated by Ang II via mitogen-activated protein kinase /ER kinase pathway [205, 206]. Future studies should focus on the pathway involved in the AT collagen deposition induced by NA.

It is noteworthy that increased TGF- β levels were observed in morbidly obese patients compared to the lean individuals [164]. TGF- β/Smad3 pathway is highly involved in pathological alterations in obesity and type II diabetes. It is demonstrated that TGF-β/Smad3 regulates insulin gene transcription in β-cells in pancreatic islets [207], while Smad3 knockout mouse display resistance to high-fat diet-induced obesity, also these mice showed improved glucose tolerance, insulin sensitivity and β-oxidation [208]. However, TGF- β-mediated fibrosis in AT is less concerned. It has been showed that, in diseased vessels, TGF-β type 1 receptor expression was enhanced, leading to a stimulation of ECM production [209], further study should focus on the investigation of TGF-β and its receptor gene and protein expression in AT between depots and disease. Additionally, microarray data in **Chapter 4** showed a significant up-regulation of TGF-β in SAT in diabetic compared to non-diabetic group, it could be explained by the hyperglycemia in diabetics, which has been proved to enhance TGF-β mediated fibrotic effect by elevating TGF-β receptor gene expression [210]. Also up-regulation of TGF-β

in SAT in diabetics may, at least partly, explain the higher collagen deposition in this group.

6.6 Interplay between AT fibrosis and angiogenesis

Current data demonstrate the elevated collagen deposition in OAT and diabetics is concomitant with excessive angiogenic response. One popular hypothesis predicts that adipocyte overexpansion results in insufficient angiogenesis, tissue hypoxia, adipocyte necrosis, inflammation and fibrosis [41, 211]. During this process, the accumulation of collagen may make the tissue stiffer and inhibit angiogenesis [125]. This hypothesis was supported by the evidence that overexpression of HIF-1α in AT of genetic mice failed to trigger an angiogenic response, but unexpectedly stimulated tissue fibrosis [212]. However, current data suggest both fibrotic and angiogenic responses are stimulated by local inflammation and hypoxia. Furthermore, vascular tone, rather than angiogenesis, may be affected by local collagen accumulation. Although the mechanism is still unclear, a recent study showed that adipocyte-derived endothrophin, a cleavage product of the collagen type VI, induced angiogenesis in mammary tumor growth via recruiting endothelial precursor cells while also contributing to tissue fibrosis [213].

6.7 Adipocyte morphology

In **Chapter 3**, the adipocyte area was measured by manually tracing the cell boundary. The result was also confirmed by measuring the adipocyte length, though these data were too preliminary to include. However, the current measurements for adipocyte size may still not be accurate enough to show the actual value *in vivo*. Unlike some other types of cell, the adipocyte is ball-shaped and lipid engorged. The shape could be altered by depletion of the cellular lipid (squeezing) or stretching during the paraffin process or be affected by the angle of dissection. Therefore, in this study, we focused on

the relative size difference between depots rather than the physiological values. Furthermore, adipocyte morphology may be also affected by collagen deposition, thus adipocytes isolated by collagenase digest may not reflect the condition *in vivo*. In future study, the development of a 3D model may be required for detailed investigation of AT structure and morphology.

6.8 The paradox between AT angiogenesis and hypoxia

The close interplay between adipogenesis and angiogenesis has been widely reported. During optimal tissue growth, there is recruitment of both adipocytes and vascular cells, which was displayed as adipocyte migration towards neovasculature [43]. However, the angiogenesis in AT of obese patients may be an adaptive response triggered by local hypoxia. Although animal models have shown that elevated angiogenic response induced by VEGFA has a protective effect in obesity, this has not been confirmed in human studies. Evidence suggests oxygen tension is lower in SAT of obese patients compared to lean individuals, but at levels not low enough to activate the VEGF signalling pathway [41]. In addition, OAT showed elevated angiogenesis-related gene expression, VEGF protein levels and higher capillary density compared to SAT, despite a more inflammatory and hypoxic microenvironment compared to SAT [37, 53]. It is noteworthy that, under hypoxia, although angiogenesis is stimulated, arteriogenesis is less affected [214]. Arteriogenesis describes the process of small pre-existing arterioles developing into functional arteries [215]. It is doubtful whether the neovasculature is mature enough to be functioning; thus vascular function, as well as its regulation of AT blood flow may be more critical in the regulation of AT functions. We presume SAT in non-diabetic obese individuals may be protected from hypoxia by its functional vasoreactivity, despite concomitant capillary rarefaction, which may explain why the VEGF pathway is not triggered in this depot [41]. Moreover, preserved vascular

function may also ensure sufficient blood supply of oxygen and maintain the local oxygen tension, which has been observed in a previous study investigating similar hyperinsulinemic non-diabetic obese individuals [38].

6.9 Diabetic effect on AT angiogenesis

Previous data showed higher angiogenic capacity in SAT of obese patients than OAT [69]. However, we found SAT showed lower capillary number and angiogenic capacity in non-diabetic versus diabetic obese individuals. This difference may be caused by most of previous work having been done using a mixed obese group with both diabetic and non-diabetic patients; and also data analysis was based on mean and mean of standard error, which was unable to show the true significance when comparing data with high variability. In our group, a strict clinical criteria was used to classify obese patients into MHO (plasma insulin level<6.5mU/l with plasma glucose <6.0 mmol/ml, excluding hypertension and dyslipidemia), PO (pathological obese, insulin>7.0 mU/l with glucose <6.0 mmol/ml) and the diabetic group. Further work should investigate the angiogenic difference between the non-diabetic sub-groups - PO and MHO. The data obtained from the angiogenesis array also needs to be extended to the samples from MHO patients, as here only the non-diabetic PO were compared to the diabetics.

6.10 AT vasculature, new target for treating obesity

Sufficient vascular supply enriched with oxygen and insulin may protect tissue from hypoxia and insulin resistance, but may also facilitate growth factor transport and accelerate AT growth. Therefore, it is tempting to suggest that inhibiting AT vasculature and consequently reducing AT growth as a reasonable treatment for obese patients. Current data suggests even though capillary density is sufficient in OAT and diabetes the AT may still be associated with tissue hypoxia, pro-inflammatory

adipokine secretion and insulin resistance. Thus, excessive angiogenesis may not contribute to metabolic benefits but only facilitate the rapid 'unhealthy' AT growth. Data from rodents demonstrates that systemic VEGF repression in various tissues showed a protective effect against high-fat diet-induced obesity by producing a browning AT phenotype [216]. However, it has been reported that anti-angiogenic therapy may also be associated with elevated risks of endothelium dysfunction and other vascular diseases [217]. In addition, rapid reduction of adipose mass in MHO patients may cause negative metabolic consequences. It should be noted that lower capillary density and larger adipocytes were observed in SAT of non-diabetic patients in this study, but SAT still appeared to be less deleterious compared with OAT. This could be a consequence of its relatively normal vascular tone and reactivity, which ensures sufficient blood supply even with less capillary numbers and angiogenesis. Therefore, the improvement of vascular function may be a better way to improve or reverse the hypoxia and insulin resistance in AT.

6.11 PVAT-derived Adiponectin

The major finding in **Chapter 5** is the demonstration of endothelium-derived adiponectin. Moreover, the adiponectin mRNA expression was significantly different between HCAEC and HUVEC. The heterogeneity of ECs between different vascular beds has been investigated in previous studies (reviewed in [218]&[219]). The major differences were summarised in **Figure 31**. Interestingly, besides the structural, morphological and genetic differences, HCAEC and HUVEC also displayed different response to inflammatory stimulation. Compared with HUVEC, there were lower levels of adhesion molecules expression in HCAEC by 4-hr treatment. However, prolonged 24-hr exposure to inflammatory stimuli elevated adhesion molecules expression in both artery and vein [220]. This suggests that endothelium-derived adiponectin could play a

protective role in response to inflammation and the consequent inflammatory molecule/cell adhesion, an initial step in atherosclerosis. Future studies may need to investigate whether there are intracellular adiponectin receptors, as well as the pathways involved in the endothelial adiponectin synthesis and regulation.

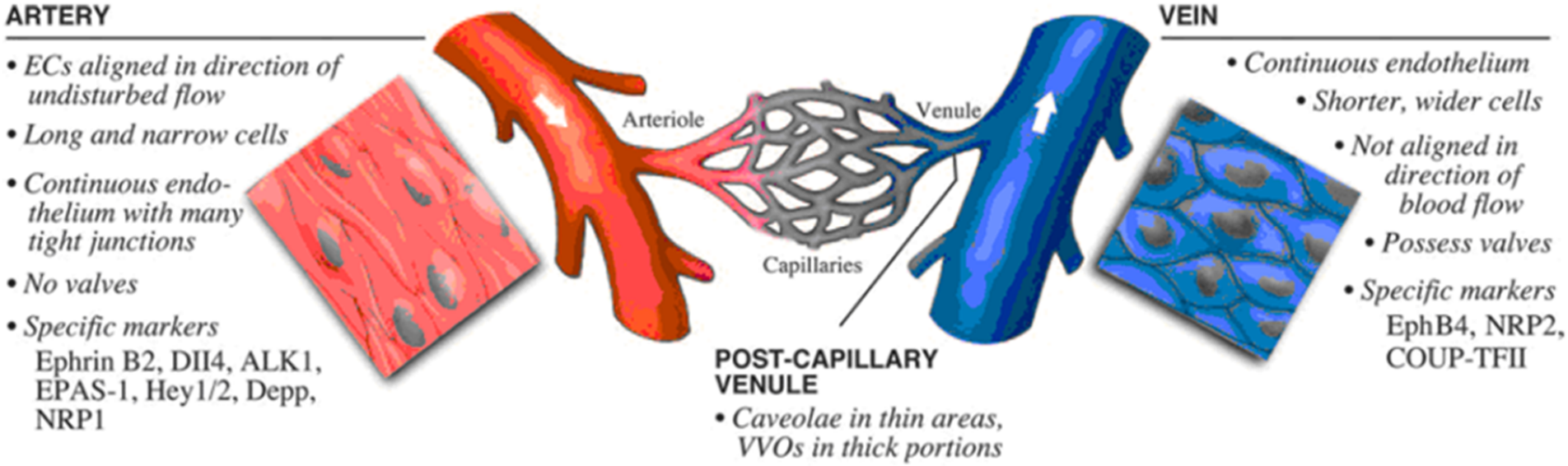

Figure. 31 Major differences in structure and ECs between artery and vein [219]

Shown are mayor EC structural and marker differences between arteries, veins, postcapillary venules, and capillaries.

6.12 Limitation

A major limitation in this thesis is the lack of lean control patients. At an initial stage of this study lean patients undergoing cholecystectomy and hernia repair surgery were recruited as controls. Although they were relatively insulin sensitive and metabolically healthy compared to the obese patients, levels of pro-inflammatory adipokines such as IL-6 were found to be high in the AT explant in these patients, which suggests they were also associated with chronic local inflammation.

Furthermore, no animal work was undertaken to supplement the current study. Dietary-induced obese mice model is widely utilized to investigate AT structure and function in obesity. However, weight gain in obese mice is more often a short-term process; it may be not representative of human obesity, in which the AT expansion may take many years. In addition, due to the anatomic difference in mice, SAT and OAT may not be precisely distinguished and also truly analogous to human abdominal depots.

6.13 Future study

6.13.1 Vasoconstriction induced by NPY and ET-1

The current study displayed the depot- and diabetes- specific difference in vasoconstriction mediated by NA. Interestingly, data from rats showed that the NA-mediated vasoconstriction could be amplified by the infusion of NPY [221]. However, the effect of NPY on microvessels embedded within AT is not clear. Preliminary data in our group suggested NPY showed vasocontractile effect on both SAT and OAT. This vasoconstriction was transient and could not be reproduced. However, the vasoconstriction was much higher in both depots of those obese patients with

hypertension or OSA. When this condition was simulated experimentally (vessel incubated with 10^{-7}M NA) in vessels from non-hypertensive, non-OSA obese patients this led to a much stronger vasoconstriction mediated by NPY, which was not observed by applying NPY alone. Thus, future investigation needs to be performed to clarify the vasoactive effects of NPY, in the presence and absence of differing levels of NA, both *in vivo* and *in vitro*.

6.13.2 Vasodilatation induced by Ach, leptin, adiponectin

Acetylcholine (Ach)-induced vasodilatation of microvessels from AT was investigated between SAT and OAT in a previous study [140] and no significant difference was reported between diabetics and non-diabetics. Furthermore, arterioles in OAT showed barely any response to Ach. However, in that study, 10^{-6} M ET-1 was applied to build the pre-constriction, which was far beyond the normal range for vessel to contract. In our group, a lower dose of ET-1 (10^{-8}M) was used and vasodilatation was shown in OAT.

Our data also suggest a significant depot difference between SAT and OAT in leptin secretion. The higher level of leptin released from SAT raised the question whether there is leptin resistance in this depot and how this might affect vasoreactivity. Preliminary evidence showed leptin induced incomplete vasodilatation in SAT by using relatively high doses of leptin (8μg/ml) while OAT relaxed more quickly and completely under a much lower dose (2μg/ml).

PVAT-derived adiponectin may have a protective anti-contractile function by increasing the bioavailability of NO [74], but whether it has similar effects on the microvessels with PVAT dissected is still unknown. Therefore, vasodilator differences between the depots also should be investigated in future studies.

6.13.3 Electron microscopic study: endothelial junction and mitochondria

The cell to cell junction is a structure formed by transmembrane adhesion molecules linked to cytoplasmic proteins between cells [222]. In endothelium, cell junctions mainly include adherens junctions and tight junctions (**Figure 32A**) [223]. Endothelial cell to cell junctions not only mediate intercellular communication, but also regulate vascular permeability [224]. Furthermore, adherens junction may be also involved in vessel morphogenesis and stability [222]. Evidence showed that inflammatory molecules such TNF and IL-1 elevate vascular permeability by binding to specific receptors generating intracellular signals, which lead to the cytoskeletal reorganization and cell gap opening (reviewed in [225]). In obese individuals, ECs in OAT showed higher levels of inflammatory gene expression than SAT [37], but whether the endothelial cell to cell junction is affected is still unclear. A preliminary study was done in 3 patients; 1 from each group - MHO, PO and diabetic. Our data showed that ECs in OAT displayed significantly larger adherens junctions compared to SAT (**Figure 32B&C)**. In addition, the structure of cell junction may be compromised in OAT (**Figure 32C**). The wider endothelial junction and 'de-structured' junction in OAT may be due to the inflammation in this depot, which may facilitate macrophage infiltration into the endothelium and increase the risk of atherosclerosis.

In this study, we also found a number of mitochondria in AT vasculature. Mitochondrial number and function are directly involved in the AT oxygenation. Data suggest oxygen consumption in mitochondria is down-regulated in obese individuals [38]. Thus, mitochondrial metabolic disorder may be a risk factor associated with AT dysfunction. But, due to the small sample size, the mitochondrial numbers could not be fully quantified in the study. This would be worth further investigation.

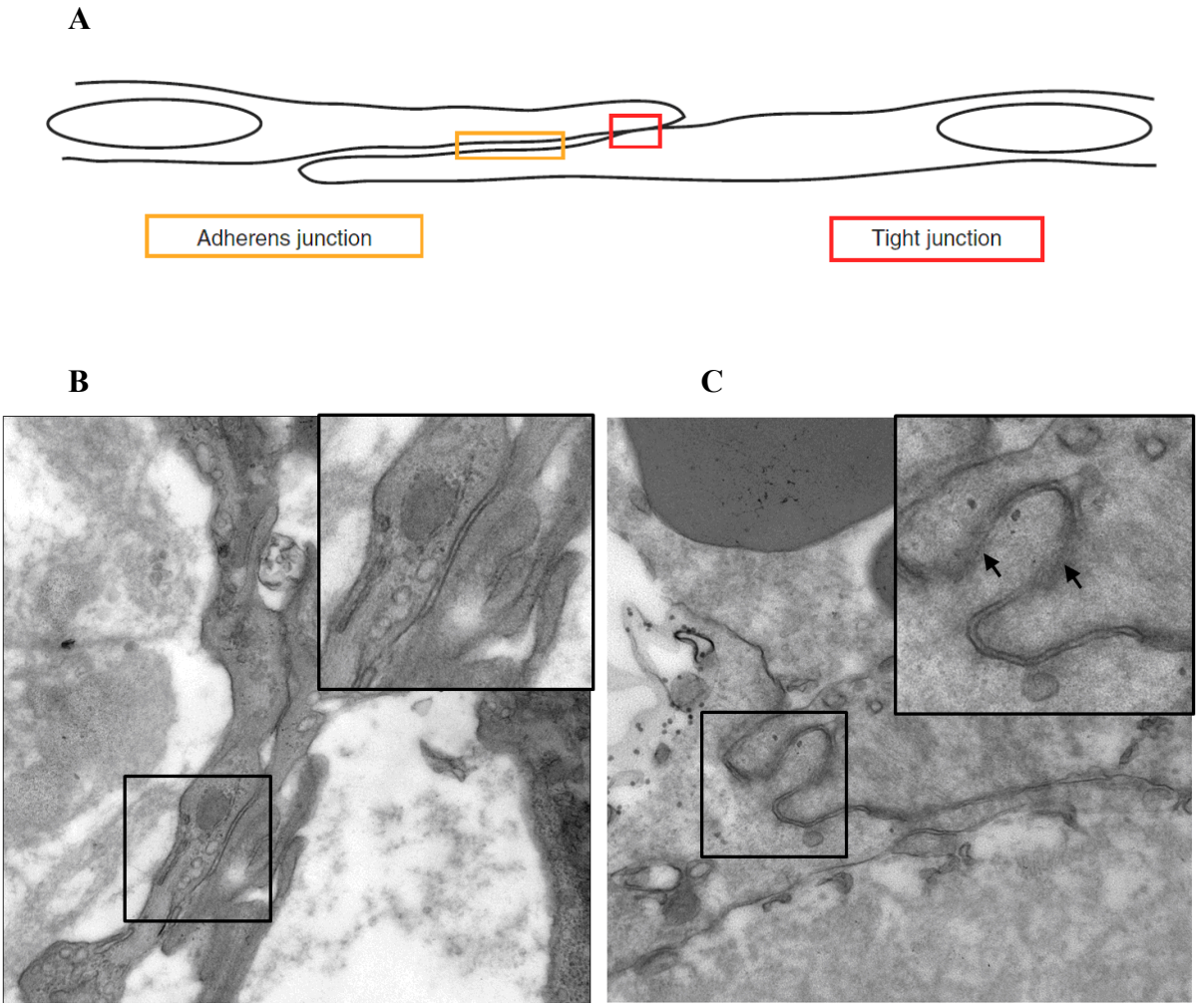

Figure 32 Junctional components in ECs and depot-specific difference in AT endothelial junction.

In ECs, there are mainly two distinct junctional domains, adherens junctions and tight junctions (A, extracted from [223])

In a non-diabetic subject, arterioles in SAT (B) displayed significantly larger junctions compared with OAT (C). Furthermore, structural alterations in OAT was observed, which suggest the impairment of endothelial junction intactness (arrows).

6.14 Conclusion

The interplay between the vasculature and AT is crucial to maintaining AT normal function and remodelling capacity. Preserved vascular NA sensitivity as well as low levels of local AT NA synthesis may play a key role to protect AT from tissue fibrosis, inflammation and hypoxia. This study demonstrated local chronically elevated NA in AT desensitized adrenergic regulation of vasoconstriction and increased vessel stiffness via elevating tissue fibrosis, perhaps consequently leading to a vascular hyporeactivity, which may be associated with AT dysfunction. Concomitantly angiogenesis was triggered, perhaps to compensate for the compromised vascular function, as observed in OAT and diabetes. Due to the vascular dysfunction, neovasculature, even at relatively normal or high levels, may not be adequate to reverse local hypoxia and inflammation but only facilitate the 'unhealthy' tissue expansion.

The endothelium-derived adiponectin suggests that ECs *per se* may produce adiponectin, which is known to be protective against the initial stages of atherosclerosis. Higher levels of adiponectin in the arteries further explains its potential advantage in CABG, but the effect of endothelium-derived adiponectin and its intracellular pathway need to be further investigated.

Chapter 7

References

1. Flegal, KM, Carroll, MD, Ogden, CL, and Curtin, LR, *Prevalence and Trends in Obesity Among US Adults, 1999-2008.* J Am Med Assoc, 2010. **303**(3): p. 235-241.

2. WHO, *Obesity and overweight.* Fact sheet N°311, 2012. **http://www.who.int/mediacentre/factsheets/fs311/en/**.

3. Alberti, KGMM, Eckel, RH, Grundy, SM, Zimmet, PZ, Cleeman, JI, Donato, KA, Fruchart, JC, James, WPT, Loria, CM, and Smith, SC, *Harmonizing the Metabolic Syndrome A Joint Interim Statement of the International Diabetes Federation Task Force on Epidemiology and Prevention; National Heart, Lung, and Blood Institute; American Heart Association; World Heart Federation; International Atherosclerosis Society; and International Association for the Study of Obesity.* Circulation, 2009. **120**(16): p. 1640-1645.

4. Sowers, JR, *Obesity as a cardiovascular risk factor.* Am J Med, 2003. **115**: p. 37-41.

5. Ross, R and Despres, JP, *Abdominal Obesity, Insulin Resistance, and the Metabolic Syndrome: Contribution of Physical Activity/Exercise.* Obesity, 2009. **17**: p. S1-S2.

6. Calabro, P, Golia, E, Riegler, L, Palmieri, R, Maddaloni, V, D'Alessandro, R, Limongelli, G, Pacileo, G, Golino, P, Russo, M, and Calabro, R, *Abdominal Obesity, Chronic Inflammation and the Cardiovascular Risk: Not All Fat Is Equal.* Horiz Cancer Res, 2010. **41**: p. 163-182.

7. Primeau, V, Coderre, L, Karelis, AD, Brochu, M, Lavoie, ME, Messier, V, Sladek, R, and Rabasa-Lhoret, R, *Characterizing the profile of obese patients who are metabolically healthy.* Int J Obesity, 2011. **35**(7): p. 971-981.

8. Andres, R, *Effect of Obesity on Total Mortality.* Int J Obesity, 1980. **4**(4): p. 381-386.

9. Arsenault, BJ, Rana, JS, Lemieux, I, Despres, JP, Warehame, NJ, Kastelein, JJP, Boekholdt, SM, and Khaw, KT, *Physical activity, the Framingham risk score and risk of coronary heart disease in men and women of the EPIC-Norfolk study.* Atherosclerosis, 2010. **209**(1): p. 261-265.

10. Karelis, AD, Messier, V, Brochu, M, and Rabasa-Lhoret, R, *Metabolically healthy but obese women: effect of an energy-restricted diet.* Diabetologia, 2008. **51**(9): p. 1752-1754.

11. Frayn, KN, Coppack, SW, Fielding, BA, and Humphreys, SM, *Coordinated regulation of hormone-sensitive lipase and lipoprotein lipase in human adipose tissue in vivo: implications for the control of fat storage and fat mobilization.* Adv Enzyme Regul, 1995. **35**: p. 163-178.

12. Karastergiou, K and Mohamed-Ali, V, *The autocrine and paracrine roles of adipokines.* Mol Cell Endocrinol, 2010. **318**(1-2): p. 69-78.

13. Mohamed-Ali, V, Pinkney, JH, and Coppack, SW, *Adipose tissue as an endocrine and paracrine organ.* Int J Obes Relat Metab Disord, 1998. **22**(12): p. 1145-1158.

14. Sethi, JK and Vidal-Puig, AJ, *Thematic review series: Adipocyte biology - Adipose tissue function and plasticity orchestrate nutritional adaptation.* J Lipid Res, 2007. **48**(6): p. 1253-1262.

15. Snijder, MB, Dekker, JM, Visser, M, Bouter, LM, Stehouwer, CDA, Kostense, PJ, Yudkin, JS, Heine, RJ, Nijpels, G, and Seidell, JC, *Associations of hip and thigh circumferences independent of waist circumference with the incidence of type 2 diabetes: the Hoorn Study.* Am J Clin Nutr, 2003. **77**(5): p. 1192-1197.

16. Lissner, L, Bjorkelund, C, Heitmann, BL, Seidell, JC, and Bengtsson, C, *Larger hip circumference independently predicts health and longevity in a Swedish female cohort.* Obes Res, 2001. **9**(10): p. 644-646.

17. Despres, JP and Lemieux, I, *Abdominal obesity and metabolic syndrome.* Nature, 2006. **444**(7121): p. 881-887.

18. Bjorntorp, P, *Hazards in Subgroups of Human Obesity.* Eur J Clin Invest, 1984. **14**(4): p. 239-241.

19. Bjorntorp, P, *Obesity and the Risk of Cardiovascular-Disease.* Ann Clin Res, 1985. **17**(1): p. 3-9.

20. Fujioka, S, Matsuzawa, Y, Tokunaga, K, and Tarui, S, *Contribution of intra-abdominal fat accumulation to the impairment of glucose and lipid metabolism in human obesity.* Metabolism, 1987. **36**(1): p. 54-59.

21. Despres, JP, Nadeau, A, Tremblay, A, Ferland, M, Moorjani, S, Lupien, PJ, Theriault, G, Pinault, S, and Bouchard, C, *Role of Deep Abdominal Fat in the Association between Regional Adipose-Tissue Distribution and Glucose-Tolerance in Obese Women.* Diabetes, 1989. **38**(3): p. 304-309.

22. Pouliot, MC, Despres, JP, Nadeau, A, Moorjani, S, Prudhomme, D, Lupien, PJ, Tremblay, A, and Bouchard, C, *Visceral Obesity in Men - Associations with Glucose-Tolerance, Plasma-Insulin, and Lipoprotein Levels.* Diabetes, 1992. **41**(7): p. 826-834.

23. Tran, TT, Yamamoto, Y, Gesta, S, and Kahn, CR, *Beneficial effects of subcutaneous fat transplantation on metabolism.* Cell Metab, 2008. **7**(5): p. 410-420.

24. Kim, JY, De Wall, EV, Laplante, M, Azzara, A, Trujillo, ME, Hofmann, SM, Schraw, T, Durand, JL, Li, H, Li, G, Jelicks, LA, Mehler, MF, Hui, DY, Deshaies, Y, Shulman, GI, Schwartz, GJ, and Scherer, PE, *Obesity-associated improvements in metabolic profile through expansion of adipose tissue.* J Clin Invest, 2007. **117**(9): p. 2621-2637.

25. Yang, X and Smith, U, *Adipose tissue distribution and risk of metabolic disease: does thiazolidinedione-induced adipose tissue redistribution provide a clue to the answer?* Diabetologia, 2007. **50**(6): p. 1127-1139.

26. Mohammed, BS, Cohen, S, Reeds, D, Young, VL, and Klein, S, *Long-term effects of large-volume liposuction on metabolic risk factors for coronary heart disease.* Obesity, 2008. **16**(12): p. 2648-2651.

27. Wajchenberg, BL, *Subcutaneous and Visceral Adipose Tissue: Their Relation to the Metabolic Syndrome.* Endocr Rev, 2000. **21**(6): p. 697-738.

28. Lee, M-J, Wu, Y, and Fried, SK, *Adipose tissue heterogeneity: Implication of depot differences in adipose tissue for obesity complications.* Mol Aspects Med, 2013. **34**(1): p. 1-11.

29. Frayn, KN, *Adipose tissue as a buffer for daily lipid flux.* Diabetologia, 2002. **45**: p. 1201-1210.

30. Smith, J, Al-Amri, M, Dorairaj, P, and Sniderman, A, *The adipocyte life cycle hypothesis.* Clin Sci (Lond), 2006. **110**(1): p. 1-9.

31. Cao, Y, *Angiogenesis as a therapeutic target for obesity and metabolic diseases.* Chem Immunol Allergy, 2014. **99**: p. 170-179.

32. Hausman, DB, DiGirolamo, M, Bartness, TJ, Hausman, GJ, and Martin, RJ, *The biology of white adipocyte proliferation.* Obes Rev, 2001. **2**(4): p. 239-254.

33. Lundgren, M, Svensson, M, Lindmark, S, Renstrom, F, Ruge, T, and Eriksson, JW, *Fat cell enlargement is an independent marker of insulin resistance and 'hyperleptinaemia'.* Diabetologia, 2007. **50**(3): p. 625-633.

34. Skurk, T, Alberti-Huber, C, Herder, C, and Hauner, H, *Relationship between adipocyte size and adipokine expression and secretion.* J Clin Endocrinol Metab, 2007. **92**(3): p. 1023-1033.

35. Tchernof, A, Belanger, C, Morisset, AS, Richard, C, Mailloux, J, Laberge, P, and Dupont, P, *Regional differences in adipose tissue metabolism in women - Minor effect of obesity and body fat distribution.* Diabetes, 2006. **55**(5): p. 1353-1360.

36. Veilleux, A, Caron-Jobin, M, Noel, S, Laberge, PY, and Tchernof, A, *Visceral adipocyte hypertrophy is associated with dyslipidemia independent of body composition and fat distribution in women.* Diabetes, 2011. **60**(5): p. 1504-1511.

37. Villaret, A, Galitzky, J, Decaunes, P, Esteve, D, Marques, MA, Sengenes, C, Chiotasso, P, Tchkonia, T, Lafontan, M, Kirkland, JL, and Bouloumie, A, *Adipose tissue endothelial cells from obese human subjects: differences among depots in angiogenic, metabolic, and inflammatory gene expression and cellular senescence.* Diabetes, 2010. **59**(11): p. 2755-2763.

38. Goossens, GH, Bizzarri, A, Venteclef, N, Essers, Y, Cleutjens, JP, Konings, E, Jocken, JW, Cajlakovic, M, Ribitsch, V, Clement, K, and Blaak, EE, *Increased adipose tissue oxygen tension in obese compared with lean men is accompanied by insulin resistance, impaired adipose tissue capillarization, and inflammation.* Circulation, 2011. **124**(1): p. 67-76.

39. Sun, K, Kusminski, CM, and Scherer, PE, *Adipose tissue remodeling and obesity.* J Clin Invest, 2011. **121**(6): p. 2094-2101.

40. Ye, JP, Gao, ZG, Yin, J, and He, Q, *Hypoxia is a potential risk factor for chronic inflammation and adiponectin reduction in adipose tissue of ob/ob and dietary obese mice.* Am J Physiol-Endoc M, 2007. **293**(4): p. E1118-E1128.

41. Pasarica, M, Sereda, OR, Redman, LM, Albarado, DC, Hymel, DT, Roan, LE, Rood, JC, Burk, DH, and Smith, SR, *Reduced Adipose Tissue Oxygenation in Human Obesity Evidence for Rarefaction, Macrophage Chemotaxis, and*

Inflammation Without an Angiogenic Response. Diabetes, 2009. **58**(3): p. 718-725.

42. Cao, Y, *Adipose tissue angiogenesis as a therapeutic target for obesity and metabolic diseases.* Nat Rev Drug Discov, 2010. **9**(2): p. 107-115.

43. Nishimura, S, Manabe, I, Nagasaki, M, Hosoya, Y, Yamashita, H, Fujita, H, Ohsugi, M, Tobe, K, Kadowaki, T, Nagai, R, and Sugiura, S, *Adipogenesis in obesity requires close interplay between differentiating adipocytes, strontal cells, and blood vessels.* Diabetes, 2007. **56**(6): p. 1517-1526.

44. Hausman, GJ and Richardson, RL, *Adipose tissue angiogenesis.* J Anim Sci, 2004. **82**(3): p. 925-934.

45. Crandall, DL, Busler, DE, McHendry-Rinde, B, Groeling, TM, and Kral, JG, *Autocrine regulation of human preadipocyte migration by plasminogen activator inhibitor-1.* J Clin Endocrinol Metab, 2000. **85**(7): p. 2609-2614.

46. Planat-Benard, V, Silvestre, JS, Cousin, B, Andre, M, Nibbelink, M, Tamarat, R, Clergue, M, Manneville, C, Saillan-Barreau, C, Duriez, M, Tedgui, A, Levy, B, Penicaud, L, and Casteilla, L, *Plasticity of human adipose lineage cells toward endothelial cells - Physiological and therapeutic perspectives.* Circulation, 2004. **109**: p. 656-663.

47. Gupta, RK, Mepani, RJ, Kleiner, S, Lo, JC, Khandekar, MJ, Cohen, P, Frontini, A, Bhowmick, DC, Ye, L, Cinti, S, and Spiegelman, BM, *Zfp423 expression identifies committed preadipocytes and localizes to adipose endothelial and perivascular cells.* Cell Metab, 2012. **15**(2): p. 230-239.

48. Tugues, S, Koch, S, Gualandi, L, Li, XJ, and Claesson-Welsh, L, *Vascular endothelial growth factors and receptors: Anti-angiogenic therapy in the treatment of cancer.* Mol Aspects Med, 2011. **32**(2): p. 88-111.

49. Hagberg, CE, Mehlem, A, Falkevall, A, Muhl, L, Fam, BC, Ortsater, H, Scotney, P, Nyqvist, D, Samen, E, Lu, L, Stone-Elander, S, Proietto, J, Andrikopoulos, S, Sjoholm, A, Nash, A, and Eriksson, U, *Targeting VEGF-B as a novel treatment for insulin resistance and type 2 diabetes.* Nature, 2012. **490**(7420): p. 426-430.

50. Shweiki, D, Itin, A, Soffer, D, and Keshet, E, *Vascular Endothelial Growth-Factor Induced by Hypoxia May Mediate Hypoxia-Initiated Angiogenesis.* Nature, 1992. **359**(6398): p. 843-845.

51. Elias, I, Franckhauser, S, Ferre, T, Vila, L, Tafuro, S, Munoz, S, Roca, C, Ramos, D, Pujol, A, Riu, E, Ruberte, J, and Bosch, F, *Adipose Tissue Overexpression of Vascular Endothelial Growth Factor Protects Against Diet-Induced Obesity and Insulin Resistance.* Diabetes, 2012. **61**(7): p. 1801-1813.

52. Tinahones, F, Salas, J, Mayas, MD, Ruiz-Villalba, A, Macias-Gonzalez, M, Garrido-Sanchez, L, DeMora, M, Moreno-Santos, I, Bernal, R, Cardona, F, and El Bekay, R, *VEGF gene expression in adult human thymus fat: a correlative study with hypoxic induced factor and cyclooxygenase-2.* PLoS One, 2009. **4**(12): p. e8213.

53. Zhang, QX, Magovern, CJ, Mack, CA, Budenbender, KT, Ko, W, and Rosengart, TK, *Vascular endothelial growth factor is the major angiogenic factor in omentum: Mechanism of the omentum-mediated angiogenesis.* J Surg Res, 1997. **67**(2): p. 147-154.

54. Pellet-Many, C, Frankel, P, Jia, H, and Zachary, I, *Neuropilins: structure, function and role in disease.* Biochem J, 2008. **411**(2): p. 211-226.

55. Herzog, Y, Kalcheim, C, Kahane, N, Reshef, R, and Neufeld, G, *Differential expression of neuropilin-1 and neuropilin-2 in arteries and veins.* Mech Dev, 2001. **109**(1): p. 115-119.

56. Koch, S, *Neuropilin signalling in angiogenesis.* Biochem Soc Trans, 2012. **40**(1): p. 20-25.

57. Zachary, I, *Neuropilins: role in signalling, angiogenesis and disease.* Chem Immunol Allergy, 2014. **99**: p. 37-70.

58. Kawasaki, T, Kitsukawa, T, Bekku, Y, Matsuda, Y, Sanbo, M, Yagi, T, and Fujisawa, H, *A requirement for neuropilin-1 in embryonic vessel formation.* Development, 1999. **126**(21): p. 4895-4902.

59. Giordano, A, Cesari, P, Capparuccia, L, Castellucci, M, and Cinti, S, *Sema3A and neuropilin-1 expression and distribution in rat white adipose tissue.* J Neurocytol, 2003. **32**(4): p. 345-352.

60. Belaid, Z, Hubint, F, Humblet, C, Boniver, J, Nusgens, B, and Defresne, M, *Differential expression of vascular endothelial growth factor and its receptors in hematopoietic and fatty bone marrow: evidence that neuropilin-1 is produced by fat cells.* Haematologica, 2005. **90**(3): p. 400-401.

61. Cao, RH, Brakenhielm, E, Wahlestedt, C, Thyberg, J, and Cao, YH, *Leptin induces vascular permeability and synergistically stimulates angiogenesis with FGF-2 and VEGF.* P Natl Acad Sci USA, 2001. **98**(11): p. 6390-6395.

62. Sierra-Honigmann, MR, Nath, AK, Murakami, C, Garcia-Cardena, G, Papapetropoulos, A, Sessa, WC, Madge, LA, Schechner, JS, Schwabb, MB, Polverini, PJ, and Flores-Riveros, JR, *Biological action of leptin as an angiogenic factor.* Science, 1998. **281**(5383): p. 1683-1686.

63. Wood, IS, Stezhka, T, and Trayhurn, P, *Modulation of adipokine production, glucose uptake and lactate release in human adipocytes by small changes in oxygen tension.* Pflugers Archiv-European Journal of Physiology, 2011. **462**(3): p. 469-477.

64. Lihn, AS, Pedersen, SB, and Richelsen, B, *Adiponectin: action, regulation and association to insulin sensitivity.* Obes Rev, 2005. **6**(1): p. 13-21.

65. Brakenhielm, E, Veitonmaki, N, Cao, R, Kihara, S, Matsuzawa, Y, Zhivotovsky, B, Funahashi, T, and Cao, Y, *Adiponectin-induced antiangiogenesis and antitumor activity involve caspase-mediated endothelial cell apoptosis.* Proc Natl Acad Sci U S A, 2004. **101**(8): p. 2476-2481.

66. Mahadev, K, Wu, X, Donnelly, S, Ouedraogo, R, Eckhart, AD, and Goldstein, BJ, *Adiponectin inhibits vascular endothelial growth factor-induced migration of human coronary artery endothelial cells.* Cardiovasc Res, 2008. **78**(2): p. 376-384.

67. Landskroner-Eiger, S, Qian, BZ, Muise, ES, Nawrocki, AR, Berger, JP, Fine, EJ, Koba, W, Deng, YF, Pollard, JW, and Scherer, PE, *Proangiogenic Contribution of Adiponectin toward Mammary Tumor Growth In vivo.* Clin Cancer Res, 2009. **15**(10): p. 3265-3276.

68. Ouchi, N, Kobayashi, H, Kihara, S, Kumada, M, Sato, K, Inoue, T, Funahashi, T, and Walsh, K, *Adiponectin stimulates angiogenesis by promoting cross-talk between AMP-activated protein kinase and Akt signaling in endothelial cells.* J Biol Chem, 2004. **279**(2): p. 1304-1309.

69. Gealekman, O, Guseva, N, Hartigan, C, Apotheker, S, Gorgoglione, M, Gurav, K, Tran, KV, Straubhaar, J, Nicoloro, S, Czech, MP, Thompson, M, Perugini, RA, and Corvera, S, *Depot-specific differences and insufficient subcutaneous adipose tissue angiogenesis in human obesity.* Circulation, 2011. **123**(2): p. 186-194.

70. Lemoine, AY, Ledoux, S, Queguiner, I, Calderari, S, Mechler, C, Msika, S, Corvol, P, and Larger, E, *Link between Adipose Tissue Angiogenesis and Fat*

Accumulation in Severely Obese Subjects. Journal of Clinical Endocrinology & Metabolism, 2012. **97**(5): p. E775-E780.

71. Levy, BI, Ambrosio, G, Pries, AR, and Struijker-Boudier, HA, *Microcirculation in hypertension: a new target for treatment?* Circulation, 2001. **104**(6): p. 735-740.

72. Vicaut, E, *Hypertension and the microcirculation: a brief overview of experimental studies.* J Hypertens Suppl, 1992. **10**(5): p. S59-68.

73. de Jongh, RT, Serne, EH, Ijzerman, RG, de Vries, G, and Stehouwer, CDA, *Impaired microvascular function in obesity - Implications for obesity-associated microangiopathy, hypertension, and insulin resistance.* Circulation, 2004. **109**(21): p. 2529-2535.

74. Greenstein, AS, Khavandi, K, Withers, SB, Sonoyama, K, Clancy, O, Jeziorska, M, Laing, I, Yates, AP, Pemberton, PW, Malik, RA, and Heagerty, AM, *Local inflammation and hypoxia abolish the protective anticontractile properties of perivascular fat in obese patients.* Circulation, 2009. **119**(12): p. 1661-1670.

75. Sobey, CG, *Potassium channel function in vascular disease.* Arterioscler Thromb Vasc Biol, 2001. **21**(1): p. 28-38.

76. Vane, JR, Anggard, EE, and Botting, RM, *Regulatory functions of the vascular endothelium.* N Engl J Med, 1990. **323**(1): p. 27-36.

77. Nacci, C, Tarquinio, M, and Montagnani, M, *Molecular and clinical aspects of endothelial dysfunction in diabetes.* Intern Emerg Med, 2009. **4**(2): p. 107-116.

78. Schiffrin, EL and Touyz, RM, *Vascular biology of endothelin.* J Cardiovasc Pharm, 1998. **32**: p. S2-S13.

79. Zhang, J, Yang, W, Hu, B, Wu, W, and Fallon, MB, *Endothelin-1 activation of the endothelin B receptor modulates pulmonary endothelial CX3CL1 and*

contributes to pulmonary angiogenesis in experimental hepatopulmonary syndrome. Am J Pathol, 2014. **184**(6): p. 1706-1714.

80. Caballero, AE, *Endothelial dysfunction in obesity and insulin resistance: A road to diabetes and heart disease.* Obes Res, 2003. **11**(11): p. 1278-1289.

81. Zeng, GY, Nystrom, FH, Ravichandran, LV, Cong, LN, Kirby, M, Mostowski, H, and Quon, MJ, *Roles for insulin receptor, PI3-kinase, and Akt in insulin-signaling pathways related to production of nitric oxide in human vascular endothelial cells.* Circulation, 2000. **101**(13): p. 1539-1545.

82. Cardillo, C, Nambi, SS, Kilcoyne, CM, Choucair, WK, Katz, A, Quon, MJ, and Panza, JA, *Insulin stimulates both endothelin and nitric oxide activity in the human forearm.* Circulation, 1999. **100**(8): p. 820-825.

83. Clark, MG, Wallis, MG, Barrett, EJ, Vincent, MA, Richards, SM, Clerk, LH, and Rattigan, S, *Blood flow and muscle metabolism: a focus on insulin action.* Am J Physiol Endocrinol Metab, 2003. **284**(2): p. E241-258.

84. Lteif, A, Vaishnava, P, Baron, AD, and Mather, KJ, *Endothelin limits insulin action in obese/insulin-resistant humans.* Diabetes, 2007. **56**(3): p. 728-734.

85. Achike, FI, To, NH, Wang, H, and Kwan, CY, *Obesity, metabolic syndrome, adipocytes and vascular function: A holistic viewpoint.* Clin Exp Pharmacol Physiol, 2011. **38**(1): p. 1-10.

86. Vecchione, C, Maffei, A, Colella, S, Aretini, A, Poulet, R, Frati, G, Gentile, MT, Fratta, L, Trimarco, V, Trimarco, B, and Lembo, G, *Leptin Effect on Endothelial Nitric Oxide Is Mediated Through Akt–Endothelial Nitric Oxide Synthase Phosphorylation Pathway.* Diabetes, 2002. **51**(1): p. 168-173.

87. Cooke, JP and Oka, RK, *Does Leptin Cause Vascular Disease?* Circulation, 2002. **106**(15): p. 1904-1905.

88. Procopio, C, Andreozzi, F, Laratta, E, Cassese, A, Beguinot, F, Arturi, F, Hribal, ML, Perticone, F, and Sesti, G, *Leptin-stimulated endothelial nitric-oxide synthase via an adenosine 5'-monophosphate-activated protein kinase/Akt signaling pathway is attenuated by interaction with C-reactive protein.* Endocrinology, 2009. **150**: p. 3584-3593.

89. Bastard, JP, Maachi, M, Lagathu, C, Kim, MJ, Caron, M, Vidal, H, Capeau, J, and Feve, B, *Recent advances in the relationship between obesity, inflammation, and insulin resistance.* Eur Cytokine Netw, 2006. **17**(1): p. 4-12.

90. Fruhbeck, G, *Pivotal role of nitric oxide in the control of blood pressure after leptin administration.* Diabetes, 1999. **48**(4): p. 903-908.

91. Leung, YM and Kwan, CY, *Dual vascular effects of leptin via endothelium: Hypothesis and perspective.* Chinese J Physiol, 2008. **51**(1): p. 1-6.

92. Quehenberger, P, Exner, M, Sunder-Plassmann, R, Ruzicka, K, Bieglmayer, C, Endler, G, Muellner, C, Speiser, W, and Wagner, O, *Leptin induces endothelin-1 in endothelial cells in vitro.* Circ Res, 2002. **90**(6): p. 711-718.

93. Loffreda, S, Yang, SQ, Lin, HZ, Karp, CL, Brengman, ML, Wang, DJ, Klein, AS, Bulkley, GB, Bao, C, Noble, PW, Lane, MD, and Diehl, AM, *Leptin regulates proinflammatory immune responses.* Faseb Journal, 1998. **12**(1): p. 57-65.

94. Antoniades, C, Antonopoulos, AS, Tousoulis, D, and Stefanadis, C, *Adiponectin: from obesity to cardiovascular disease.* Obes Rev, 2009. **10**(3): p. 269-279.

95. Xi, W, Satoh, H, Kase, H, Suzuki, K, and Hattori, Y, *Stimulated HSP90 binding to eNOS and activation of the PI3-Akt pathway contribute to globular adiponectin-induced NO production: Vasorelaxation in response to globular adiponectin.* Biochem Bioph Res Co, 2005. **332**(1): p. 200-205.

96. Fesus, G, Dubrovska, G, Gorzelniak, K, Kluge, R, Huang, Y, Luft, FC, and Gollasch, M, *Adiponectin is a novel humoral vasodilator.* Cardiovascular Research, 2007. **75**(4): p. 719-727.

97. Tan, KCB, Xu, A, Chow, WS, Lam, MCW, Ai, VHG, Tam, SCF, and Lam, KSL, *Hypoadiponectinemia is associated with impaired endothelium-dependent vasodilation.* Journal of Clinical Endocrinology & Metabolism, 2004. **89**(2): p. 765-769.

98. Chudek, J and Wiecek, A, *Adipose tissue, inflammation and endothelial dysfunction.* Pharmacol Rep, 2006. **58 Suppl**: p. 81-88.

99. Ohkawa, F, Ikeda, U, Kawasaki, K, Kusano, E, Igarashi, M, and Shimada, K, *Inhibitory effect of interleukin-6 on vascular smooth muscle contraction.* Am J Physiol, 1994. **266**(3 Pt 2): p. H898-902.

100. Schrader, LI, Kinzenbaw, DA, Johnson, AW, Faraci, FM, and Didion, SP, *IL-6 deficiency protects against angiotensin II induced endothelial dysfunction and hypertrophy.* Arterioscler Thromb Vasc Biol, 2007. **27**(12): p. 2576-2581.

101. Brian, JE, Jr. and Faraci, FM, *Tumor necrosis factor-alpha-induced dilatation of cerebral arterioles.* Stroke, 1998. **29**(2): p. 509-515.

102. Meijer, RI, Serne, EH, Smulders, YM, van Hinsbergh, VW, Yudkin, JS, and Eringa, EC, *Perivascular adipose tissue and its role in type 2 diabetes and cardiovascular disease.* Curr Diab Rep, 2011. **11**(3): p. 211-217.

103. Gu, P and Xu, A, *Interplay between adipose tissue and blood vessels in obesity and vascular dysfunction.* Rev Endocr Metab Disord, 2013. **14**(1): p. 49-58.

104. Lee, RMKW, Lu, C, Su, LY, and Gao, YJ, *Endothelium-dependent relaxation factor released by perivascular adipose tissue.* J Hypertens, 2009. **27**(4): p. 782-790.

105. Lohn, M, Dubrovska, G, Lauterbach, B, Luft, FC, Gollasch, M, and Sharma, AM, *Periadventitial fat releases a vascular relaxing factor.* Faseb Journal, 2002. **16**(9): p. 1057-1063.

106. Gao, YJ, Lu, C, Su, LY, Sharma, AM, and Lee, RMKW, *Modulation of vascular function by perivascular adipose tissue: the role of endothelium and hydrogen peroxide.* Brit J Pharmacol, 2007. **151**(3): p. 323-331.

107. Eringa, EC, Bakker, W, and van Hinsbergh, VWM, *Paracrine regulation of vascular tone, inflammation and insulin sensitivity by perivascular adipose tissue.* Vasc Pharmacol, 2012. **56**(5-6): p. 204-209.

108. Yudkin, JS, Eringa, E, and Stehouwer, CDA, *"Vasocrine" signalling from perivascular fat: a mechanism linking insulin resistance to vascular disease.* Lancet, 2005. **365**(9473): p. 1817-1820.

109. Richelsen, B, *Factors regulating the production of prostaglandin E2 and prostacyclin (prostaglandin I2) in rat and human adipocytes.* Biochem J, 1987. **247**(2): p. 389-394.

110. Traupe, T, Lang, M, Goettsch, W, Munter, K, Morawietz, H, Vetter, W, and Barton, M, *Obesity increases prostanoid-mediated vasoconstriction and vascular thromboxane receptor gene expression.* J Hypertens, 2002. **20**(11): p. 2239-2245.

111. Traupe, T, D'Uscio, LV, Muenter, K, Morawietz, H, Vetter, W, and Barton, M, *Effects of obesity on endothelium-dependent reactivity during acute nitric oxide synthase inhibition: modulatory role of endothelin.* Clin Sci (Lond), 2002. **103 Suppl 48**: p. 13S-15S.

112. Axelrod, L, *Insulin, Prostaglandins, and the Pathogenesis of Hypertension.* Diabetes, 1991. **40**(10): p. 1223-1227.

113. Tobin, L, Simonsen, L, Galbo, H, and Bulow, J, *Vascular and metabolic effects of adrenaline in adipose tissue in type 2 diabetes.* Nutr Diabetes, 2012. **2**: p. e46.

114. Mohamed-Ali, V, Flower, L, Sethi, J, Hotamisligil, G, Gray, R, Humphries, SE, York, DA, and Pinkney, J, *beta-Adrenergic regulation of IL-6 release from adipose tissue: in vivo and in vitro studies.* J Clin Endocrinol Metab, 2001. **86**(12): p. 5864-5869.

115. Prieto, D, *Physiological regulation of penile arteries and veins.* Int J Impot Res, 2008. **20**(1): p. 17-29.

116. Spraul, M, Ravussin, E, Fontvieille, AM, Rising, R, Larson, DE, and Anderson, EA, *Reduced sympathetic nervous activity. A potential mechanism predisposing to body weight gain.* J Clin Invest, 1993. **92**(4): p. 1730-1735.

117. Rumantir, MS, Vaz, M, Jennings, GL, Collier, G, Kaye, DM, Seals, DR, Wiesner, GH, Brunner-La Rocca, HP, and Esler, MD, *Neural mechanisms in human obesity-related hypertension.* J Hypertens, 1999. **17**(8): p. 1125-1133.

118. Vargovic, P, Ukropec, J, Laukova, M, Cleary, S, Manz, B, Pacak, K, and Kvetnansky, R, *Adipocytes as a new source of catecholamine production.* FEBS Lett, 2011. **585**(14): p. 2279-2284.

119. Tatemoto, K, Carlquist, M, and Mutt, V, *Neuropeptide Y--a novel brain peptide with structural similarities to peptide YY and pancreatic polypeptide.* Nature, 1982. **296**(5858): p. 659-660.

120. Tang-Christensen, M, Vrang, N, Ortmann, S, Bidlingmaier, M, Horvath, TL, and Tschop, M, *Central administration of ghrelin and agouti-related protein (83-132) increases food intake and decreases spontaneous locomotor activity in rats.* Endocrinology, 2004. **145**(10): p. 4645-4652.

121. Lundberg, JM, Franco-Cereceda, A, Lacroix, JS, and Pernow, J, *Neuropeptide Y and sympathetic neurotransmission.* Ann N Y Acad Sci, 1990. **611**: p. 166-174.

122. Pernow, J, Ohlen, A, Hokfelt, T, Nilsson, O, and Lundberg, JM, *Neuropeptide Y: presence in perivascular noradrenergic neurons and vasoconstrictor effects on skeletal muscle blood vessels in experimental animals and man.* Regul Pept, 1987. **19**(5-6): p. 313-324.

123. Wahlestedt, C, Hakanson, R, Vaz, CA, and Zukowska-Grojec, Z, *Norepinephrine and neuropeptide Y: vasoconstrictor cooperation in vivo and in vitro.* Am J Physiol, 1990. **258**(3 Pt 2): p. R736-742.

124. Kalra, SP and Kalra, PS, *NPY and cohorts in regulating appetite, obesity and metabolic syndrome: beneficial effects of gene therapy.* Neuropeptides, 2004. **38**(4): p. 201-211.

125. Sun, K, Tordjman, J, Clement, K, and Scherer, PE, *Fibrosis and adipose tissue dysfunction.* Cell Metab, 2013. **18**(4): p. 470-477.

126. Keophiphath, M, Achard, V, Henegar, C, Rouault, C, Clement, K, and Lacasa, D, *Macrophage-secreted factors promote a profibrotic phenotype in human preadipocytes.* Mol Endocrinol, 2009. **23**(1): p. 11-24.

127. Sun, K, Halberg, N, Khan, M, Magalang, UJ, and Scherer, PE, *Selective inhibition of hypoxia-inducible factor 1alpha ameliorates adipose tissue dysfunction.* Mol Cell Biol, 2013. **33**(5): p. 904-917.

128. Divoux, A, Tordjman, J, Lacasa, D, Veyrie, N, Hugol, D, Aissat, A, Basdevant, A, Guerre-Millo, M, Poitou, C, Zucker, JD, Bedossa, P, and Clement, K, *Fibrosis in human adipose tissue: composition, distribution, and link with lipid metabolism and fat mass loss.* Diabetes, 2010. **59**(11): p. 2817-2825.

129. Khan, T, Muise, ES, Iyengar, P, Wang, ZV, Chandalia, M, Abate, N, Zhang, BB, Bonaldo, P, Chua, S, and Scherer, PE, *Metabolic dysregulation and adipose tissue fibrosis: role of collagen VI.* Mol Cell Biol, 2009. **29**(6): p. 1575-1591.

130. Pasarica, M, Gowronska-Kozak, B, Burk, D, Remedios, I, Hymel, D, Gimble, J, Ravussin, E, Bray, GA, and Smith, SR, *Adipose Tissue Collagen VI in Obesity.* Journal of Clinical Endocrinology & Metabolism, 2009. **94**(12): p. 5155-5162.

131. Raines, EW, *The extracellular matrix can regulate vascular cell migration, proliferation, and survival: relationships to vascular disease.* Int J Exp Pathol, 2000. **81**(3): p. 173-182.

132. Lan, TH, Huang, XQ, and Tan, HM, *Vascular fibrosis in atherosclerosis.* Cardiovasc Pathol, 2013. **22**(5): p. 401-407.

133. Oben, JA, Roskams, T, Yang, S, Lin, H, Sinelli, N, Li, Z, Torbenson, M, Thomas, SA, and Diehl, AM, *Norepinephrine induces hepatic fibrogenesis in leptin deficient ob/ob mice.* Biochem Biophys Res Commun, 2003. **308**(2): p. 284-292.

134. Rassler, B, Marx, G, Schierle, K, and Zimmer, HG, *Catecholamines Can Induce Pulmonary Remodeling in Rats.* Cell Physiol and Biochem, 2012. **30**(5): p. 1134-1147.

135. Zebekakis, PE, Nawrot, T, Thijs, L, Balkestein, EJ, van der Heijden-Spek, J, Van Bortel, LM, Struijker-Boudier, HA, Safar, ME, and Staessen, JA, *Obesity is associated with increased arterial stiffness from adolescence until old age.* J Hypertens, 2005. **23**(10): p. 1839-1846.

136. Giltay, EJ, Lambert, J, Elbers, JM, Gooren, LJ, Asscheman, H, and Stehouwer, CD, *Arterial compliance and distensibility are modulated by body composition in both men and women but by insulin sensitivity only in women.* Diabetologia, 1999. **42**(2): p. 214-221.

137. Steinberg, HO, Chaker, H, Leaming, R, Johnson, A, Brechtel, G, and Baron, AD, *Obesity/insulin resistance is associated with endothelial dysfunction.*

Implications for the syndrome of insulin resistance. J Clin Invest, 1996. **97**(11): p. 2601-2610.

138. Grassi, G, Seravalle, G, Scopelliti, F, Dell'Oro, R, Fattori, L, Quarti-Trevano, F, Brambilla, G, Schiffrin, EL, and Mancia, G, *Structural and functional alterations of subcutaneous small resistance arteries in severe human obesity.* Obesity, 2010. **18**(1): p. 92-98.

139. Van Gaal, LF, Mertens, IL, and De Block, CE, *Mechanisms linking obesity with cardiovascular disease.* Nature, 2006. **444**(7121): p. 875-880.

140. Farb, MG, Ganley-Leal, L, Mott, M, Liang, Y, Ercan, B, Widlansky, ME, Bigornia, SJ, Fiscale, AJ, Apovian, CM, Carmine, B, Hess, DT, Vita, JA, and Gokce, N, *Arteriolar Function in Visceral Adipose Tissue Is Impaired in Human Obesity.* Arterioscler Thromb Vasc Biol, 2012. **32**(2): p. 467-473.

141. Georgescu, A, Popov, D, Constantin, A, Nemecz, M, Alexandru, N, Cochior, D, and Tudor, A, *Dysfunction of human subcutaneous fat arterioles in obesity alone or obesity associated with Type 2 diabetes.* Clin Sci (Lond), 2011. **120**(10): p. 463-472.

142. Barton, M, Baretella, O, and Meyer, MR, *Obesity and risk of vascular disease: importance of endothelium-dependent vasoconstriction.* Br J Pharmacol, 2012. **165**(3): p. 591-602.

143. Fried, M, Hainer, V, Basdevant, A, Buchwald, H, Deitel, M, Finer, N, Greve, JW, Horber, F, Mathus-Vliegen, E, Scopinaro, N, Steffen, R, Tsigos, C, Weiner, R, and Widhalm, K, *Interdisciplinary European guidelines for surgery for severe (morbid) obesity.* Obes Surg, 2007. **17**(2): p. 260-270.

144. Matthews, DR, Hosker, JP, Rudenski, AS, Naylor, BA, Treacher, DF, and Turner, RC, *Homeostasis model assessment: insulin resistance and beta-cell*

function from fasting plasma glucose and insulin concentrations in man. Diabetologia, 1985. **28**(7): p. 412-419.

145. Hausman, GJ, *Cytochemistry for lectins, actin, nucleotide tetrazolium reductases and several phosphatases in the porcine semitendinosus muscle: vascular development in young pigs.* J Anim Sci, 1989. **67**(5): p. 1375-1386.

146. Matsumoto, S, Morikawa, K, and Yanagida, M, *Light microscopic structure of DNA in solution studied by the 4',6-diamidino-2-phenylindole staining method.* J Mol Biol, 1981. **152**(2): p. 501-516.

147. Dashwood, MR, Dooley, A, Xu, SW, Abraham, DJ, and Souza, DSR, *Does periadventitial fat-derived nitric oxide play a role in improved saphenous vein graft patency in patients undergoing coronary artery bypass surgery?* Journal of Vascular Research, 2007. **44**: p. 175-181.

148. Chomczynski, P and Sacchi, N, *Single-step method of RNA isolation by acid guanidinium thiocyanate-phenol-chloroform extraction.* Anal Biochem, 1987. **162**(1): p. 156-159.

149. Smith, PK, Krohn, RI, Hermanson, GT, Mallia, AK, Gartner, FH, Provenzano, MD, Fujimoto, EK, Goeke, NM, Olson, BJ, and Klenk, DC, *Measurement of protein using bicinchoninic acid.* Anal Biochem, 1985. **150**(1): p. 76-85.

150. Friedewald, WT, Levy, RI, and Fredrickson, DS, *Estimation of the concentration of low-density lipoprotein cholesterol in plasma, without use of the preparative ultracentrifuge.* Clin Chem, 1972. **18**(6): p. 499-502.

151. Alvarez, GE, Beske, SD, Ballard, TP, and Davy, KP, *Sympathetic neural activation in visceral obesity.* Circulation, 2002. **106**(20): p. 2533-2536.

152. Straznicky, NE, Grima, MT, Sari, CI, Eikelis, N, Lambert, EA, Nestel, PJ, Esler, MD, Dixon, JB, Chopra, R, Tilbrook, AJ, Schlaich, MP, and Lambert, GW, *Neuroadrenergic dysfunction along the diabetes continuum: a comparative*

study in obese metabolic syndrome subjects. Diabetes, 2012. **61**(10): p. 2506-2516.

153. Alvarez, GE, Ballard, TP, Beske, SD, and Davy, KP, *Subcutaneous obesity is not associated with sympathetic neural activation.* Am J Physiol Heart Circ Physiol, 2004. **287**(1): p. H414-418.

154. Bartness, TJ and Bamshad, M, *Innervation of mammalian white adipose tissue: implications for the regulation of total body fat.* Am J Physiol, 1998. **275**(5 Pt 2): p. R1399-1411.

155. Lambert, GW, Straznicky, NE, Lambert, EA, Dixon, JB, and Schlaich, MP, *Sympathetic nervous activation in obesity and the metabolic syndrome--causes, consequences and therapeutic implications.* Pharmacol Ther, 2010. **126**(2): p. 159-172.

156. Rizzoni, D, De Ciuceis, C, Porteri, E, Semeraro, F, and Rosei, EA, *Structural alterations in small resistance arteries in obesity.* Basic Clin Pharmacol Toxicol, 2012. **110**(1): p. 56-62.

157. Ball, N, Danks, JL, Dorudi, S, and Nasmyth, PA, *Desensitization by noradrenaline of responses to stimulation of pre- and postsynaptic adrenoceptors.* Br J Pharmacol, 1982. **76**(1): p. 201-210.

158. Abraham, GJ and Nasmyth, PA, *Desensitization of the rat aortic strip to vasopressin by infusions of noradrenaline [proceedings]*. Br J Pharmacol, 1976. **57**(3): p. 458P.

159. Simonsen, L, Bulow, J, Astrup, A, Madsen, J, and Christensen, NJ, *Diet-induced changes in subcutaneous adipose tissue blood flow in man: effect of beta-adrenoceptor inhibition.* Acta Physiol Scand, 1990. **139**(2): p. 341-346.

160. Ruiz-Ortega, M, Rodriguez-Vita, J, Sanchez-Lopez, E, Carvajal, G, and Egido, J, *TGF-beta signaling in vascular fibrosis.* Cardiovasc Res, 2007. **74**(2): p. 196-206.

161. Annes, JP, Munger, JS, and Rifkin, DB, *Making sense of latent TGFbeta activation.* J Cell Sci, 2003. **116**(Pt 2): p. 217-224.

162. Leask, A and Abraham, DJ, *TGF-beta signaling and the fibrotic response.* FASEB J, 2004. **18**(7): p. 816-827.

163. Santana, AB, de Souza Oliveira, TC, Bianconi, BL, Barauna, VG, Santos, EW, Alves, TP, Silva, JC, Fiorino, P, Borelli, P, Irigoyen, MC, Krieger, JE, and Lacchini, S, *Effect of high-fat diet upon inflammatory markers and aortic stiffening in mice.* Biomed Res Int, 2014. **2014**: p. 914102.

164. Pereira, S, Teixeira, L, Aguilar, E, Oliveira, M, Savassi-Rocha, A, Pelaez, JN, Capettini, L, Diniz, MT, Ferreira, A, and Alvarez-Leite, J, *Modulation of adipose tissue inflammation by FOXP3+ Treg cells, IL-10, and TGF-beta in metabolically healthy class III obese individuals.* Nutrition, 2014. **30**(7-8): p. 784-790.

165. Aprahamian, TR, *Elevated adiponectin expression promotes adipose tissue vascularity under conditions of diet-induced obesity.* Metabolism, 2013.

166. Niu, J, Wang, K, Zhelyabovska, O, Saad, Y, and Kolattukudy, PE, *MCP-1-induced protein promotes endothelial-like and angiogenic properties in human bone marrow monocytic cells.* J Pharmacol Exp Ther, 2013.

167. Costa, PZ and Soares, R, *Neovascularization in diabetes and its complications. Unraveling the angiogenic paradox.* Life Sci, 2013. **92**(22): p. 1037-1045.

168. Adham, SA and Coomber, BL, *Glucose is a key regulator of VEGFR2/KDR in human epithelial ovarian carcinoma cells.* Biochem Biophys Res Commun, 2009. **390**(1): p. 130-135.

169. Morita, Y, Maeda, K, Kondo, T, Ishii, H, Matsudaira, K, Okumura, N, Mitsuhashi, H, Shibata, R, Murohara, T, and on behalf of the Nagoya Acute Myocardial Infarction Study, G, *Impact of Adiponectin and Leptin on Long-Term Adverse Events in Japanese Patients With Acute Myocardial Infarction.* Circ J, 2013.

170. Cheng, KK, Lam, KS, Wang, Y, Huang, Y, Carling, D, Wu, D, Wong, C, and Xu, A, *Adiponectin-induced endothelial nitric oxide synthase activation and nitric oxide production are mediated by APPL1 in endothelial cells*, Diabetes, 2007. p. 1387-1394.

171. Perri, A, Vizza, D, Lofaro, D, Gigliotti, P, Leone, F, Papalia, T, and Bonofiglio, R, *Adiponectin Is Expressed and Secreted by Tubular Epithelial Renal Cells.* Nephrology Dialysis Transplantation, 2013. **Epub ahead of print**.

172. Okamoto, Y, Arita, Y, Nishida, M, Muraguchi, M, Ouchi, N, Takahashi, M, Igura, T, Inui, Y, Kihara, S, Nakamura, T, Yamashita, S, Miyagawa, J, Funahashi, T, and Matsuzawa, Y, *An adipocyte-derived plasma protein, adiponectin, adheres to injured vascular walls.* Horm Metab Res, 2000. **32**: p. 47-50.

173. Eringa, EC, Bakker, W, Smulders, YM, Serne, EH, Yudkin, JS, and Stehouwer, CD, *Regulation of vascular function and insulin sensitivity by adipose tissue: focus on perivascular adipose tissue.* Microcirculation, 2007. **14**(4-5): p. 389-402.

174. Komura, N, Maeda, N, Mori, T, Kihara, S, Nakatsuji, H, Hirata, A, Tochino, Y, Funahashi, T, and Shimomura, I, *Adiponectin protein exists in aortic endothelial cells.* PLoS One, 2013. **8**(8): p. e71271.

175. Tschritter, O, Fritsche, A, Thamer, C, Haap, M, Shirkavand, F, Rahe, S, Staiger, H, Maerker, E, Haring, H, and Stumvoll, M, *Plasma adiponectin concentrations*

predict insulin sensitivity of both glucose and lipid metabolism. Diabetes, 2003. **52**(2): p. 239-243.

176. Kadowaki, T, Yamauchi, T, Kubota, N, Hara, K, Ueki, K, and Tobe, K, *Adiponectin and adiponectin receptors in insulin resistance, diabetes, and the metabolic syndrome.* J Clin Invest, 2006. **116**(7): p. 1784-1792.

177. Souza, DS, Johansson, B, Bojo, L, Karlsson, R, Geijer, H, Filbey, D, Bodin, L, Arbeus, M, and Dashwood, MR, *Harvesting the saphenous vein with surrounding tissue for CABG provides long-term graft patency comparable to the left internal thoracic artery: results of a randomized longitudinal trial.* J Thorac Cardiovasc Surg, 2006. **132**(2): p. 373-378.

178. Sims, FH, *A comparison of coronary and internal mammary arteries and implications of the results in the etiology of arteriosclerosis.* Am Heart J, 1983. **105**(4): p. 560-566.

179. Li, CJ, Sun, HW, Zhu, FL, Chen, L, Rong, YY, Zhang, Y, and Zhang, M, *Local adiponectin treatment reduces atherosclerotic plaque size in rabbits.* J Endocrinol, 2007. **193**(1): p. 137-145.

180. Bahadori, B, Neuer, E, Schumacher, M, Fruhwald, F, Eber, B, Klein, W, Topak, H, and Wascher, TC, *Prevalence of coronary artery disease in obese versus lean men with angina pectoris and positive exercise stress test.* Am J Cardiol, 1996. **77**(11): p. 1000-1001.

181. Emdin, M, Gastaldelli, A, Muscelli, E, Macerata, A, Natali, A, Camastra, S, and Ferrannini, E, *Hyperinsulinemia and autonomic nervous system dysfunction in obesity: effects of weight loss.* Circulation, 2001. **103**(4): p. 513-519.

182. Goodpaster, BH, Wolfe, RR, and Kelley, DE, *Effects of obesity on substrate utilization during exercise.* Obes Res, 2002. **10**(7): p. 575-584.

183. Bruce, CR, Mertz, VA, Heigenhauser, GJ, and Dyck, DJ, *The stimulatory effect of globular adiponectin on insulin-stimulated glucose uptake and fatty acid oxidation is impaired in skeletal muscle from obese subjects.* Diabetes, 2005. **54**(11): p. 3154-3160.

184. Cannon, B, Nedergaard, J, Lundberg, JM, Hokfelt, T, Terenius, L, and Goldstein, M, *'Neuropeptide tyrosine' (NPY) is co-stored with noradrenaline in vascular but not in parenchymal sympathetic nerves of brown adipose tissue.* Exp Cell Res, 1986. **164**(2): p. 546-550.

185. Bulow, J, Astrup, A, Christensen, NJ, and Kastrup, J, *Blood flow in skin, subcutaneous adipose tissue and skeletal muscle in the forearm of normal man during an oral glucose load.* Acta Physiol Scand, 1987. **130**(4): p. 657-661.

186. Dimitriadis, G, Lambadiari, V, Mitrou, P, Maratou, E, Boutati, E, Panagiotakos, DB, Economopoulos, T, and Raptis, SA, *Impaired postprandial blood flow in adipose tissue may be an early marker of insulin resistance in type 2 diabetes.* Diabetes Care, 2007. **30**(12): p. 3128-3130.

187. Flechtner-Mors, M, Jenkinson, CP, Alt, A, Biesalski, HK, Adler, G, and Ditschuneit, HH, *Sympathetic regulation of glucose uptake by the alpha1-adrenoceptor in human obesity.* Obes Res, 2004. **12**(4): p. 612-620.

188. Boschmann, M, Krupp, G, Luft, FC, Klaus, S, and Jordan, J, *In vivo response to alpha(1)-adrenoreceptor stimulation in human white adipose tissue.* Obes Res, 2002. **10**(6): p. 555-558.

189. Lafontan, M, Barbe, P, Galitzky, J, Tavernier, G, Langin, D, Carpene, C, Bousquet-Melou, A, and Berlan, M, *Adrenergic regulation of adipocyte metabolism.* Hum Reprod, 1997. **12 Suppl 1**: p. 6-20.

190. Sotornik, R, Brassard, P, Martin, E, Yale, P, Carpentier, AC, and Ardilouze, JL, *Update on adipose tissue blood flow regulation.* Am J Physiol Endocrinol Metab, 2012. **302**(10): p. E1157-1170.

191. De Ciuceis, C, Porteri, E, Rizzoni, D, Corbellini, C, La Boria, E, Boari, GE, Pilu, A, Mittempergher, F, Di Betta, E, Casella, C, Nascimbeni, R, Rosei, CA, Ruggeri, G, Caimi, L, and Rosei, EA, *Effects of weight loss on structural and functional alterations of subcutaneous small arteries in obese patients.* Hypertension, 2011. **58**(1): p. 29-36.

192. Blaak, EE, van Baak, MA, Kemerink, GJ, Pakbiers, MT, Heidendal, GA, and Saris, WH, *Beta-adrenergic stimulation and abdominal subcutaneous fat blood flow in lean, obese, and reduced-obese subjects.* Metabolism, 1995. **44**(2): p. 183-187.

193. Millet, L, Barbe, P, Lafontan, M, Berlan, M, and Galitzky, J, *Catecholamine effects on lipolysis and blood flow in human abdominal and femoral adipose tissue.* J Appl Physiol (1985), 1998. **85**(1): p. 181-188.

194. Patel, JN, Eisenhofer, G, Coppack, SW, and Miles, JM, *Norepinephrine spillover in forearm and subcutaneous adipose tissue before and after eating.* J Clin Endocrinol Metab, 1999. **84**(8): p. 2815-2819.

195. Vollenweider, P, Tappy, L, Randin, D, Schneiter, P, Jequier, E, Nicod, P, and Scherrer, U, *Differential effects of hyperinsulinemia and carbohydrate metabolism on sympathetic nerve activity and muscle blood flow in humans.* J Clin Invest, 1993. **92**(1): p. 147-154.

196. Gentile, CL, Orr, JS, Davy, BM, and Davy, KP, *Modest weight gain is associated with sympathetic neural activation in nonobese humans.* Am J Physiol Regul Integr Comp Physiol, 2007. **292**(5): p. R1834-1838.

197. Chen, W, Sang, JY, Liu, DJ, Qin, J, Huo, YM, Xu, J, and Wu, ZY, *Desensitization of G-protein-coupled receptors induces vascular hypocontractility in response to norepinephrine in the mesenteric arteries of cirrhotic patients and rats.* Hepatobiliary Pancreat Dis Int, 2013. **12**(3): p. 295-304.

198. Ferguson, SS, *Evolving concepts in G protein-coupled receptor endocytosis: the role in receptor desensitization and signaling.* Pharmacol Rev, 2001. **53**(1): p. 1-24.

199. Gluszek, J, *Ischaemic heart disease and hypertension in patients with chronic obstructive pulmonary disease and obstructive sleep apnoea.* Pneumonol Alergol Pol, 2013. **81**(6): p. 567-574.

200. Fu, Y, Xiao, H, and Zhang, Y, *Beta-adrenoceptor signaling pathways mediate cardiac pathological remodeling.* Front Biosci (Elite Ed), 2012. **4**: p. 1625-1637.

201. Johnson, RJ, Gordon, KL, Suga, S, Duijvestijn, AM, Griffin, K, and Bidani, A, *Renal Injury and Salt-Sensitive Hypertension After Exposure to Catecholamines.* Hypertension, 1999. **34**(1): p. 151-159.

202. Reichenbach, DD and Benditt, EP, *Catecholamines and cardiomyopathy: The pathogenesis and potential importance of myofibrillar degeneration.* Human Pathol, 1970. **1**(1): p. 125-150.

203. Diez, J, Panizo, A, Gil, MJ, Monreal, I, Hernandez, M, and Pardo Mindan, J, *Serum markers of collagen type I metabolism in spontaneously hypertensive rats: relation to myocardial fibrosis.* Circulation, 1996. **93**(5): p. 1026-1032.

204. Laviades, C, Varo, N, Fernandez, J, Mayor, G, Gil, MJ, Monreal, I, and Diez, J, *Abnormalities of the extracellular degradation of collagen type I in essential hypertension.* Circulation, 1998. **98**(6): p. 535-540.

205. Kato, H, Suzuki, H, Tajima, S, Ogata, Y, Tominaga, T, Sato, A, and Saruta, T, *Angiotensin II stimulates collagen synthesis in cultured vascular smooth muscle cells.* J Hypertens, 1991. **9**(1): p. 17-22.

206. Tharaux, PL, Chatziantoniou, C, Fakhouri, F, and Dussaule, JC, *Angiotensin II activates collagen I gene through a mechanism involving the MAP/ER kinase pathway.* Hypertension, 2000. **36**(3): p. 330-336.

207. Lin, HM, Lee, JH, Yadav, H, Kamaraju, AK, Liu, E, Zhigang, D, Vieira, A, Kim, SJ, Collins, H, Matschinsky, F, Harlan, DM, Roberts, AB, and Rane, SG, *Transforming growth factor-beta/Smad3 signaling regulates insulin gene transcription and pancreatic islet beta-cell function.* J Biol Chem, 2009. **284**(18): p. 12246-12257.

208. Tan, CK, Leuenberger, N, Tan, MJ, Yan, YW, Chen, Y, Kambadur, R, Wahli, W, and Tan, NS, *Smad3 deficiency in mice protects against insulin resistance and obesity induced by a high-fat diet.* Diabetes, 2011. **60**(2): p. 464-476.

209. Chen, YL, Wu, HW, and Jiang, MJ, *Transforming growth factor-beta1 gene and protein expression associated with atherogenesis of cholesterol-fed rabbits.* Histol Histopathol, 2000. **15**(2): p. 421-428.

210. Yang, YL, Guh, JY, Yang, ML, Lai, YH, Tsai, JH, Hung, WC, Chang, CC, and Chuang, LY, *Interaction between high glucose and TGF-beta in cell cycle protein regulations in MDCK cells.* J Am Soc Nephrol, 1998. **9**(2): p. 182-193.

211. Rutkowski, JM, Davis, KE, and Scherer, PE, *Mechanisms of obesity and related pathologies: the macro- and microcirculation of adipose tissue.* FEBS J, 2009. **276**(20): p. 5738-5746.

212. Halberg, N, Khan, T, Trujillo, ME, Wernstedt-Asterholm, I, Attie, AD, Sherwani, S, Wang, ZV, Landskroner-Eiger, S, Dineen, S, Magalang, UJ, Brekken, RA, and Scherer, PE, *Hypoxia-Inducible Factor 1 alpha Induces*

Fibrosis and Insulin Resistance in White Adipose Tissue. Mol Cell Biol, 2009. **29**(16): p. 4467-4483.

213. Park, J and Scherer, PE, *Adipocyte-derived endotrophin promotes malignant tumor progression.* J Clin Invest, 2012. **122**(11): p. 4243-4256.

214. Simons, M, *Angiogenesis - Where do we stand now?* Circulation, 2005. **111**(12): p. 1556-1566.

215. Heil, M, Eitenmuller, I, Schmitz-Rixen, T, and Schaper, W, *Arteriogenesis versus angiogenesis: similarities and differences.* Journal of Cellular and Molecular Medicine, 2006. **10**(1): p. 45-55.

216. Lu, XD, Ji, Y, Zhang, LQ, Zhang, YT, Zhang, SZ, An, Y, Liu, P, and Zheng, YW, *Resistance to Obesity by Repression of VEGF Gene Expression through Induction of Brown-Like Adipocyte Differentiation.* Endocrinology, 2012. **153**(7): p. 3123-3132.

217. Cabebe, E and Wakelee, H, *Role of anti-angiogenesis agents in treating NSCLC: focus on bevacizumab and VEGFR tyrosine kinase inhibitors.* Curr Treat Options Oncol, 2007. **8**(1): p. 15-27.

218. Aird, WC, *Phenotypic heterogeneity of the endothelium: I. Structure, function, and mechanisms.* Circ Res, 2007. **100**(2): p. 158-173.

219. Aird, WC, *Phenotypic heterogeneity of the endothelium: II. Representative vascular beds.* Circ Res, 2007. **100**(2): p. 174-190.

220. Scott, DW, Vallejo, MO, and Patel, RP, *Heterogenic endothelial responses to inflammation: role for differential N-glycosylation and vascular bed of origin.* J Am Heart Assoc, 2013. **2**(4): p. e000263.

221. Macho, P, Perez, R, Huidobro-Toro, JP, and Domenech, RJ, *Neuropeptide Y (NPY): a coronary vasoconstrictor and potentiator of catecholamine-induced coronary constriction.* Eur J Pharmacol, 1989. **167**(1): p. 67-74.

222. Dejana, E, Tournier-Lasserve, E, and Weinstein, BM, *The control of vascular integrity by endothelial cell junctions: molecular basis and pathological implications.* Dev Cell, 2009. **16**(2): p. 209-221.

223. Lampugnani, MG, *Endothelial cell-to-cell junctions: adhesion and signaling in physiology and pathology.* Cold Spring Harb Perspect Med, 2012. **2**(10).

224. Dejana, E, *Endothelial adherens junctions: implications in the control of vascular permeability and angiogenesis.* J Clin Invest, 1997. **100**(11 Suppl): p. S7-10.

225. Dejana, E, Corada, M, and Lampugnani, MG, *Endothelial cell-to-cell junctions.* FASEB J, 1995. **9**(10): p. 910-918.